IntechOpen

Shale Gas

New Aspects and Technologies

Edited by Ali Al-Juboury

SHALE GAS - NEW ASPECTS AND TECHNOLOGIES

Edited by **Ali Al-Juboury**

Shale Gas - New Aspects and Technologies
http://dx.doi.org/10.5772/intechopen.70911
Edited by Ali Al-Juboury

Contributors

Abdul Haris, Agus Riyanto, Bayu Seno, Husein Agil Almunawar, Martogu Benedict Marbun, Iskandarsyah Mahmudin, Prima Erfido Manaf, Nadia Shafie Zadeh, Shahriar Talebi, Ali Ismail Al-Juboury, Muhammed Abed Mazeel Thani, Raghda Ahmed El-Nagar, Alaa Ghanem, Maher Nessim, Yunsheng Wei, Ailin Jia, Junlei Wang, Yadong Qi, Chengye Jia

Notice

First published in London, United Kingdom, 2018 by IntechOpen
eBook (PDF) Published by IntechOpen, 2019
IntechOpen is the global imprint of INTECHOPEN LIMITED, registered in England and Wales, registration number: 11086078, The Shard, 25th floor, 32 London Bridge Street
London, SE19SG – United Kingdom
Printed in Croatia

British Library Cataloguing-in-Publication Data
A catalogue record for this book is available from the British Library

Additional hard and PDF copies can be obtained from orders@intechopen.com

Shale Gas - New Aspects and Technologies
Edited by Ali Al-Juboury

p. cm.

Print ISBN 978-1-78923-618-7

Online ISBN 978-1-78923-619-4

eBook (PDF) ISBN 978-1-83881-479-3

Meet the editor

Ali Al-Juboury is a professor at the Geology Department of Mosul University, Iraq. He earned his BSc in Geology and MSc in Sedimentology from Mosul University, Iraq, in 1980 and 1983, respectively, and his PhD from Comenius University, Slovakia, in 1992. During 33 years of academic work at Salahaddin and Mosul universities, Iraq, he published 82 papers in local and international peer-reviewed journals in the fields of petroleum geology, sedimentology, geochemistry, and economic geology. He is a member of numerous international societies and serves on the editorial board of the *Iraqi Geological Journal*, *International Sedimentology and Stratigraphy Journal of Oil and Gas Basins*, Azerbaijan, *SciFed Journal of Biofuel and Bioenergetics*, and the *International Journal of Geophysics and Geochemistry* (American Association of Science and Technology). Prof. Al-Juboury has also received several awards, among which are the Distinguished Scholars Award from the Arab Fund for Economic and Social Development, Kuwait, in 2009 and the Islamic States Science and . Technology (Geology) Award in 2014.

Contents

Preface

Shale gas is one of the so-called "unconventional resources" because it requires specialized techniques and tools to achieve economic production. Commonly, these resources are oil or gas-bearing formations with very low permeability and porosity. Shale gas is an unconventional natural gas found in shale rocks and is composed primarily of methane (60–95% v/v), ethane, and propane.

This book contains five chapters that focus on contributions and new technologies and prospects on shale gas reserves in selected regions of the world. Generally, contributions are geographically distributed from Canada, China, Iraq, Indonesia, and Egypt.

The first chapter, "An overview of new developments in shale gas: induced seismicity aspect" by Nadia Shafie Zadeh and Shahriar Talebi, provides as extensive review of new technologies developed to monitor induced microseismicity and their applications on shale gas development.

The second chapter, "Unconventional resources of shale hydrocarbon in Sumatra Island, Indonesia" by Abdul Haris, Agus Riyanto, Bayu Seno, Husein Agil Almunawar, Martogu Benedict Marbun, Iskandarsyah Mahmudin, and Prima Erfido Manaf, uses integrated geochemical, geomechanical, petrophysical, and geophysical analyses to assess shale reservoirs on the island of Sumatra, Indonesia, and to explore the shale hydrocarbon prospect.

Chapter 3, "Silurian gas-rich "hot shale" from Akkas gas field, Western Iraq: geological importance and updated hydrocarbon potential and reservoir development estimations of the field" by Ali Ismail Al-Juboury and Muhammed Abed Mazeel Thani, gives a description of Silurian "hot shale" as a major source rock on the Arabian Peninsula, which is also regarded as the source of non-associated gas in the region and one of the common natural gases formed in shale of the Silurian period of Earth's history (400–450 million years ago) worldwide. The study also sets out assumptions about Akkas gas field development.

Chapter 4, "Current technologies and prospects of shale gas development in China" by Yunsheng Wei, Ailin Jia, Junlei Wang, Yadong Qi, and Chengye Jia, compares the shale gas developing conditions between China and the United States, reviews the developing practice and technological innovations, and gives a summary of the progress in key technologies of evaluating shale gas development in the past few years. The work also attempts to establish shale gas development theory, optimization of evaluation methods, and control of development cost as the core tasks in large-scale shale gas development

The final chapter, Chapter 5, "Capture of CO_2 from natural gas using ionic liquids" by Raghda Ahmed El-Nagar, Alaa Ali Ghanem, and Maher Ibrahim Nessim, includes an introduction to ionic liquids, their history and types, which were used in different applications such

as removal of carbon dioxide from natural gas. The work deals with the synthesis of different types of ionic liquids and their characterizations using different traditional techniques.

In general, *Shale Gas—New Aspects and Technologies* introduces an overview of some new advances in technologies and prospects on shale gas reserves. Each work is of great interest in terms of new discoveries of promising reserves, application of new technologies and syntheses, and their impact on shale gas development as one of the cleanest consuming non-renewable energy sources.

We have benefited from comments and suggestions offered by many expertise reviewers whose comments and contributions play an important and recognizable role in finalizing the high quality of the book chapters.

We would like to thank Rob Westaway, Qingmin Meng, Yongliang Xu, Nadia Shafiezadeh, Satish Kumar, Shuangfang Lu, Wei Yu, and Leonid Grigoryev.

We are also indebted to the support of IntechOpen Science in the publishing of this book.

Prof. Dr. Ali Ismail Al-Juboury
Mosul University, Iraq

Chapter 1

An Overview of New Developments in Shale Gas: Induced Seismicity Aspect

Nadia Shafie Zadeh and Shahriar Talebi

Additional information is available at the end of the chapter

http://dx.doi.org/10.5772/intechopen.76542

Abstract

New advances in technology such as advances in horizontal drilling, the use of multi-well drilling pads, and multi-stage hydraulic fracturing allow for the economic consideration of recovering formerly uneconomic, yet proven resources. Hydraulic fracturing perturbs the local stress field and causes slip/shearing in naturally fractured shale formations. Monitoring this process using microseismic techniques provides a valuable tool helping to detect the progression of the treatment and understand the efficacy of the operation. This article provides basic definitions regarding shale gas and development of shale gas reservoirs along with results of many new developments in the field of monitoring induced seismicity associated with hydraulic fracturing operations and characterizing of the efficacy of such operations.

Keywords: shale gas, induced seismicity, microseismic monitoring, hydraulic fracturing optimization

1. Introduction

Unconventional resources such as shale gas are energy reserves under study and development. "Unconventional resources" is a useful term for resources that are trapped, and not primarily controlled by buoyancy forces. In other words, unconventional resources are oil or gas-bearing formations where the permeability and porosity are very low. This makes it extremely difficult or impossible for oil or natural gas to naturally flow through pores and into a production well. For this reason, unconventional resources require specialized techniques and tools to achieve economic production. Unconventional resources can be classified into different groups according to their type, origin and deposition. Shale gas, shale oil, tight

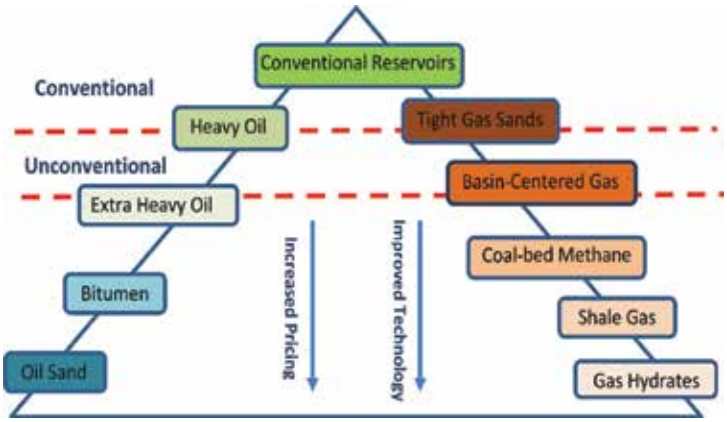

Figure 1. Petroleum resources triangle.

gas sands, oil shale, coal-bed methane, oil sands, and methane hydrates are all considered unconventional gases and tight oil. Shale gas is the focus of this study and refers to natural gas that is locked within shale formations. **Figure 1** illustrates the relative relationship between different unconventional and conventional resources by a resource triangle.

2. Shale gas

Natural gas, particularly shale gas, is an abundant energy resource that will be playing an active role in future energy demand and enabling the nation to transition to higher support on renewable energy sources.

2.1. Definition

Shale gas is unconventional natural gas, which is primarily methane (60–95% v/v), ethane and propane. This natural gas is found in shale rocks, some of which were formed during a Silurian period of Earth's history (400–450 million years ago). Shale gas is generally considered a dry gas which means that it is essentially methane in it but not much else, though some formations do produce wet gas that means in addition to methane, the gas contains compounds like ethane and butane. Shale is composed of fine-grained silt and clay particles that accumulated at the bottom of relatively enclosed bodies of water. These bodies of water had a high organic matter content. Shale typically functions as both the reservoir and the source rocks for the natural gas.

Some of the methane formed from the organic matter buried with the sediments remained locked in the tight, low-permeability shale layers, becoming shale gas though the gas is generated and stored in situ in gas shale as both sorbed gas on organic matter and free gas in fractures or pores. As such, shale contained gas is considered a self-sourced reservoir. Global discoveries of shale gas reserves will affect the geopolitical map of energy production. Shale gas is expected to be one of the leading sustainable energy sources in the twenty-first century [1, 2].

http://dx.doi.org/10.5772/intechopen.76542

2.2. Origin

Gas from shale is typically generated in two different ways; although a mixture of gas types is possible too. Thermogenic gas originates from cracking of organic matter or the secondary cracking of oil, while biogenic gas is generated from microbes in areas of freshwater recharge [3, 4]. Thermogenic gas is associated with a mature organic matter that has been subjected to relatively high temperature and high pressure in order to form hydrocarbons. Considering all other factors being equal, the more mature organic matter is the more in situ gas resources generate. Vitrinite reflectance (% Ro) is representative of organic maturity, and its value can vary. The value above 1% implies that the organic matter is adequately mature to be considered as an effective source rock [5, 6]. Further, biogenic gas is associated with either mature or immature organic matter and can add substantially to the shale gas reservoir [7].

2.3. Shale gas reservoirs

Shale gas reservoirs generally recover less gas, e.g., less than <5% up to 20% (v/v) relative to conventional gas reservoirs (approximately 50–90% (v/v)) [8]. Some naturally fractured shale reservoirs can have a recovery as high as 50–60% (v/v). Aside from the low permeability of the shale formation in shale gas reservoirs, the critical properties of shale formations regarding gas-containing potential are total organic content and their thermal maturity. The former key property refers to the total amount of organic material present in the host rock. The higher the total organic content, the better the potential for hydrocarbon generation. The latter key property is an indicator to measure the degree to which organic material in the rock has been heated over geological time and converted into the liquid or gas form of hydrocarbons. Gas storage characteristics of shale reservoirs are in practice different from conventional reservoirs. In shale gas reservoirs, besides the presence of gas in the porous matrix (similar to what is found in conventional reservoirs), gas can be found in the form of bound or absorbed to the surface of organic matters in the shale. Therefore, the key element of the production outline of the reservoir is the relative contributions and combinations of these two sources of free gas from matrix pores and from desorption of absorbed gas. The initial reservoir pressure, the petrophysical properties of the shale formation and its adsorption characteristics are the parameters that determine the amount and distribution of gas within the shale formation.

There are three main processes during gas production. The first process is the depletion of gas from the fracture network, which rapidly declines due to limited storage capacity. The second process is the depletion of gas stored in the matrix, and the third is desorption where the adsorbed gas is released from the rock as pressure declines within the reservoir. The rate of production via the latter process depends on the amount of declined reservoir pressure. Pressure changes within the reservoir usually occur very slowly because of the low permeability of the rock. Therefore, to increase the production via this latter process, the small well spacing needs to decrease the reservoir pressure significantly enough to cause the adsorbed gas to be desorbed. Key inputs that play a crucial role in volumetric analysis of evaluation of each shale gas resources are: the maturity of the organic matter, the type of gas generated and stored in the reservoir (biogenic or thermogenic gas), the total organic carbon (TOC) content, the permeability/porosity of the reservoir, and matrix and sorbed gas saturation. One

of the common approaches for resource evaluation is a probabilistic approach where the key parameters can be modeled using mathematical distributions and combined in Monte Carlo simulations to derive a resulting distribution [9]. The combination of TOC (known as a measure of organic richness), the thickness of organic shale, and organic maturity are key attributes to estimate the economic viability of a shale gas reservoir [2, 7, 10, 11]. The permeability of the matrix is the most important parameter that influences the sustainable gas production from the reservoir [12]. Natural or induced fracture density, and consequently the permeability of the shale matrix is the most important factor to sustain yearly production, since gas has to diffuse from the low permeability matrix to fractures. A higher matrix permeability leads to a higher rate of diffusion and higher rate of flow and production [2, 7, 12, 13]. Microfractures within shale formations can have a critical role in both economic production [14] and creating an induced fracture network resulting from the interaction with those natural microfractures. This statement needs further research and analysis both numerically and experimentally to determine their role in shale gas development and production. The other important factor to be considered is the thickness of the shale formation. A general rule is that a thicker shale gas reservoir is a better target. Though as drilling and completion techniques are improving, the necessary thickness of a shale gas reservoir to be developed economically may decrease.

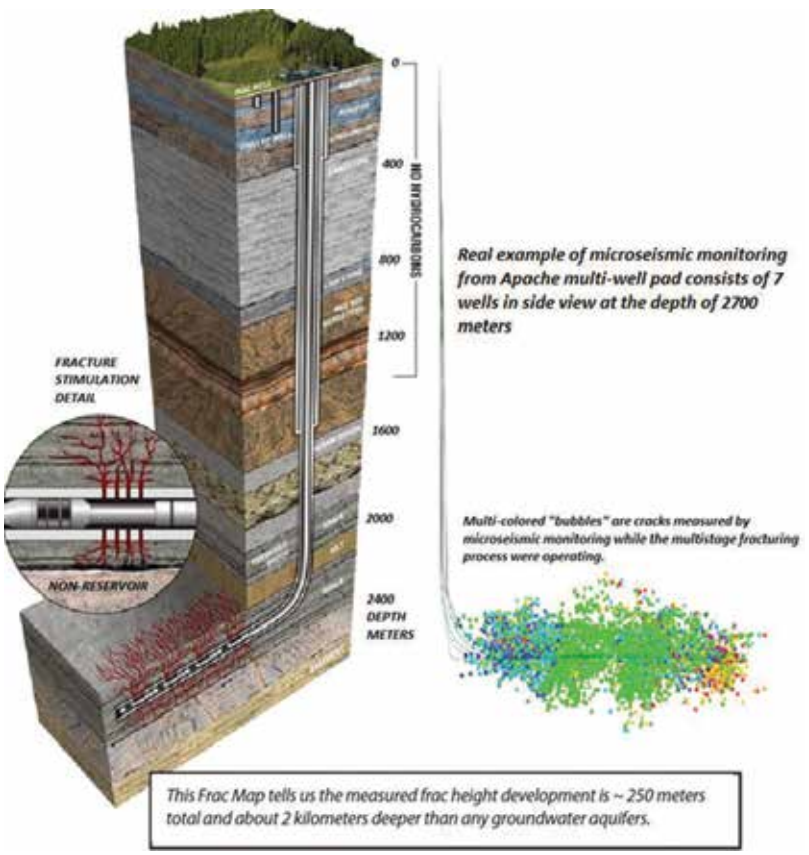

Figure 2. Horizontal well completions and multistage hydraulic fracturing (modified from: Apache Canada Ltd., Canadian Society for Unconventional Gas (CSUG)).

http://dx.doi.org/10.5772/intechopen.76542

2.4. Shale gas development

Natural gas will not willingly flow to any vertical well drilled through it because of low permeability of shales. The combination of horizontal well completions and multi-stage hydraulic fracture treatments have been crucial to the expansion of shale gas development. **Figure 2** illustrates the process of horizontal well completions and multistage hydraulic fracturing including microseismic events recorded during hydraulic fracturing operations. This technique is a necessary operation to complete the horizontal drilling technique since these wells have an extended horizontal leg section, and combining these two techniques can provide the effective stimulation of the reservoir. Previous to the successful application of these two technologies, similar resources in many basins were ignored because production was not considered economically feasible. The low natural permeability of shale has limited the production of gas shale resources because such low permeability allows only minor volumes of gas to flow naturally to a wellbore. This characteristic of low matrix permeability represents a key difference between shale and other gas reservoirs and must be surmounted for gas shales to be economically viable. The description of technologies essential for a successful shale gas extraction operation is outside the scope of this study.

3. Development in induced seismicity of shale gas

Large-scale fluid injections under high pressures can cause seismicity by reducing the effective normal stress on pre-existing discontinuities and causing them to slip. **Figure 3** illustrates the different mechanisms that create induced earthquakes. Induced earthquakes occur because of geomechanical changes in the reservoir because of the fracturing process [15–19]. Earthquakes may occur by increasing the excess pore pressure acting on a fault and/or by changing the shear and normal stress acting on the fault plane [20]. This phenomenon was

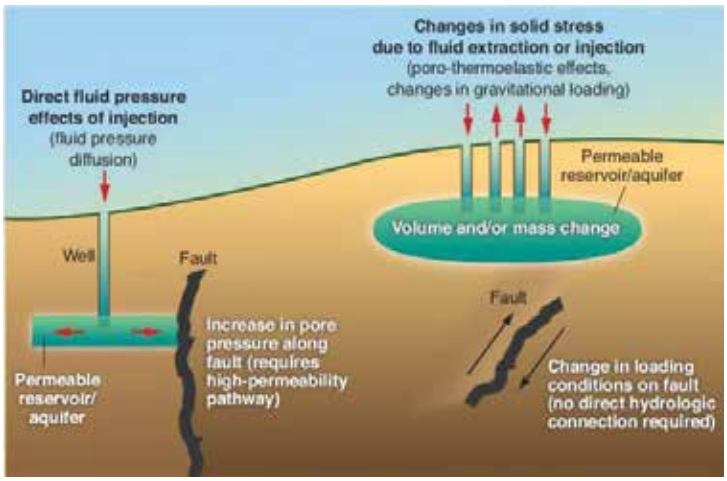

Figure 3. Different mechanisms cause induced earthquakes; earthquakes may be induced by increasing the pore pressure acting on a fault (left) or by changing the shear and normal stress acting on the fault (right) [20].

observed over half a century ago during Denver [21] and Rangely [22] experiments. Smaller-scale experiments later extended this conclusion to much smaller microseismic events, especially when clear evidence of a double-couple source was provided by fault-plane solutions [23, 24]. Seismicity refers to recorded earthquakes caused primarily by fault movement, which are typically events greater than 0.5 ML.

Induced Seismicity are earthquakes (events) resulting from human activity. Microseismic monitoring describes both the recording and processing of very low magnitude events produced by hydraulic fracturing. Typically, these events range from −3.0 to 0.5 ML. Hypocenter is the point within the earth where an earthquake starts. Hypocenters include both the horizontal surface location and depth of an event. Microseismic monitoring is a valuable tool for understanding the efficacy of hydraulic fracture treatments. The determination of event locations and magnitudes leads to estimations of the geometry of the fracture zone and the dynamics of the fracturing process. With sufficient resolution, the hypocenters may even reveal failure planes or other underlying structures controlling the distribution of events and interest petroleum engineers to test various hypotheses on fracture growth.

3.1. Induced microseismicity monitoring and its applications

Induced microseismic monitoring is a geophysical remote-sensing technology that gives the ability to detect and locate associated fracturing processes, which could be either in real-time or in post-processing mode. A typical field deployment involves installation of an array of continuously recording three-component geophones within an observational well(s) near the zone of interest, and/or a set of surface sensors. Besides the oil and gas industry application, which is relatively new, the seismological and mining research communities have developed microseismic monitoring technologies for years [25–27]. Microseismic monitoring aims to detect, locate, and describe the nature of microseismic events resulting from any geomechanical changes for caprock integrity, wellbore integrity and/or optimization of hydraulic fracturing in the oil and gas industry. When hydraulic fracturing monitoring and its optimization are the goals, microseismic events usually occur in large numbers within cloud-like distributions that imitate underlying fracture networks. This method allows monitoring of fracturing treatments in real-time with the aim of detecting the extent of the stimulated rock volume, and thus the success of the treatment. It can also lead to possible improvements in reservoir drainage. Oil and gas companies have set aside significant funds ($100's MM) for microseismic monitoring, but face extraordinary technological challenges to utilize the results in their full capacity. These challenges are consequences of inadequate insights of seismological and geomechanical processes associated with induced microseismicity.

3.2. Microseismic monitoring in shale gas development

There has been a growing number of reports about the application of microseismic techniques in Shale Gas reservoirs for characterizing fracture growth and geometry, as this technique is an established and reliable one for this purpose. Some studies have relied on surface equipment when seismicity was high enough to be recorded on the surface. However, the majority of cases are based on the use of downhole microseismic equipment that focuses on much

smaller events, which simply cannot be detected on surface due to attenuation. The Horn River Basin in northeastern British Columbia (BC) in Canada has hosted many pilot studies and research with regard to the development of Shale Gas reservoirs. Thousands of hydraulic fracturing operations have been performed in the area and anomalous seismicity has been observed in the last decade [28, 29]. The Canadian National Seismograph Network (CNSN) operative throughout Canada is designed to monitor large-scale seismicity and has a minimum magnitude detection limit of 2.0 ML.

The BC Oil and Gas commission [28] performed a comprehensive study on this phenomenon in three areas of the Horn River Basin. The investigation established that during the period of April 2009–December 2011, there was a link between events observed within remote and isolated areas of the Horn River Basin and hydraulic fracturing in the proximity of pre-existing faults. A local seismograph array was deployed for a couple of months within that period and recorded 19 events. A total of 38 events were analyzed. The events recorded ranged in magnitude between 2.2 and 3.8 ML on the Richter scale.

In the Etsho study area, hydraulic fracturing of Horn River Shales was performed in horizontal wells using multiple stages of slickwater fracturing, which consists of pumping a water-based fluid, chemicals, and proppant combination that has low-viscosity to increase the fluid flow. Microseismic monitoring showed that fracture growth was confined to the target shale layers. Hydraulic fracturing operations in the February 2007 to July 2011 period involved 14 different pads and 90 wells with more than 1600 hydraulic fracturing stage completion operations [28].

As a result of the previous study, eight new seismograph stations were added to the existing two of the CNSN in the area. The new investigation focused on the Montney Trend of BC that represents over a third of the province's recoverable natural gas reserves [29] under development since mid-2000s. The area has seen thousands of horizontal gas wells and hundreds of wastewater disposal wells. CNSN recorded 231 events attributed to gas and oil activities in the area from August 2013 to October 2014. Hydraulic Fracturing operations were at the root of 193 of these events that were in the range 1.0–4.4 ML. Wastewater disposal was the cause of 38 events in the 1.2–2.9 ML. The study period covered about 7500 hydraulic fracturing stages. Only 11 were felt on the surface without causing any damage on the surface. No loss of wellbore containment was observed either. **Figure 4** shows the comparison between wastewater disposal-induced seismicity and hydraulic fracturing ones. The investigation confirmed that the mechanism at the root of observed seismicity was the reactivation of pre-existing faults due to increasing pore pressure due to fluid injection. It also demonstrated the critical importance of a dense array in understanding induced seismicity. Moreover, some active faults could be precisely delineated that can be crucial in risk assessment and mitigation of this phenomenon.

The Marcellus Shale formation in Greene County Pennsylvania was subject to a comprehensive investigation of induced seismicity using six horizontal gas wells [30]. The objectives were to find the maximum fracture height in hydraulic fracturing operations and to determine if any natural gas or fluids had migrated upward to an overlying gas field 3800 ft above. The investigation included microseismic monitoring using vertical geophone arrays, gas pressure

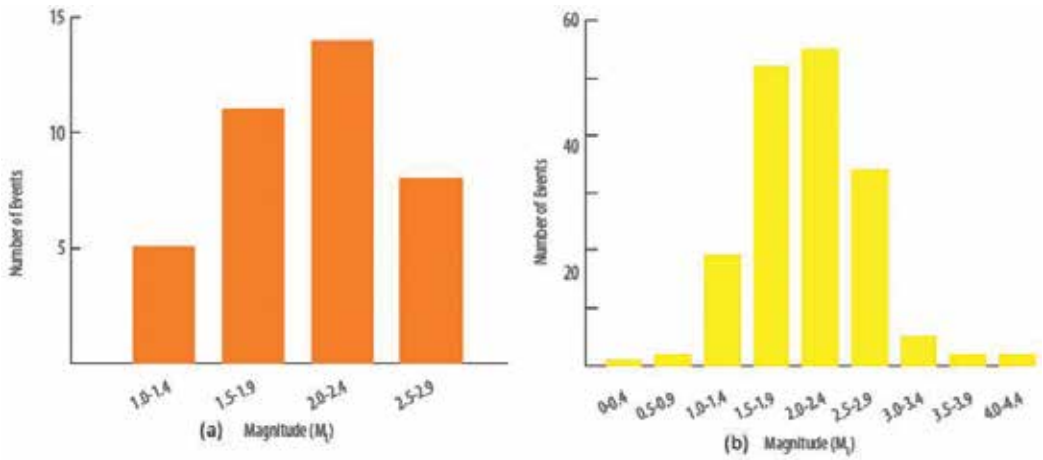

Figure 4. Number of events versus magnitude for (a) wastewater disposal wells induced events, (b) hydraulic fracture induced events (modified from: BC Oil and Gas Commission [29]).

and production histories of three wells, chemical and isotopic analyses of produced gas from seven wells, and monitoring for perfluorocarbon traces of gas from two wells [30]. The findings showed no evidence of gas migration from Marcellus Shale and no evidence of brine migration from this formation. It was demonstrated that the impact of hydraulic fracturing operations did not extend to the overlying shallower gas field and no detectable gas or fluid migration took place in that formation.

Seismicity (M > 3) observed in the Western Canada Sedimentary Basin in the 1985–2015 period has been investigated recently by Atkinson et al. [31]. This basin is where most of Canada's shale gas developments are concentrated. The data set included seismicity induced by hydraulic fracturing, wastewater disposal and production. Both seismicity rates and the number of hydraulic fracturing wells rose sharply between 2010 and 2015, and more than half of all seismicity occurred in close proximity of hydraulic operations in both time and space [31]. The authors pointed out that hydraulic fracturing is responsible for a larger proportion of observed seismicity rather than wastewater injection operations. They also noted that their findings are markedly in contrast with those from similar studies focused on the Central United States where wastewater injections were responsible for most of the induced seismicity. McGarr [32] proposed a linear equation, and it shows the maximum seismic moment as a function of total volume of liquid injected up to the time of the largest induced earthquake. For most of case histories mentioned here, magnitude exceeds the maximum bounds provided by the McGarr relation as shown in **Figure 5**. For many of the events above the McGarr line, it has been proven that use of the maximum volume value might just allow the point to come beneath the line. However, two events are clearly above the line, even with the combination of the maximum volume and the minimum magnitude; these are the August 2014 M 4.4 and August 2015 M 4.6 events near Fort St. John [29, 33–35].

Ellsworth [20] has reviewed many cases of induced seismicity reported previously and points out that seismic activity in the central and eastern United States has increased dramatically

http://dx.doi.org/10.5772/intechopen.76542

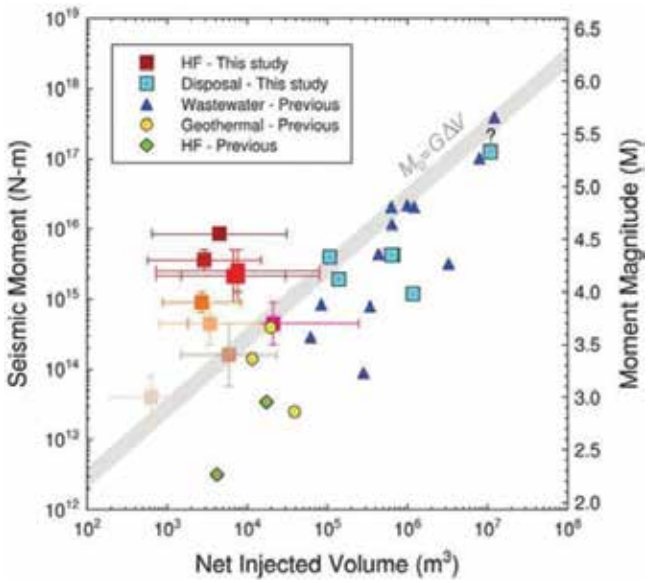

Figure 5. Seismic moment versus net injected volume from Atkinson et al. [31]. The authors have shown their own results (squares) and those from previous studies. The gray band shows the maximum magnitude predicted by McGarr [32] for shear modulus G in the range 20–40 Gpa.

in the recent past. Ellsworth relates this observation to cases of hydraulic fracturing and disposal of wastewater injected in deep wells. The mechanics of this phenomenon is analyzed and described. The intimate relationship between the development of unconventional gas fields and new technologies are well explained, and many cases are enumerated. The author pointed out the importance of well documenting the specifics of each operation in the ability to get to the root of the observations and described how important that was in the case of pioneering experiments of Denver and Rangely mentioned above. A case study of microseismic imaging of hydraulic fracturing in the Barnett shale gas reservoir in Texas demonstrated some complications about the use of microseismic results in reservoir simulations [36].

While the technology is mature and well established when dealing with detecting fracture geometry and growth, the author states that the disability of the technique in distinguishing between seismicity induced by fracture opening and closing. In addition, more detailed information about the fracturing process and mechanism need to be implemented in order to make the technique more valuable for reservoir management.

Zeng et al. [37] describe results from a multi-stage hydraulic fracturing experiment carried out in a horizontal well of a shale gas reservoir using a surface broadband 3C seismic array. They state that it is possible to detect and locate small events ($M < -1$) with a relatively sparse array, particularly for shallow reservoirs. Their focal mechanism analysis of the observed seismic activity was consistent with the regional stress field. The seismicity formed into two clusters; one fell into a small volume surrounding the horizontal well, and another group fell 500 m away from the well. Both groups of events showed similar properties in their focal mechanisms. The authors point out that in order to reduce the hazard of such operations, a

better understanding of the pre-existing fractures, the tectonic stress regime in the region, and appropriate design and management of the injection operation would be necessary.

A combination of surface and downhole sensors were used to monitor microseismic activity associated with hydraulic fracturing of a shale gas reservoir in China [38]. The results were used in real-time to optimize pre-pad fluid parameters, perforation and temporary additive releasing time to optimize fracturing operation. The authors mentioned that the average shale gas production's rate was increased 2–5 times through optimization using real-time microseismic monitoring, and they could prove the benefit of using this technique by later production tests, too. The real-time results played a vital role in the immediate evaluation and optimization of fracture parameters. The gas field under study is the largest commercially available shale gas field in the world outside North America. Another study conducted by Yaowen et al. [39] built further on the success of the previous paper and provides guidelines for the optimization of fracturing parameters at the later stage.

Kaka et al. [40] presented the results of the microseismic monitoring of a multistage stimulation experiment of a shale gas reservoir in Saudi Arabia. A string of 12 3C-sensors with 30.5 m spacing was used, and a total of 415 events were recorded. The objective of the study was to better understand fracture growth during the operation and the role of pre-existing fractures in the process. No changes were observed in the direction of local stresses along the treatment well. Significant changes in total length and aspect ratio (length/width) of the fracture induced in different stages have been observed. The authors enumerated parameters that may have had a role in this observation such as in situ fracturing, local rock heterogeneity or the influence of the treatment parameters. The conclusion made from their observations was that early and late stages of stimulation show the longest fracture networks, with events induced further away from the initiation point. They did not find any immediate relationship between treatment parameters (peak pressure and pumping rate) and fracture extension. Sensitivity analysis using the Monte Carlo simulation method was attempted to clarify location uncertainties. The results of these simulation methods show a higher location uncertainty for events located at the early stages, consequently restrained interpretation from monitored seismicity in the early stages. One of the main purposes of their study was to develop a methodology for generating dynamic, high-resolution seismic and geomechanical models of shale reservoirs before, during and after stimulation, and interpreting the models regarding fracture susceptibility and fracture dynamics.

3.3. Emerging trends

The abundance of applications of microseismic monitoring in gas reservoirs in recent years and the high quality of collected 3C data have been accompanied by attempts to extract more detailed information about the fracturing process from recorded signals. The basic motivation of these attempts, understandably, has to do with the need to reduce production expenses. Hence, application of new seismic techniques that can actually help achieve this objective through increasing the efficiency of production and rate of production has been welcome. In this section, we enumerate some of such initiatives presented in recent years. The list is not in any way exhaustive, but it is a sample of recent efforts in this regard.

http://dx.doi.org/10.5772/intechopen.76542

Application of seismic moment tensor inversion techniques is one promising trend in the analysis and interpretation of microseismicity related to shale gas reservoirs. The technique is fundamentally superior to fault plane solution determination in that it does not include a priori assumption about the mechanism of failure. It allows, in simple terms, for the source mechanism to be decomposed into three components: a double-couple component that is expected to be of a pure shear failure source, an isotropic component that can be described as an explosive or implosive source, and the so-called compensated linear vector dipole (CLVD) [25].

Baig and Urbancic [41] have presented a case of such studies for a collection of 147 microseismic events recorded during a fracture treatment using three borehole arrays. The authors have adopted the method of Gephart and Forsyth [42], originally applied to California earthquakes, to their microseismic data by considering the double-couple approximations of their moment tensors. The idea is that seismic moment tensor is a symmetric second-order tensor with six independent components. Mapping the total amplitudes of the P, S_V, and S_H phases to the focal sphere surrounding the source should determine this tensor. For monitoring hydraulic fractures, at least two linear borehole arrays non-coplanar with the event are required for identifying the full resolution of all six independent components of the tensor. These six independent components include three geometric parameters controlled by the orientation of the fracture and the sense of slip on; one parameter is the total seismic moment, the second is to control the relative strength of the double-couple, and the last using compensated linear vector dipole and isotropic components [41]. **Figure 6** illustrates the radiation patterns from various failure mechanisms according to different crack modes.

Using the algorithm proposed by Gephart and Forsyth [42] and considering the double-couple approximations of the seismic moment tensors, Baig and Urbancic [41] could invert the measured strain axes in the treatment zone represented by the seismic moment tensors for the stress regime that best fits these events. Each suit of results provides a set of P (pressure) and T (tension) axes,

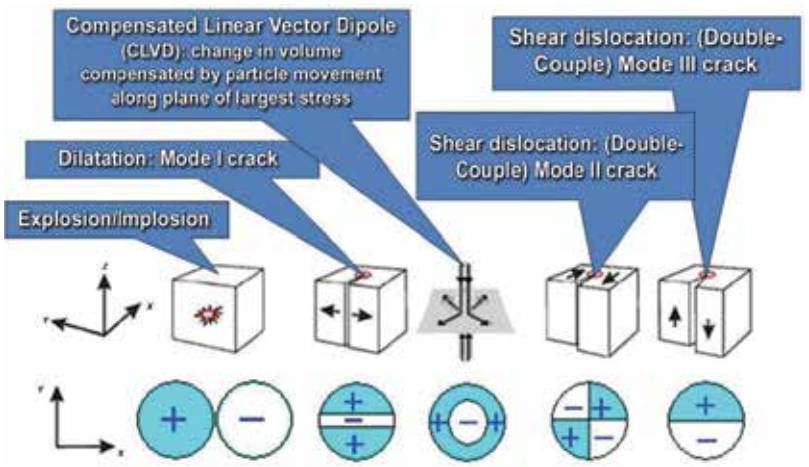

Figure 6. Different modes of failure create various moment tensors visualized by the beach ball diagrams, which are stereographic projections of the P-wave radiation patterns over the focal sphere [41].

just like for a focal mechanism plot. Then they search for an in-situ stress field that minimizes the total rotation required for the strain axes for the data set at hand. The results showed distinct differences among different stages of fracturing. For instance, **Figure 7** shows the locations and moment tensor solution for 147 events recorded in the study using three borehole arrays during one hydraulic fracturing operation. According to this figure, the events fall along a vertical plane trending N40°E and the presence of a variety of mechanisms, suggesting that the events cannot be categorized as simple shear failures but consist of volumetric components of failure.

Urbancic and Mountjoy [43] also reported the results of the moment tensor inversion. The former have applied the technique to two distinct microseismic clusters observed during production cycles of two wells with remarkably different types of source mechanism. They attribute this difference to changes observed in fracture types, which became active and production methods. The latter applied the technique to a microseismic data set recorded at a shale gas reservoir in order to estimate fracture planes and orientations, volumetric strain, crack movements and timing and relationships with pumping operations.

Norton et al. [44] have used Amplitude Variation with Offset (AVO) inversion to estimate elastic properties and fault mapping to identify potential barriers that could affect fracture propagation in a shale gas reservoir. They argued that by correlating the results of the two techniques in parallel could provide valuable information about the local heterogeneity within the reservoir and the effect on the fracture simulation programs. Xu et al. [45] presented results of microseismic monitoring of hydraulic fracturing simulation in a tight sand reservoir. They stated that although the use of a single well has been widely adopted, much better results could be obtained with a dual-well set up regarding fracture delineation and location accuracy. Both surface and downhole microseismic equipment have been employed to monitor a shale gas field in China [39]. The results helped to evaluate reservoir stimulation in order to optimize fracturing operation.

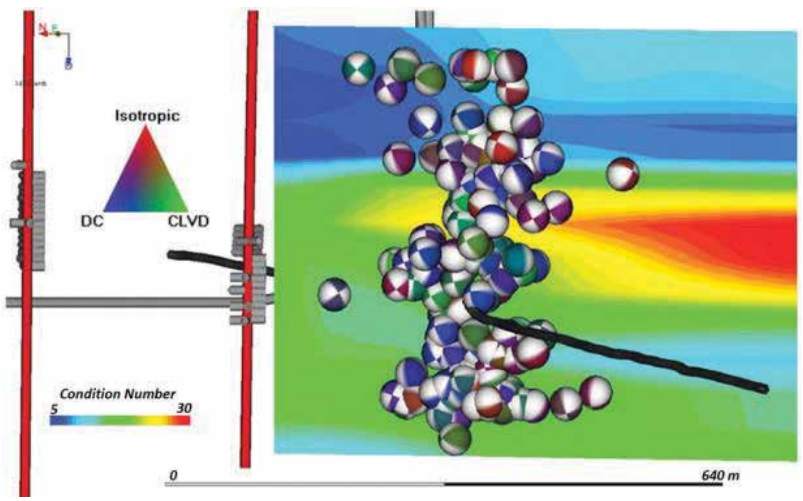

Figure 7. The moment tensors for 147 events plotted with the condition number that determines how well one can invert for the mechanism of the event [41].

Xu et al. [45] studied the hydraulic fracturing stimulation using microseismic monitoring of two wells simultaneously in low porosity and low permeability formation in Ordos basin with the aim of improving fracture geometry and optimization of good placement. Comparing with single-well microseismic monitoring, they concluded that the dual-well technique could explain features in far more precise details and accuracy and then subsequently can reduce uncertainty. Maxwell and Norton [46–48] discussed a case study on Montney formation (NE British Columbia, Canada) with the focus on integrating the microseismic data with the available geotechnical/geomechanical resources. They concluded that the combination of this data could provide valuable information to deeper insights about hydraulic fracturing behavior, optimal hydraulic fracturing geometry, and optimal production rates. In general, it leads to more optimized completion design with closer perforation clusters and increased reservoir contact in future wells.

One of the most controversial discussions in shale gas development is the interaction between natural fractures in fractured shale reservoirs and hydraulically induced fractures resulting from multi-stage hydraulic fracturing. In general, three main scenarios describe the interaction between these two sets of fractures. When a fracture has been created by the hydraulic fracturing method, the propagation of that induced fracture may cross a natural fracture without any change in propagation direction, terminate against a natural fracture and then continues to propagate along the natural fracture, or terminate and then open the natural fracture, as new fractures initiate from the natural fracture. Huang et al. [49] conducted a comprehensive study coupling a geomechanic-microseismic model using numerical simulation. They have run the model under different situations such as various fracture intensities, different number and orientation of fracture sets, hydraulic-natural fracture crossing versus arrest scenarios, and various frictional properties for the natural fractures for two horizontal wells from the Barnett Shale. They concluded that the number and orientation of fracture sets, fracture frictional properties, wellbore orientation, and fracture spacing/intensity are the governing factors influencing complex fracture network geometry, reactivation patterns, and synthetic microseismic events.

Rutqvist et al. [50] studied the reactivation of natural fractures and faults and induced microseismicity regarding hydraulic fracturing operations in shale gas reservoirs. They developed and conducted three-dimensional coupled fluid-flow and geomechanical modeling of fault activation where a horizontal injection well intersects a steeply dipping fault. A three-hour hydraulic fracture operation was modeled, and the results indicated that shale-gas hydraulic fracturing along faults would not likely induce seismic events that could be felt on ground surface. The results indicated several small microseismic events, as well as aseismic deformations along with the fracture propagation. The magnitudes of the created events ranged from −2.0 to 0.5, excluding one case regarding a very brittle fault with low residual shear strength for which the magnitude was 2.3, an event that would possibly go unrecognized or might be felt by humans at its epicenter. A dependency on injection depth and fault dip was found after conducting sensitivity analyses on various parameters such as injection depth, fault dip, and slip-weakening model parameters. That dependency could be attributed to the variation of the shear stress on the fault plane and the variation of stress during the reactivation process. The plastic zone, according to the results, expanded up to 200 m from the injection well at the end of the hydraulic fracturing operation.

Shahid et al. [51] did an inclusive review on numerical simulation analyses and strategies using commercial codes or developing new specific codes for modeling hydraulic fracturing, the natural fracture reactivation, and induced microseismicity associated with either hydraulic fracturing operation itself or the interaction between hydraulically induced fractures and natural fractures and discontinuities. There are different numerical models to use for this purpose according to the assumption/s of the studies. For example, there are different approaches depending on the 2D or 3D assumption, or considering media under study as continuous or discontinuous media. It is obvious that if the interaction between a natural fracture and an induced one is the subject of the study, the DFN (discrete fracture network) must be considered. In term of shale gas reservoir modeling, there are plenty of "unknown unknowns," and there is a certain number of "known unknowns." The "known facts" are the best place to start with to come up with general ideas accepted by professionals and experts. One of the known facts is that shale is naturally fractured and another one is that the induced hydraulic fractures will open and activate these existing natural fractures.

In some recent publications and presentations, the concept of Stimulated Reservoir Volume (SRV) has been connected to microseismic. It is proposed that by gathering and interpreting microseismic data and detecting microseismic events in a shale well subjected to multistage hydraulic fracturing, the size of the stimulated reservoir volume can be estimated. Shreds of evidence that dispute them equally counter the amount of evidence supporting such claims [52]. Furthermore, it has been proven that misinterpreting the size of the Stimulated Reservoir Volume can result in substantial inconsistencies in predicting the potential of a well [52].

As another application of induced seismicity monitoring in the oil and gas industry, wellbore integrity in shale gas development can be considered as an outcome of using that technology as it has been long used for Cyclic Steam Stimulation (CCS) projects to observe, detect, and locate casing failure or slip due to steam injection in thermal oil recovery operations [53–55].

4. Discussion

Shale gas exploitation is no longer an inefficient operation with the availability of improved technology, as the demand and preference for this clean form of hydrocarbon have made Shale Gas an energy in order. The production and development of shale gas from one reservoir to another around the world are swiftly increasing. Real-time monitoring of microseismic events allows optimizing the hydraulic stimulation process by modifying the fracture stage design while pumping into the formation. Recording micro-seismic events to monitor rock fracturing in 3D space and time during the stimulation process allows one to confirm the rock volume and formation geometry being stimulated. As a result, future well placement and completion designs can be optimized for cost-effective drainage of unconventional reservoirs. The technological advances that led to the initial exploitation of shale gas reservoirs, namely horizontal drilling and multi-stage fracture stimulations, were not entirely new to the industry. This supports the concept that advanced technologies must be aligned with in-depth knowledge and understanding of the potential and possible challenge/s for best outcomes.

The increased application of micro-seismic monitoring in the field of shale gas exploitation seems like an obvious technology to complement fracture stimulation treatments.

Microseismic monitoring of fracture stimulations has seen huge growth in the past decade, in line with the increase in shale gas development activity. Although the technology is not new, monitoring of microseismic events has been used in mine safety monitoring for years. It is still a relatively new technique in the oil and gas industry, and in some ways, not an entirely developed technology. Although it is a comparatively simple method to detect microseismic events, to locate them correctly in the subsurface is not an easy task. The aim of many current advanced seismic developments is to use the clustering of microseismic events and their character/attributes to evaluate the volume of stimulated rock and compare it to the volume of pumped fracturing fluids.

An extensive review of new technologies developed to monitor induced microseismicity has been carried out. The application of these technologies and their impact on shale gas development have been reviewed in this article.

Author details

Nadia Shafie Zadeh* and Shahriar Talebi

*Address all correspondence to: nadia.shafiezadeh@canada.ca

Natural Resources Canada (NRCan), Ottawa, Canada

References

[1] Bustin RM. Geology Report: Where are the High-potential Reigns Expected to be in Canada and the U.S. Capturing Opportunities in Canadian Shale Gas, Second Annual Shale Gas Conference, the Canadian Institute, Calgary; Jan 31-Feb 1 2006

[2] Bustin AMM, Bustin RM, Cui X. Importance of fabric on production of gas shales. In: Proceedings of the Unconventional Gas Conference SPENO: 114167; Keynote, Colorado; Feb 10-12, 2008. p. 29. DOI: 10.2118/114167-MS

[3] Martini AM, Nusslein LM, Petsch ST. Enhancing microbial gas from unconventional reservoirs: Geochemical and microbiological characterization of methane-rich fractured black shales. Final report, No: R-520, GRI-05/0023, Research Partnership to Secure Energy for America, Washington, DC. 2004. pp. 1-8

[4] Shurr GW, Ridgley JR. Unconventional shallow gas biogenic systems. American Association of Petroleum Geologists Bulletin. 2002;**86**(11):1939-1969

[5] ASTM D7708-11, Standard Test Method for Microscopical Determination of the Reflectance of Vitrinite Dispersed in Sedimentary Rocks

[6] ASTM D2798-99, Standard Test Method for Microscopical Determination of the Reflectance of Vitrinitein a Polished Specimen of Coal

[7] Speight JG. Shale Gas Production Processes. Gulf Professional Publishing. 2013. p. 162. DOI: 10.1016/B978-0-12-404571-2.00005-4. ISBN: 978-0-12-404571-2

[8] Faraj B, Williams H, Addison G, McKinstry B. Gas Potential of Selected Shale Formations in the Western Canadian Sedimentary Basin, Gas TIPS. Vol. 10(1). Houston, TX: Hart Energy Publishing; 2004. pp. 21-25

[9] Chan JC, Kroese DP. Efficient estimation of large portfolio loss probabilities in t-copula models. European Journal of Operational Research. 2010;**205**(2):361-367. DOI: 10.1016/j.ejor.2010.01.003

[10] Davies DK, Bryant WR, Vessell RK, Burkett PJ. In: Bennett RH, Bryant WR, Hulbert MH, editors. Microstructure of Fine-Grained Sediments: From Mud to Shale. New York: Springer-Verlag; 1991. pp. 109-119

[11] Pemberton GS, Gingras MK. Classification and characterizations of biogenically enhanced permeability. AAPG Bulletin. 2005;**89**:1493-1517

[12] Walser DW, Pursell DA. Making mature shale gas plays commercial: Process and natural parameters. In: Society of Petroleum Engineers, Eastern Regional Meeting; Lexington, Kentucky, USA; October 17-19. 2007. SPE-110127. DOI: 10.2118/110127-MS

[13] Cramer DD. Stimulating unconventional reservoirs: Lessons learned, successful practices, areas for improvement. In: Unconventional Gas Conference; Keystone; February 10-12, 2008. Society of Petroleum Engineers, SPE-114172. DOI: 10.2118/114172-MS

[14] Tinker SW, Potter EC. Unconventional gas research and technology needs. In: Society of Petroleum Engineers R&D Conference: Unlocking the Molecules; April 26-27; San Antonio, Texas. Available from: www.spe.org/spe-app/spe/meeting/RDC/2007/tech_program.htm

[15] Pearson C. The relationship between microseismicity and high pore pressure during hydraulic stimulation experiments in low permeability granitic rocks. Journal of Geophysical Research. 1981;**B9**:7855-7864. DOI: 10.1029/JB086iB09p07855

[16] Warpinski NR, Wolhart SL, Wright CA. Analysis and prediction of microseismicity induced by hydraulic fracturing. SPE Journal. 2004;**9**(1):24-33. DOI: 10.2118/87673-PA

[17] Warpinski N. Microseismic monitoring: inside and out. Journal of Petroleum Technology. 2009:**61**(11):80-85. SPE-118537-JPT. DOI: 10.2118/118537-JPT

[18] Warpinski N. Understanding hydraulic fracture growth, effectiveness, and safety through microseismic monitoring. In: Bunger AP, McLennan J, Jeffrey R, editors. Effective and Sustainable Hydraulic Fracturing. 2013. DOI: 10.5772/55974. ISBN: 978-953-51-1137-5

[19] McGarr A, Simpson D, Seeber L. 40 case histories of induced and triggered seismicity. In: Lee WHK, Jennings P, Kisslinger C, editors. International Handbook of Earthquake and Engineering Seismology. Vol. 81(A). 2002. pp. 647-661

[20] Ellsworth WL: Injection-induced earthquakes. Science. 2013;**341**(6142):8. DOI: 10.1126/science.1225942

[21] Healy JH, Rubey WW, Griggs DT, Raleigh CB. The Denver earthquakes. Science. 1968;**161**(3848):1301-1310. DOI: 10.1126/science.161.3848.1301

[22] Raleigh CB, Healy JH, Bredehoeft JD. Faulting and Crustal Stress at Rangely, Colorado, in Flow and Fracture of Rocks. Washington, DC: American Geophysical Union; 1972. pp. 275-284. DOI: 10.1029/GM016p0275

[23] Cash D, Homuth EF, Keppler H, Pearson C, Sasaki S. Fault plane solutions for micro-earthquakes induced at the Fenton Hill hot dry rock geothermal site: Implication for the state of stress near a quaternary volcanic center. Journal of Geophysical Research Letters. 1983;**10**:1141-1144. DOI: 10.1029/GL010i012p01141

[24] Talebi S, Cornet FH. Analysis of the microseismicity induced by a fluid injection in a granitic rock mass. Journal of Geophysical Research Letters. 1987;**14**:227-230. DOI: 10.1029/GL014i003p00227

[25] Gibowicz SJ, Kijko A. An Introduction to Mining Seismology. Academic Press; 1994. p. 404. ISBN: 0-12-282120-3

[26] Bolt BA. Inside the Earth: Evidence from Earthquakes. San Francisco: W.H. Freeman& Company; 1982. 191 p

[27] Stein S, Wysession M. An introduction to Seismology, Earthquakes, and Earth Structure. Wiley-Blackwell; 2003. 498 p. ISBN-10: 0865420785

[28] B.C. Oil and Gas Commission. Investigation of Observed Seismicity in the Horn River Basin. 2012. p. 29. Available from: ogc.communications@bcorg.ca

[29] B.C. Oil and Gas Commission. Investigation of Observed Seismicity in the Montney Trend. 2014. p. 32. Available from: ogc.communications@bcorg.ca

[30] US Department of Energy. An Evaluation of Fracture Growth and Gas/Fluid Migration as Horizontal Marcellus Shale Gas Wells are Hydraulically Fractured in Greene County, Pennsylvania, Office of Fossil Energy, NETL-TRS-3-2014. 2014. Available from: http://www.netl.doe.gov/File%20Library/Research/onsite%20research/publications/NETL-TRS-3-2014_Greene-County-Site_20140915_1_1.pdf

[31] Atkinson GM, Eaton DW, Ghofrani H, Walker D, Cheadle B, Schultz Shcherbakov R, Tiampo K, Gu J, Harrington RM, Liu Y, van der Baan M, Kao H. Hydraulic fracturing and seismicity in the Western Canada sedimentary basin. Seismological Research Letters. 2016;**87**(3):17. DOI: 10.1785/0220150263

[32] McGarr A. Maximum magnitude earthquakes induced by fluid injection. Journal of Geophysical Research, Solid Earth. 2014. DOI: 10.1002/2013JB010597

[33] B.C. Oil and Gas Commission. Fracturing (fracing) and disposal of fluids fact sheet. 2010. http://www.bcogc.ca/documents/publications/Fact%20Sheets/Fracturing_and_Disposal_of_Fluids_FINAL.pdf

[34] B.C. Oil and Gas Commission. Safety Advisory 2010: Communication during fracture stimulation. http://www.bcogc.ca/documents/safetyadvisory/SA%20201003%20Communication%20During%20Fracture%20Stimulation.pdf

[35] B.C. Oil and Gas Commission. Water Use in Oil and Gas Activities. Victoria (BC); 2012

[36] Abdulaziz AM. Microseismic imaging of hydraulically induced-fractures in gas reservoirs: A case study in Barnett shale gas reservoir, Texas, USA. Open Journal of Geology. 2013;**3**:361-369. DOI: 10.4236/ojg.2013.35041

[37] Zeng X, Zhang H, Zhang X, Wang H, Zhang Y, Liu Q. Surface microseismic monitoring of hydraulic fracturing of a shale-gas reservoir using short-period and broadband seismic sensors. Seismological Research Letters. 2014;**85**(3). DOI: 10.1785/0220130197

[38] Furong W, Yuanyuan Y, Chen Y. Real-time microseismic monitoring technology for hydraulic fracturing in shale gas reservoirs: A case study from the Southern Sichuan Basin. Natural Gas Industry B. 2017;**4**:68-71. DOI: 10.1016/j.ngib.2017.07.010

[39] Yaowen L, Rugang L, Yuan Z, Dongwei G, Huaili Z, Ting L, Chi Z. Application of surface-downhole combined microseismic monitoring technology in the Fuling shale gas field and its enlightenment. Natural Gas Industry B. 2017;**4**:62-67. DOI: 10.1016/j.ngib.2017.07.009

[40] Kaka SI, Reyes-Montes JM, Al-Shuhail A, Al-Shuhail AA, Jervis M. Analysis of microseismic events during a multistage hydraulic stimulation experiment at a shale gas reservoir. In: Petroleum Geoscience. The Geological Society of London for GSL and EAGE; 2017. p. 10. DOI: 10.1144/petgeo2016-086

[41] Baig A, Urbancic T. Microseismic moment tensors: A path to understanding frac growth. Special Section: Microseismic, Engineering Seismology Group Canada. 2010;**29**(3):320-342. DOI: 10.1190/1.3353729

[42] Gephart J, Forsyth DW. An improved method for determining the regional stress tensor using earthquake focal mechanism data: An application to the San Fernando earthquake sequence. Journal of Geophysical Research, Solid Earth. 1984;**89**(B11):9305-9320. DOI: 10.1029/JB089iB11p09305

[43] Urbancic T, Mountjoy K. Microseismic Monitoring: Increases Efficiency and Performance In Liquids-Rich Plays, The "Better Business" Publication Serving the Exploration/Drilling/Production Industry. The American Oil and Gas Reporter, Special Report: Reservoir Characterization. 2011. Reproduced for ESG Solutions with permission from The American Oil & Gas Reporter. Available from: www.aogr.com

[44] Norton M, Hovdebo W, Cho D, Maxwell S, Jones M. Integration of surface seismic and microseismic for the characterization of a shale gas reservoir. CSEG Recorder, Official Publication of the Canadian Society of Exploration Geophysicists. 2011;**36**:01

[45] Xu Y, Mu L, Yang XG, Zhao W, Wang X, Lim TK, Li Y. Understating tight oil reservoir hydraulic fracturing stimulation using two wells simultaneous microseismic monitoring approach. In: International Petroleum Technology Conference; 26-28 March 2013; Beijing, China, IPTC: 16529-MS. DOI: 10.2523/IPTC-16529-MS

[46] Maxwell SC, Norton M. Enhancing shale gas reservoir characterization using hydraulic fracturing microseismic data. Unconventional and CCS. 2012;**30**:7. Available from: 2012 EAGE, www.firstbreak.org

[47] Maxwell SC. Microseismic hydraulic fracture imaging; the path toward optimizing shale gas production. The Leading Edge. 2011;**30**(3):340-346. DOI: 10.1190/1.3567266

[48] Maxwell SC. Microseismic: Growth born from success. The Leading Edge. 2010;**29**(3): 338-343. DOI: 10.1190/1.3353732

[49] Huang J, Safari R, Mutlu U, Burns K, Geldmacher I. Natural-Hydraulic Fracture Interaction: Microseismic Observations and Geomechanical Predictions, Unconventional Resources Technology Conference; 25-27 August, 2014; Colorado, USA, URTeC: 1921503. DOI: 10.1190/INT-2014-0233.1

[50] Rutqvist J, Rinaldi AP, Cappa F, Moridis GJ. Modeling of fault activation and seismicity by injection directly into a fault zone associated with hydraulic fracturing of shale-gas reservoirs. Journal of Petroleum Science and Engineering. 2015;**127**:377-386. DOI: 10.1016/j.petrol.2015.01.019

[51] Shahid ASA, Fokker PA, Rocca V. A review of numerical simulation strategies for hydraulic fracturing, natural fracture reactivation and induced microseismicity prediction. The Open Petroleum Engineering Journal. 2016;**9**(Suppl-1, M5):72-91. DOI: 10.2174/1874834101609010072

[52] Mohaghegh SD. Shale Analytics, Data-Driven Analytics in Unconventional Resources. Springer International Publishing; 2017. DOI: 10.1007/978-3-319-48753-3. ISBN 978-3-319-48751-9

[53] Talebi S, Nechtschein S, Boone TJ. Seismicity and casing failure due to steam stimulation in oil sands. Pure and Applied Geophysics. 1998;**153**(1):219-233

[54] Talebi S, Boone TJ, Eastwood JE. Injection induced microseismicity in Colorado shales. Pure and Applied Geophysics. 1998;**153**(1):95-111

[55] Boone TJ, Nechtschein S, Smith R, Youck D, Talebi S. Microseismic monitoring for fracturing in the Colorado Shales above a thermal oil recovery operation. In: 37th US Rock Mechanics Symposium, ARMA-99-1069; 1999, June 6-9. p. 10

Chapter 2

Unconventional Resources of Shale Hydrocarbon in Sumatra Basin, Indonesia

Abdul Haris, Agus Riyanto, Bayu Seno,
Husein Agil Almunawar, Martogu Benedict Marbun,
Iskandarsyah Mahmudin and Prima Erfido Manaf

Additional information is available at the end of the chapter

http://dx.doi.org/10.5772/intechopen.75600

Abstract

Sumatra Basin is the largest hydrocarbon producer in Indonesia, which was produced from North Sumatra, Central Sumatra and South Sumatra Basins. Looking at the large accumulation of hydrocarbons that have been produced from Sumatra Basin, it opens the possibility of hydrocarbon potential, which is trapped in shale source rock. The integrated study, which includes geochemical, geomechanical, petrophysical and geophysical analysis, was performed to assess shale reservoir in Sumatra Basin. The geochemical assessment of the Baong formation of North Sumatra Basin show that the total organic content (TOC) ranges from 2 to 3.5 wt.% and is categorized into fair to very good. The geophysical and geomechanical assessment shows the shale layer is indicated by an acoustic impedance, which is higher than 2490 ft/s*g/cc, with rock strength of 3000 Psi and the brittleness index of 0.48. In Central Sumatra Basin, we assessed Brownshale of Pematang formation. The geochemical analysis shows that the Brownshale has TOC ranges from 0.15 to 2.71 wt.%, which can be categorized into poor to very good. In South Sumatra Basin, we focused on Talang Akar formation (TAF). The geochemical result shows that the TOC ranged from 0.35 to 3.66 wt.% and is categorized into poor to very good.

Keywords: hydrocarbon shale, integrated geochemical, geomechanical, petrophysical and geophysical, Sumatra basin

1. Introduction

Sumatera is the most productive island for oil and gas production coming from three major basins, that is, North, Central and South Sumatra Basin. However, today's production of oil

and gas has been depleted because many fields have been reaching the maximum of recovery factor. Exploration activities are intensified to increase the potential of new oil and gas. The potential of oil and gas originating from the unconventional reservoir is potentially observed. The geological agency report showed the total potential of shale gas reserves in Sumatra Island reached 233 trillion cubic feet (TCF) [1]. This enormous resource has yet to be developed.

Understanding the characteristics of the shale hydrocarbons is very important, particularly the characteristic that is related to in situ parameters of the shale hydrocarbons. The organic richness of shale layer is represented by total organic carbon (TOC). The potential shale gas is commonly presented by TOC > 2 wt% [1], while for shale oil is indicated by TOC > 1 wt% [2]. The shale maturity is represented by vitrinite reflectance (Ro), which commonly ranges from 1.1 to 1.4% for shale gas [1] and from 0.6 to 1.1% for shale oil [2].

The productivity of shale hydrocarbon is influenced by shale layer thickness, which is related to the technical strategy in producing hydrocarbon. The shale layer thickness of shale gas should be higher than 30 meters [1], while shale oil's must be higher than 15 meters [3]. The last parameter that should be considered is the depth of shale reservoir, which is related to overpressure conditions. The potential depth is in the depth range of 1000–5000 m [1]. In addition, **Table 1** shows a comparison of the prospect criteria for shale oil and shale gas for US cases, and shale gas for Indonesian cases [1].

Until now, shale hydrocarbon reservoir has never been developed in Indonesia. To reduce the risk of failure in the exploration, various studies are required to minimize the level of uncertainty.

Criteria	Data range shale oil US	Data range shale gas US	Data range shale gas
TOC	>1% [2]	2–5% [6] and 3–10% (Marcellus shale)	> 2 wt% [1]
Thermal maturity (Ro)	0.6–1.1% for oil window, but sometimes can reach 1.4% [2]	> 1.4 for dry gas and 1.1–1.4 for wet gas [5], Tmax >450	> 1.1–1.4%, 1–1.3% for wet gas and > 1.3% for dry gas
Kerogen type	The ideal condition is type I, II or IIs. [2] HI > 250, 250–800 mg/g	Type II or III	Type II
Shale thickness	> 15 m [3], > 50 m [2]	Minimum 15–20 m [6], 32 m [7], 20–100 m (Haynesville Shale)	> 30 m
Depth	> 1500 m [3], > 1000 m [8]	200 m (antrim shale), 1300 m (marcellus shale)	1000–5000 m
Mineralogy (clay content)	Clay (low) < 35% Silica (significant) > 30% Less carbonate [2]	Clay <40%	Clay <10%

Table 1. Comparison of the prospect criteria for shale oil and shale gas for US cases [5] and shale gas for Indonesian cases [1].

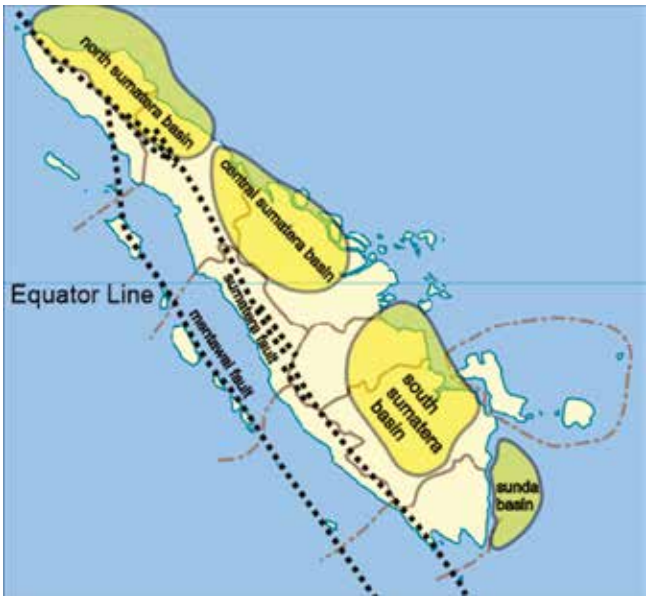

Figure 1. Sumatera Island that includes three main basins (north, central and South Sumatra basin).

In this chapter, we describe the mathematical application, geological and geophysical methods for studying shale hydrocarbons in the North, Central and South Sumatra basin. The study area is shown in **Figure 1**. We applied the advanced data processing technique that includes multilinear regression, linear least square, seismic inversion and geostatistical modeling.

2. Geochemical assessment

The hydrocarbon that was generated in the shale reservoir started with the oil formation that had undergone various stages of chemical reaction caused by temperature and pressure on organic material of the shale. The organic material in the first stage underwent digenesis and made up a kerogen (temperature < 1000°C). In the next stage kerogen changes to become a bitumen, and finally they form hydrocarbons through mutagenesis (oil at temperatures 1000–1500°C and gas at temperatures 1500–2300°C). The organic material that becomes hydrocarbon is only a few percent and the remaining is still in the form of kerogen. This condition that makes the geochemical assessment is important [4].

Geochemical assessment is the critical step for shale hydrocarbon exploration. The main purpose of the geochemical assessment is to assess the quantity, quality and maturity of the shale reservoir. Hydrocarbon content of shale reservoir is a complex function of TOC, Ro, porosity, pressure and temperature. There are several parameters that must be acquired for geochemical assessment. The most accurate parameter is the parameter that is obtained from

laboratory measurements, by using such methods as Leco, Rock-Eval Pyrolysis, to quantify TOC, kerogen type and maturity level. TOC is the amount of organic carbon expressed as weight percent of the dry rock [9]. There is a minimum TOC value to classify that shale reservoir is potential to becoming a source rock [10]. The next parameter is kerogen type, which is determined by using a cross plot between hydrogen index and oxygen index (Van

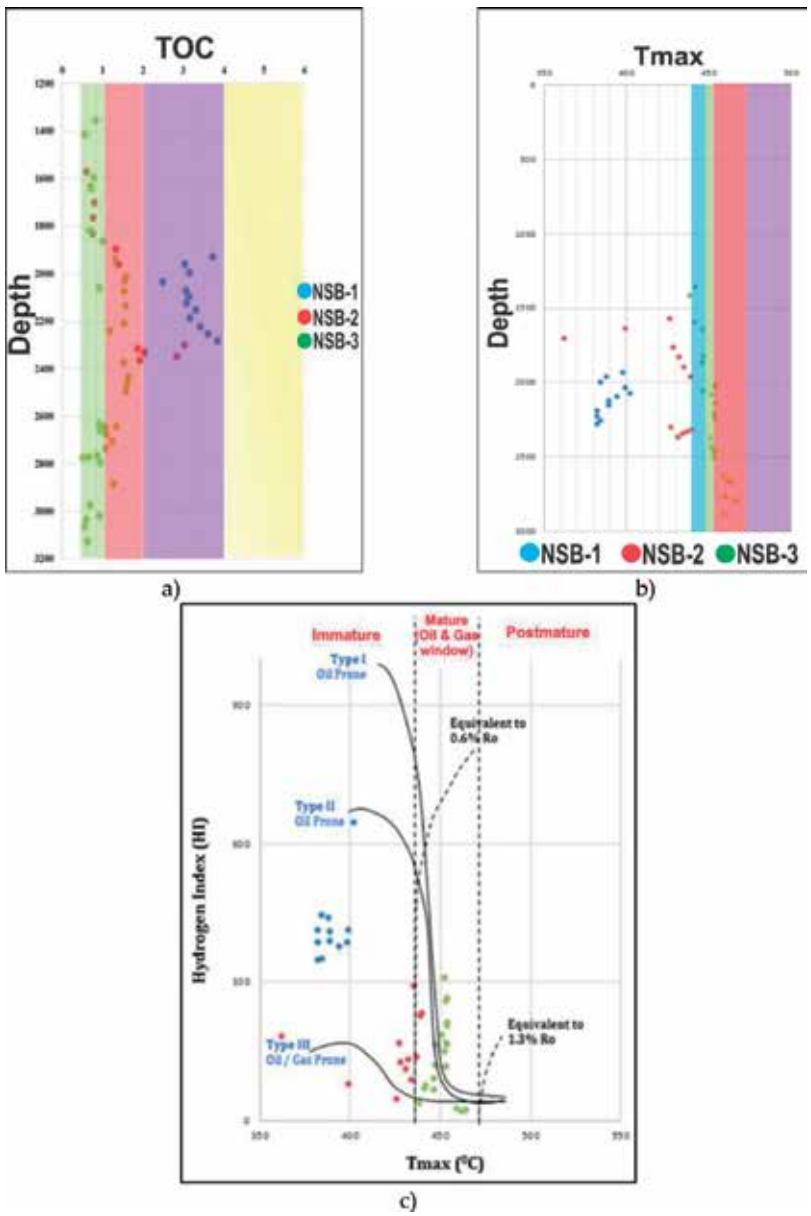

Figure 2. Geochemical assessment of shale hydrocarbon of Baong shale formation in North Sumatra basin, where (a) TOC, (b) Tmax as a function of depth and (c) the relationship between Tmax and HI [11].

Krevelen diagram) and comparison between the hydrogen index and Tmax. The maturity level of organic matters is determined by vitrinite reflectance (Ro) and Tmax. Hydrocarbons can be produced from organic-rich shale with TOC > 1 wt%, Ro from 0.6–1.1% and HI of >200 mg H/g [10].

The study area of North Sumatra Basin is located in Telaga Said and Pantai Pakam area. The conventional reservoir comes from the sand of Ketapang formation, limestone of Belumai formation and source rock of Baong shale formation. In shale hydrocarbon exploration, Baong shale formation plays as a source rock and reservoir as well. The geochemical assessment of Baong shale formation was taken from three well log data (i.e., NSB-1, NSB-2 and NSB-3). The TOC measurement of a core sample from three well log data, which is shown in **Figure 2a**, ranges from 0.5 to 4 wt %. These TOC values are classified as fair to very good. In addition, Tmax ranges from 350–500°C as shown in **Figure 2b**. Referring to Tmax, the Baong shale formation is classified in the category from immature to early mature. **Figure 2c** shows the Krevelen diagram of a core sample of three well log data that indicated the kerogen type of Baong shale formation. The diagram shows that Baong shale formation is categorized into the type II with the maturity level in oil window so that has potential to produce oil.

Geochemical assessment of the Central Sumatra basin was carried out based on our previous studies. A core sample of Pematang Brown shale formation was taken from CSB-1 well. Geochemical assessment on CSB-1 well is shown in **Table 2** [12]. TOC ranges from 0.04 to 4.74 wt%, which is categorized as poor to excellent. This category corresponds to the result of S1 + S2 analysis that shows the potential value from low to moderate. In addition, kerogen type of Pematang Brown Shale is classified as kerogen type III, which has potential to produce gas. In terms of maturity level, we found that Ro ranges from 0.5 to 0.8% with Tmax from 435 to 445°C, which shows maturity level early mature to mature.

Further geochemical assessment based on a core sample from the next two wells (i.e., CSB-2 and CSB-3 well) shows that Pematang Brown Shale formation of Central Sumatra is classified into early mature phase with Tmax 435°C and Ro 0.55% at depth of 6400 ft as shown in **Figure 3a**. In terms of organic richness, this formation is indicated by organic richness varying from

Depth (ft)	Organic richness (wt%)	HC potential (S1 + S2) mgHC/g rock)	Hydrogen index (HI)
6000–6190	Fair (0.98–1.03)	Low (1.91)	Low (159)
6200–6850	Poor (0.26–0.44)	Low (0.07–1.00)	Low (22–186)
7350–8350	Very good (2.01–4.74)	Moderate (2.78–7.65)	Low (189)
8400–8910	Fair (0.74–1.70)	Moderate (2.01)	Low (136–199)
8940–9190	Good (2.09–2.66)	Moderate (2.61–4.35)	Low (136–199)
9240–9710	Fair (0.54–1.57)	High (4.04–8.11)	Moderate (206–350)

Table 2. The geochemical properties of shale rock of CSB-1 well in Pematang Brown shale formation.

0.49 to 1 wt% that is categorized as fair quality. The classification of kerogen type, Pematang Brown Shale formation, is classified into kerogen type III, which is shown in **Figure 3b** and **c**. This means that Pematang Brown Shale formation has the capability to produce gas.

Geochemical assessment of shale hydrocarbon in the South Sumatra basin was focused on Talang Akar formation, which was derived from SSB well. **Figure 4** shows the geochemical assessment of shale hydrocarbon of Talang Akar formation in South Sumatra basin. The shale hydrocarbon reveals that organic richness varies from 0.35 to 3.66 wt% that is categorized as poor to very good. In addition, the hydrogen index ranges from 107 to 278, which shows the potential to produce oil and gas. This potential is confirmed by maturity level, which ranges from 0.54 to 1.3%. This maturity level is classified as the early mature phase.

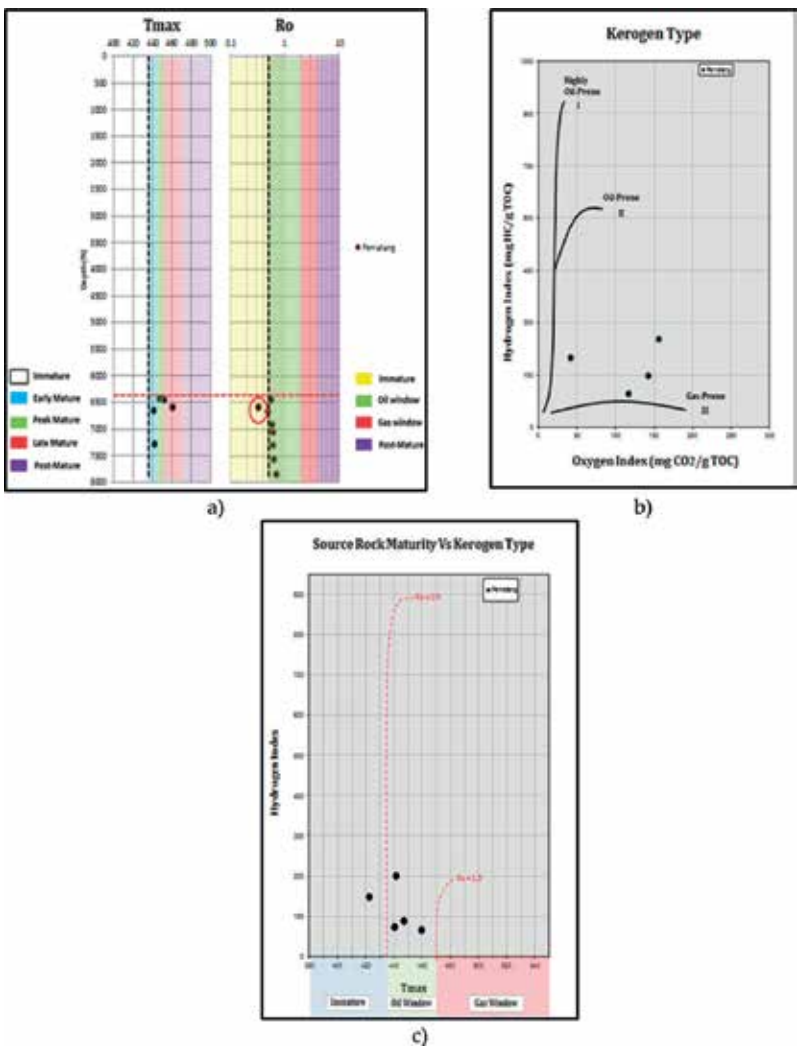

Figure 3. Geochemical assessment of Pematang formation of Central Sumatra basin based on CSB-2 and CSB-3 well. Maturity level is indicated by (a) Tmax (left) and (b) Ro as a function of depth (right). Kerogen type is indicated by (a) van Krevelen diagram and (b) the relationship between HI and Tmax [13].

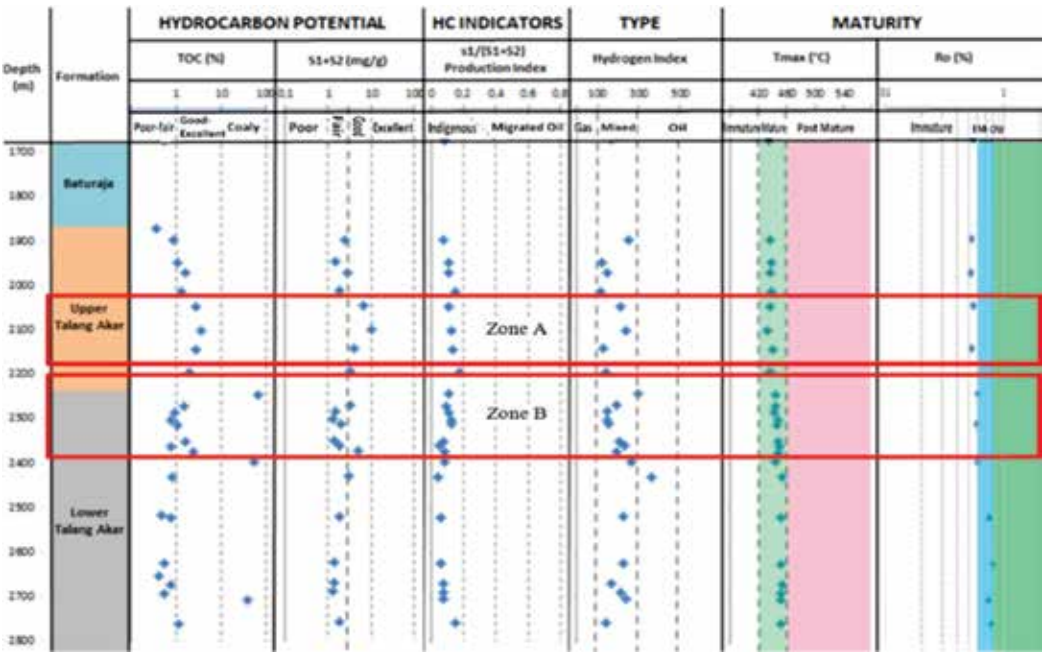

Figure 4. Geochemical assessment of shale hydrocarbon of Talang Akar formation in South Sumatra basin, which was derived from SSB well [14].

3. Geomechanical assessment

To achieve a great success in shale hydrocarbons exploration, the integrated assessment by implementing the geomechanical assessment should be applied to complement the previous geochemical assessment [15]. The natural character of the shale layer is indicated by very low permeability; therefore, we need hydraulic fracturing to increase shale permeability [16]. The key success in hydraulic fracturing is related to the geomechanical understanding of the shale layer such as the brittleness index and the rock strength.

There are some criteria of the mechanical properties for shale reservoir to be able to be fractured; the shale reservoir must have a low rock's strength and Poisson ratio and high Young's modulus [17]. The mechanical properties of shale reservoir are also influenced by the mineral composition contained in shale reservoir. Rock strength is dependent on porosity, quartz-dolomite and kerogen fraction. This means the rock strength decreases when shale porosity increases [17] and the quartz-dolomite and kerogen fraction of shale increases as well [18]. The increasing kerogen fraction in the shale will increase horizontal shear stress and in contrast will decrease the shear wave velocity. As a consequence the Poisson ratio of the shale decreases with decreasing shear wave velocity. In addition, the increasing quartz-dolomite fraction will decrease the vertical shear strain and as a consequence the Young's modulus of the shale increases.

The change of diagenetic to silica-rich shale is caused by the transformation from smectite to illite. This change may increase brittleness [7]. The presence of smectite makes the density of the shale decrease and the shear wave velocity of the shale will increase; thus, the shale kerogen fraction decreases. In particular, brittleness increases with decreasing TOC. However, brittleness may decrease as pressure and temperature increase.

According to Wang and Gale [7] brittleness index is a function of mineral composition and diagenesis. The modified equation of Jarvie et al. is shown in Eq. 1 [17].

$$BI = \frac{Q + Dol}{(Q + Dol + Lm + Cl + TOC)} \tag{1}$$

where *BI* presents the brittleness index, *Q* states the percentage of quartz mineral, *Dol* corresponds to the percentage of dolomite, *Cl* presents the total clay, and *Lm* presents limestone mineral. The increasing dolomite may increase brittleness since dolomite is more brittle than limestone. As a consequence, increasing TOC may increase ductility [8]. In addition, the brittleness is a function of diagenesis caused by changes in temperature and fluid composition associated with the tectonic system and burial history. This means that the most prospect reservoir for shale hydrocarbon is brittle reservoir, which is indicated by high Young's modulus and low Poisson ratio [19]. Further, the brittleness index might be determined by normalizing Young's modulus and Poisson ratio [19]. The relationship of Young's modulus and Poisson ratio is presented in Eqs. (2)–(4).

$$YM_{Britteness} = \left[\frac{YM - YM_{min}}{YM_{max} - YM_{min}}\right] x100 \tag{2}$$

$$PR_{Britteness} = \left[\frac{PR - PR_{max}}{PR_{min} - PR_{max}}\right] x100 \tag{3}$$

$$BI_{Average} = \frac{YM_{Britteness} + PR_{Britteness}}{2} \tag{4}$$

where *YM* represents Young's modulus, *YMmin* is the minimum Young's modulus for a certain interval and YMmax is the maximum Young's Modulus. While *PR* represents Poisson ratio, *PRmin* is the minimum Poisson ratio and *PRmax* is the maximum Poisson ratio.

In this study, the geomechanical assessment is only carried out in the North Sumatra and Central Sumatra basin due to the limitation of mineralogy data. In term of mineralogy analysis, the brittleness index (BI) was calculated by using Jarvie et al. equation, which was modified by Wang and Gale as shown in Eq. 1 [2, 7]. The equation was modified by incorporating dolomite content that caused the increase of BI.

The presence of mineral fraction in BI calculation is significant. On the other hand, Eq. 1 does not consider plagioclase mineral. However, the result of mineralogy identification shows that the presence of plagioclase mineral is quite significant, which is indicated by the fraction of 2–6%. Thereby, we incorporate the plagioclase mineral into Eq. 1 in calculating BI. The calculated BI using Jarvie and Wang shows a good agreement of BI, which is shown in a similar trend.

Figure 5 illustrates that BI is strongly connected to rock strength, in which the rock strength decreases with increasing brittleness index for the Baong formation of North Sumatra basin. In this case, the Baong formation of North Sumatra basin is identified by TOC ranging from 2 to 3.5 wt%. In terms of geomechanical, this formation is indicated by brittleness index of 0.48 and rock strength of 3000 Psi. Theoretically the potential shale reservoir is indicated by high

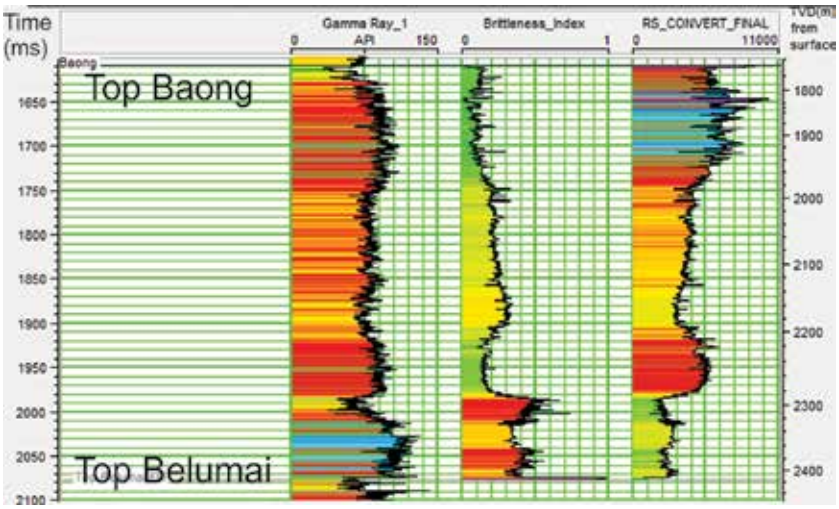

Figure 5. Geomechanical assessment of Baong shale formation of North Sumatra Basin, which was derived from NSB well. The left panel is gamma ray log, the mid-panel is BI and the right panel is rock strength [11].

TOC, high BI and low rock strength; therefore, the Baong formation of North Sumatra basin can be classified into fair or moderate quality that has potential to be developed.

In addition, the geomechanical assessment was carried out in the Pematang Brown Shale formation of Central Sumatra basin that is based on the mineralogy content. **Table 3** presents X-Ray Diffraction (XRD) analysis of the sample data of CSB-2 well. The result of X-Ray Diffraction (XRD) analysis is then used to determine the BI. Our calculation shows that the Pematang Brown Shale formation is indicated by high BI, which is greater than 0.48. This calculated BI has a good agreement with the calculated BI in North Sumatra basin.

4. Predicting total organic content using multilinear regression

The previous TOC calculation is only related to the core sample for certain depth. To derive the TOC data that cover the whole depth of well log data, we performed TOC prediction by using multilinear regression approach. This TOC prediction was applied to all available well log data (i.e., NSB-1, CSB-1 to CSB-5, and SSB-1 well) from North, Central and South Sumatra basin.

Our approach by using multilinear regression for Baong shale formation of North Sumatra Basin shows the relationship between TOC and available log data as presented in Eq. 5 [11].

$$\begin{aligned} TOC \;=\; & 1.8994 - 0.GR + 1.0176 \times Density + 20.893 \times Neutron \\ & - 0.0488 \times Sonic + 0.321 \times Resistivity \end{aligned} \tag{5}$$

Eq. 5 is then used to predict the TOC log of NSB-1 well. The same approach is continuously applied from the CSB-1 to CSB-5 well for Pematang Brown Shale formation. The relationship

No	Litho	Clay minerals (%)				Carbonate minerals (%)			Other minerals (%)				Total (%)		
		Smectite	Ilite	Kaolinite	Chlorite	Calcite	Dolomite	Siderite	Quartz	K-Feldspar	Plagioclase	Pyrite	Clay	Carbonate	Other
1	Sand	—	3	10	—	—	—	—	87	—	—	—	13	_	87
2	Shale	—	30	45	—	—	—	—	25	—	—	—	75	_	25
3	Sand	—	3	24	—	—	—	1	72	—	—	—	27	1	72
4	Sand	—	7	14	5	—	—	—	74	—	—	—	26	—	74
5	Sand	—	4	7	—	—	—	—	89	—	—	—	11	—	89
6	Sand	—	2	3	—	—	—	—	95	—	—	—	5	—	95

Table 3. The X-ray diffraction analysis for CSB-2 well.

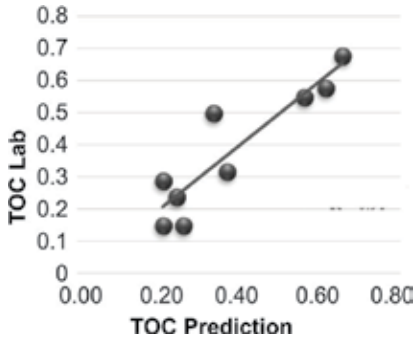

Figure 6. The relationship between predicted and measured TOC from the lab.

between organic richness and available log data for Pematang Brown Shale formation of Central Sumatra basin is presented in Eq. 6 [13].

$$\text{TOC} = -14.8534 + (-0.0168 \times \text{GR}) + (3.9498 \times \text{Density}) + (4.7925 \times \text{Neutron}) + (0.0751 \times \text{Sonic}) + (0.0651 \times \text{Resistivity}) \quad (6)$$

Figure 6 shows the relationship between predicted and measured TOC from the lab. The result shows a good agreement among them.

The relationship between TOC and available log data for Talang Akar formation of South Sumatra basin is presented in Eq. 7 [14].

$$\text{TOC} = -1.74 + 0.00038 \times \text{GR} + 1.023 \times \text{Density} - 0.0058\,2^{*}\,\text{Neutron} + 0.00\,62^{*}\,\text{Sonic} \quad (7)$$

These relationships were successfully applied to all well log data (i.e., NSB-1, CSB-1 to CSB-5, and SSB-1 well) from North, Central and South Sumatra basin.

5. Sweet spot of shale hydrocarbon distribution

Understanding the prospect reservoir for shale hydrocarbon exploration is significantly controlled by mapping the geochemical and geomechanical properties. The previous section has discussed geochemical and geomechanical analysis for one dimension of the well location, which does not cover the spatial distribution. Seismic data that have spatial coverages are then used to spatially distribute the geochemical and geomechanical properties [20, 21].

The relationship between seismic and geochemical and geomechanical properties may be approached with acoustic impedance properties [22]. Thereby, transforming the seismic into acoustic impedance (AI), which is produced by applying seismic inversion, is required [23]. This approach can be understood because AI has a strong correlation to the geochemical and geomechanical properties that are possible for mapping the TOC and rock strength distribution. Obviously, the sweet spot of shale hydrocarbon distribution could be identified based on the geochemical and geomechanical properties.

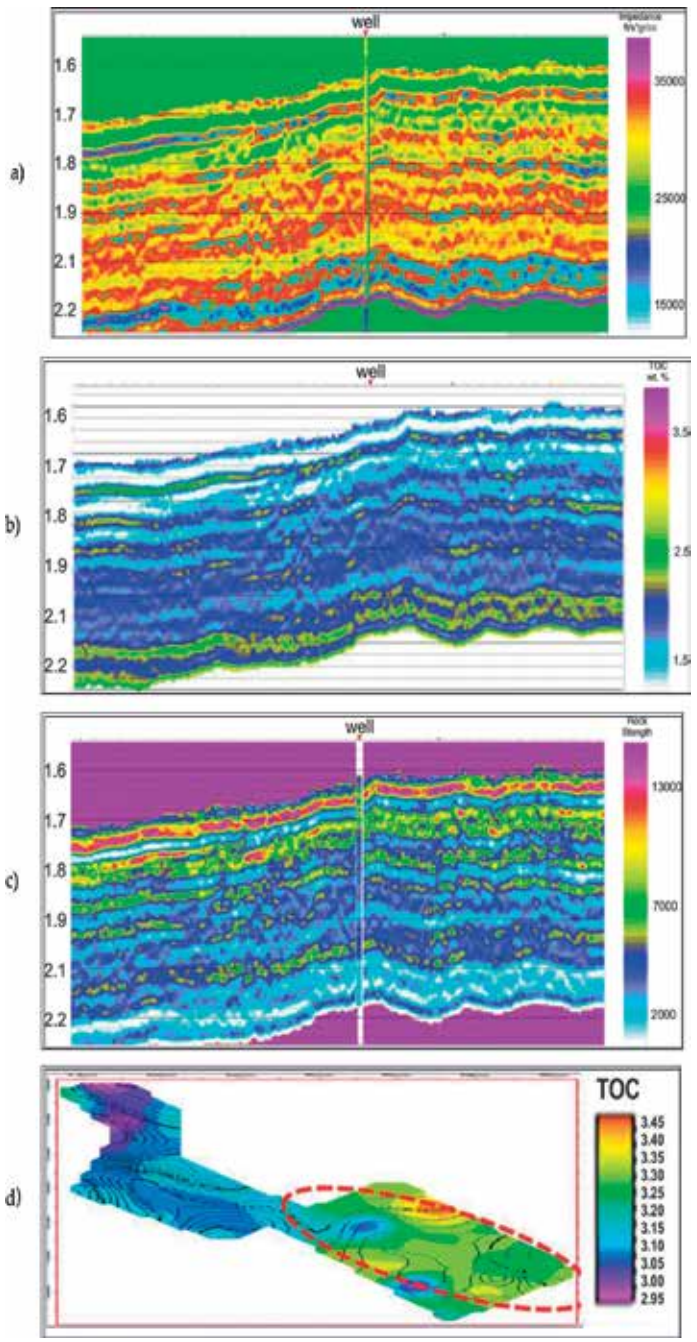

Figure 7. The spatial distribution in term of section and map, where (a) acoustic impedance, (b) organic richness, (c) rock strength, and (d) the organic richness of Baong shale formation of North Sumatra basin. The dashed line is the sweet spot of shale hydrocarbon distribution [11].

6. Sweet spot of Baong Shale formation of North Sumatra Basin

Figure 7 shows the spatial distribution in terms of the seismic section, where AI section was transformed into a section of TOC and rock strength section and TOC map of Baong Shale formation of North Sumatra basin. The zone, which is surrounded by dashed-line, is the sweet spot of potential shale hydrocarbon [11]. **Figure 7a** is acoustic impedance section, which was derived from seismic data. **Figure 7b** and **c** illustrate the TOC and rock strength section, respectively, which were derived from acoustic impedance section.

Baong Shale formation is located in the lower part of the section as shown by the white ellipse. The prospect layers were indicated by the low AI (blue), high TOC (green) and low rock strength (light blue). To see the spatial distribution of the sweet spot for the shale hydrocarbon development, we extracted TOC and rock strength along the top Baong shale horizon to map TOC and rock strength. The sweet spot of shale hydrocarbon distribution may be easily mapped by observing **Figure 7d**, which overlaid the rock strength (contour) and TOC map (color legend). The sweet spot of shale hydrocarbon distribution was identified in the southeastern part of the map.

7. Pematang Brown Shale, Central Sumatra Basin

The same procedure was performed to Pematang Brown shale formation of Central Sumatra basin. Seismic inversion was conducted to derive the acoustic impedance section, which is shown in **Figure 8a**. The AI section was then transformed to the TOC as shown in **Figure 8b** and rock strength as shown in **Figure 8c**. Pematang Brown Shale formation is located on the bottom of the basin area indicated by the low AI (purple), high TOC (green to yellow) and low rock strength (green to yellow). The sweet spot of shale hydrocarbon is illustrated in **Figure 8d**, which is the integrated map between TOC (contour) and rock strength (color legend). The sweet spot is indicated by the white tight boundary with rock strength of 10,000 psi and TOC of 1 wt%. In terms of structural geology, the sweet spot area might be identified as a basin where the sediment was deposited [24]. The diagenesis transformed sediment turns into the mature phase by sedimentation in high temperature.

8. Talang Akar formation, South Sumatra Basin

The sweet spot identification on Talang Akar formation was performed by dividing the formation into upper Talang Akar and Lower Talang Akar. A different approach was carried out due to the lack of geomechanical data, where only TOC map was produced. **Figure 9** shows the sweet spot distribution of shale hydrocarbon of Talang Akar formation of South Sumatra basin. **Figure 9a** and **b** illustrate the AI and TOC map for upper Talang Akar formation, respectively, while **Figure 9c** and **d** present the AI and TOC map for lower Talang Akar

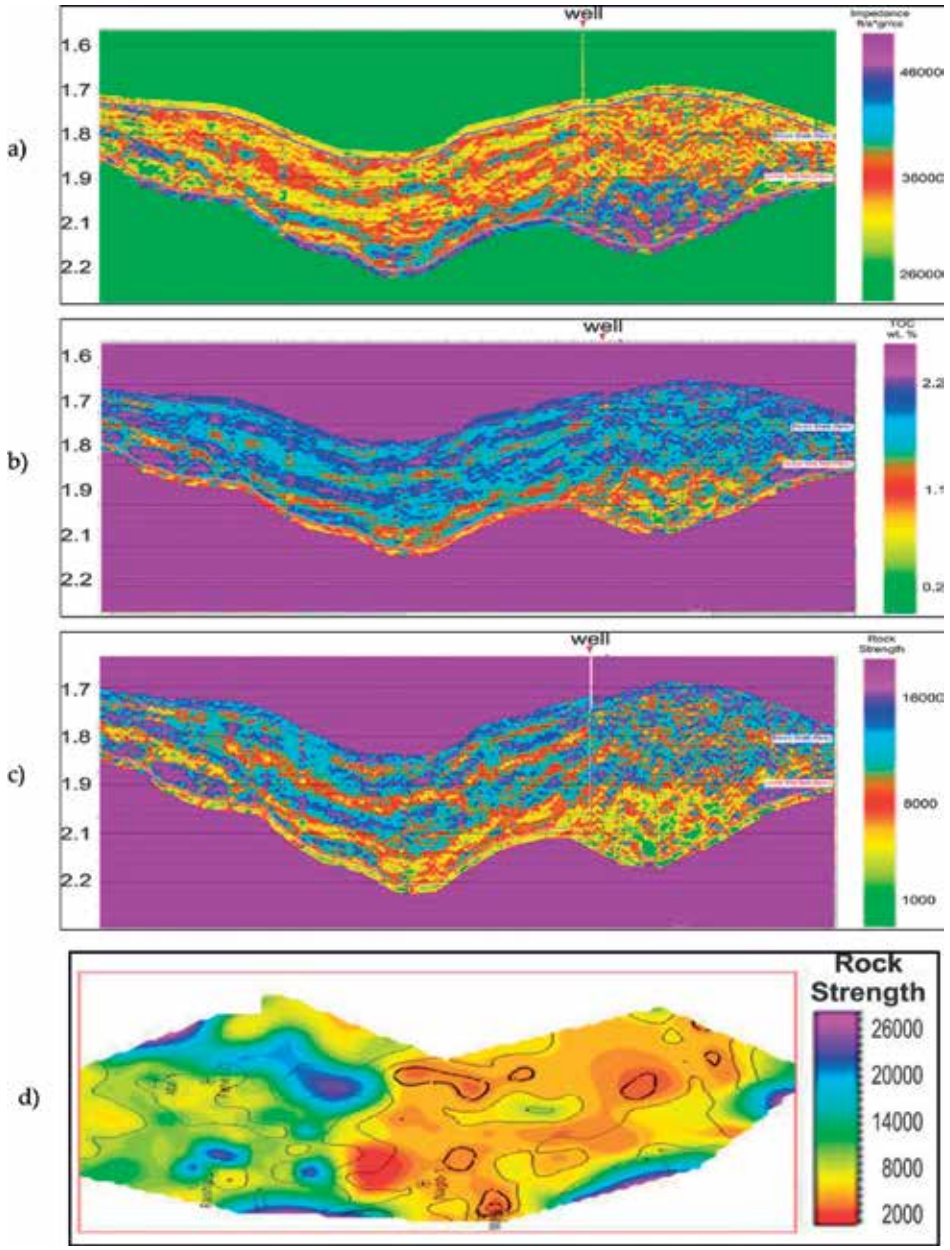

Figure 8. The spatial distribution in term of section and map (a) acoustic impedance, (b) organic richness, (c) rock strength and (d) rock strength map that is overlaid with TOC contour for identifying sweet spot potential of shale hydrocarbon of Pematang Brown shale Central Sumatra Basin [13].

formation, respectively [14]. The sweet spot of shale hydrocarbon is illustrated by red dashed line, which is indicated by low acoustic impedance (less than 27,500 ft/s*gr/cc) and relatively high TOC (greater than 2%). This sweet spot of shale hydrocarbon is classified as good quality.

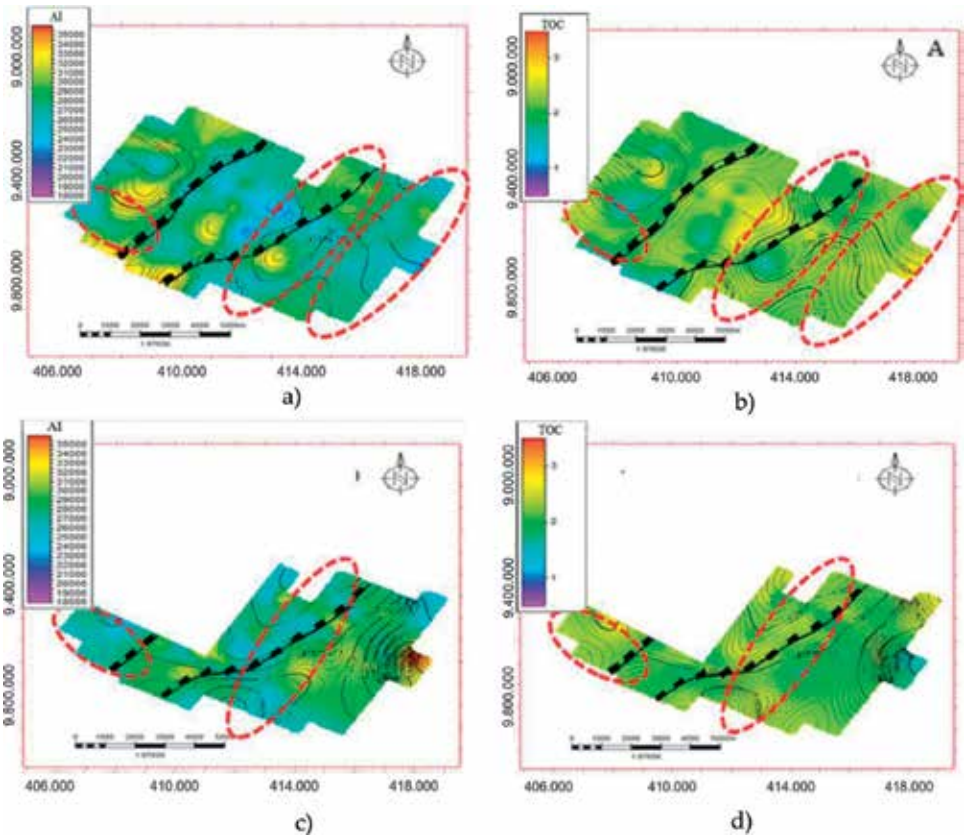

Figure 9. Sweet spot distribution of shale hydrocarbon, which is indicated by red dashed line, for upper Talang Akar formation in AI map (a) TOC map, (b) the lower Talang Akar formation is illustrated in AI map (c) TOC map, (d) sweet spot zone indicated with relatively low AI and high TOC [14].

9. Reservoir modeling approach for shale hydrocarbon

Reservoir modeling approach was carried to assess shale hydrocarbon in terms of the three-dimensional framework. This three-dimensional framework was performed based on sequential Gaussian simulation of geostatistical approach, which was focused on Pematang Brown Shale formation of Central Sumatra basin. The three-dimensional framework was then filled up by TOC and Brittleness Index.

Figure 10 shows the modeled shale hydrocarbon reservoir, which is represented by brittleness index and TOC. The illustrated model in the two-dimensional map is shown in **Figure 10a** for brittleness index and **Figure 10b** for TOC. We identify that sweet spot distribution is associated with the brittle area, which is indicated in red. The brittle area means that reservoir might be easily fractured for exploration purposes. In terms of brittleness index, the sweet spot is dominantly distributed in the southern part of the field, which is confirmed by TOC map.

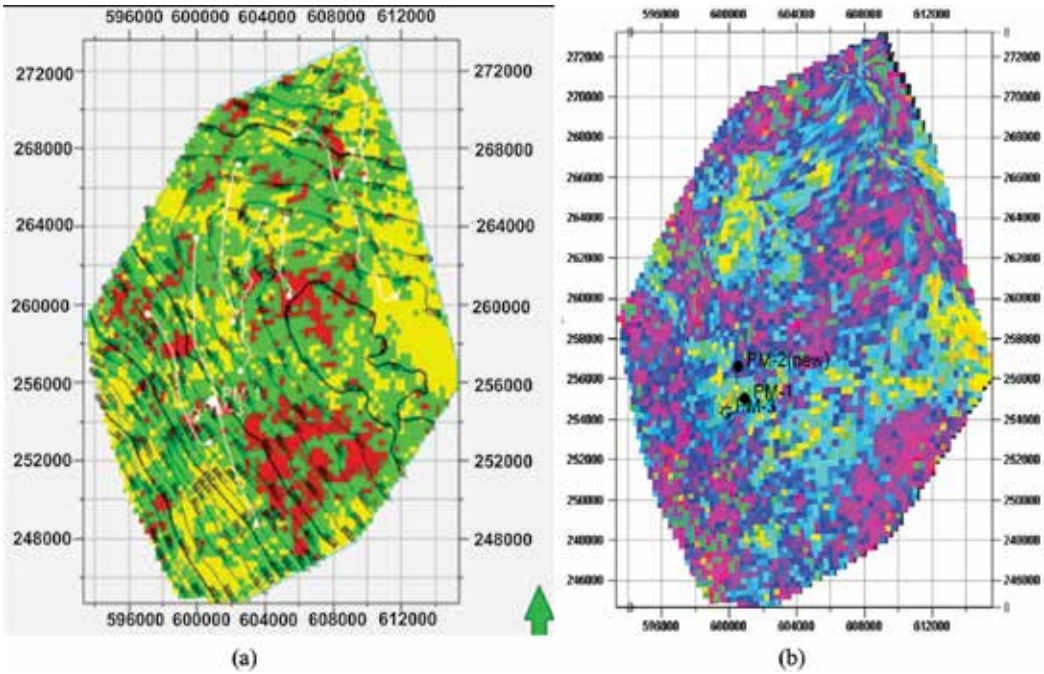

Figure 10. The modeled shale hydrocarbon reservoir, which is represented by brittleness index (a) and TOC (b), which is approached by geostatistical modeling [12, 25].

10. Conclusions

In terms of geochemical and geomechanical methods, the shale of Baong formation of North Sumatra basin is supposed to be developed for shale hydrocarbon. This conclusion is confirmed by potential level from TOC was classified from fair to very good, with kerogen type was classified into type II that associated with gas prone. The sweet spot identification was successfully performed by combining geochemical and geomechanical assessment, where the sweet spot was focused in the southeastern part of the field. The geochemical assessment shows that shale reservoir is indicated by TOC ranging from 2 up to 3.5 wt% and brittleness index of 0.48, while geomechanical assessment shows the rock strength is less than 3000 Psi.

Pematang Brown Shale Formation of Central Sumatra basin is identified as fair to excellent based on prospect level. This formation is categorized into a mature phase that has potential to produce oil. This conclusion is confirmed by mud log data at CSB-2 well that shows oil indicator at the depth of 8500 ft. The sweet spot is identified based on the intersection between geochemical and geomechanical assessment, where shale hydrocarbon distribution was indicated by TOC ranging from fair to good and deposited in the thickness of up to 50 ft. In terms of geomechanical assessment, the brittleness index is identified as greater than 0.48 and rock strength is less than 10,000 Psi.

The geochemical and geomechanical assessment of Talang Akar formation of South Sumatra Basin illustrates that two interest zones in the depth interval of 2030–2182 m, called as Upper Talang Akar formation, and 2204–2396 m, called as Lower Talang Akar formation, are considered as a potential zone for shale hydrocarbon exploration. These two prospect zones are classified as good to excellent quality in terms of organic richness criteria and fulfill sufficient maturity levels.

Conflict of interest

The authors declare that there is no conflict of interest.

Author details

Abdul Haris*, Agus Riyanto, Bayu Seno, Husein Agil Almunawar, Martogu Benedict Marbun, Iskandarsyah Mahmudin and Prima Erfido Manaf

*Address all correspondence to: abdulharis@sci.ui.ac.id

Geology and Geophysics Study Program, FMIPA Universitas Indonesia, Depok, Jawa Barat, Indonesia

References

[1] Sukhyar R, Fakhruddin R. Unconventional Oil and Gas Potential in Indonesia with Special Attention to Shale Gas and Coal Bed Methane. Jakarta: Badan Geologi KESDM; 2013

[2] Jarvie DM. Shale resource system for oil and gas: Part 1-shale gas resources system. In: Breyer JA, editor. Shale Reservoirs – Giant Resources for the 21st Century. AAPG Memoir. 2012a;**97**:69-87

[3] Charpentier RR, Cook TA. USGS Methodology for Assessing Continuous Petroleum Resources. U. S. Geological Survey Open-File Report. 2011. Vol. 1167. pp. 1-73

[4] Waples DW. Geochemistry in Petroleum Exploration. Dordrecht, Netherlands: Springer Science & Business Media; 2013. pp. 55-180

[5] Andrews IJ. The Jurassic Shales of the Weald Basin: Geology and Shale Oil and Shale Gas Resource Estimation. London, UK: British Geological Survey for Department of Energy and Climate Change; 2014

[6] dan Baker Hughes GCA. Shale Gas Workshop Houston. Houston: Gaffney Cline and Associates; 2011

[7] Wang Fred P, dan Gale Julia FW. Screening Criteria for Shale Gas Systems: Gulf Coast Association of Geological Societies Transactions. 2009;**59**:779-793

[8] U.S. Energy Information Administration (USEIA). Technically Recoverable Shale Oil and Shale Gas Resources: An Assessment of 137 Shale Formation in 41 Countries Outside the United States. Report; 2013

[9] Verma S, Marfurt K. A Way of TOC Characterization on Barnett and Woodford Shale. Search and Discovery Article #80429. Norman, OK: University of Oklahoma; 2014

[10] Peters Kenneth E, dan Cassa Mary R. Applied source rock geochemistry. AAPG Memoir. 1994:60

[11] Haris A, Seno B, Riyanto A, Bachtiar A. Integrated approach for characterizing unconventional reservoir shale hydrocarbon: Case study of North Sumatra Basin. In IOP Conference Series: Earth and Environmental Science. Bristol, UK: IOP Publishing; 2017 April;**62**(1):012023

[12] Haris A, Marbun MB, Bachtiar A, Riyanto A. Geochemical analysis of shale gas reservoir based on well log and 3D seismic data in Pematang formation, central Sumatera Basin. In: AIP Conference Proceedings. New York, USA: AIP Publishing; 2017 July;**1862**(1):030176

[13] Haris A, Almunawwar HA, Riyanto A, Bachtiar A. Shale hydrocarbon potential of brown Shale, Central Sumatera Basin based on seismic and well data analysis. In: IOP Conference Series: Earth and Environmental Science. 2017, April;**62**(1):012018. IOP Publishing

[14] Manaf PE, Suparno S, Haris A, Usman A, Riyanto A. Organic shale analysis using geochemical data and seismic attributes: Case study of Talang Akar formation, south Sumatera Basin. In: AIP Conference Proceedings. 2017, July;**1862**(1):030178. AIP Publishing

[15] Rickman R, Mullen MJ, Petre JE, Grieser WV, Kundert D. A Practical use of shale petrophysics for stimulation design optimization: all shale plays are not clones of the Barnett Shale. In: SPE Annual Technical Conference and Exhibition; 2008, January. Society of Petroleum Engineers

[16] Mair R, Bickle M, Goodman D, Koppelman B, Roberts J, Selley R, Younger P. Shale Gas Extraction in the UK: A Review of Hydraulic Fracturing; 2012

[17] Dradjat, Anggoro S. 2013. Dasar-Dasar Explorasi dan Exploitasi Gas Shale. IAGI. 2013

[18] Hui J, Sonnenberg Stephen A, Fredrick SJ. Source Rock Evaluation for the Bakken Petroleum System in the Williston Basin, North Dakota, and Montana; 2012. AAPG #20156

[19] Grieser, dan Bray JM. Identification of production potential in unconventional reservoir. SPE 106623, SPE Production and Operator Symposium held in Oklahoma City, Oklahoma, USA, 31 March – 3 April; 2007

[20] Sharma Ritesh Kumar, dan Chopra Satinder. New attribute for determination of lithology and brittleness. AAPG Article #41368; 2014

[21] Løseth H, Wensaas L, Gading M, Duffaut K, Springer M. Can hydrocarbon source rocks be identified on seismic data? Geology. 2011;**39**(12):1167-1170

[22] Perbawa A, Kusuma B, Winardhi S. Integration of Seismic Inversion, Pore Pressure Prediction, and TOC Prediction in Preliminary Study of Shale Gas Exploration. In 37th HAGI Annual Convention & Exhibition; 2012

[23] Prasad M. Rock physic of unconventional. The Leading Edge. 2009;**28**(1):34-38

[24] Williams HH, Eubank RT. Hydrocarbon habitat in the rift graben of the Central Sumatra Basin, Indonesia. In: Lambiase JJ, editor. Hydrocarbon Habitat in Rift Basins. London, UK: Geological Society Special Publication; 1995;**80**:331-337

[25] Iskandarsyah HA, Riyanto A. Brittleness modelling of shale gas reservoir: Case study of Pematang formation, Central Sumatera basin. In: AIP Conference Proceedings. New York, USA: AIP Publishing; 2017 July;**1862**(1):030165

Chapter 3

Silurian Gas-Rich "Hot Shale" from Akkas Gas Field, Western Iraq: Geological Importance and Updated Hydrocarbon Potential and Reservoir Development Estimations of the Field

Ali Ismail Al-Juboury and
Muhammed Abed Mazeel Thani

Additional information is available at the end of the chapter

http://dx.doi.org/10.5772/intechopen.77246

Abstract

The Silurian hot shale is encountered in the Akkas field, which is regarded as one of the largest gas fields in Iraq. It contains 5.68 tscf of initial gas in place of which 4.55 tscf is estimated to be recoverable. There is also the potential of condensate and other prospects in deeper formations. The well test confirmed the presence of natural gas with a flow rate of 6–8 MMscfd. Silurian shale contains two organic-rich black hot shale beds that are fissile with high-gamma uranium radiation. Silurian hot shales are geologically important from different sides. Stratigraphically, Silurian graptolites are used to delineate the time transgressive depositional advance of marine clastics across the Arabian Peninsula after the melting of Ordovician glaciers. For assessment of the hydrocarbon generation in the Paleozoic of Iraq, the hot shales of the Akkas Formation are low-sulfur, high-gravity oil, condensate, and gas and are considered as an important gas-rich formation in the region. From petrological and mineralogical view, the presence of distinctive minerals and some elements are important to interpret the depositional and climatic situation at Silurian time. This chapter also sets out assumptions about Akkas gas field development.

Keywords: gas-rich shale, hydrocarbon potential, importance, reservoir estimation, Akkas field, western Iraq

1. Introduction

The lower Silurian shales especially the characteristics "hot shale" are a major source rock on the Arabian Peninsula [1–3]. They are regarded as the source of the non-associated gas in the North Field of Qatar and of the oil in central Saudi Arabia and western Iraq [4, 5]. They are also the origin of 80–90% of Paleozoic-sourced hydrocarbons in North Africa [1]. This prolific basal Silurian source level not only occurs over wide areas of Arabia and North Africa, but source rocks are also present at a similar level in the interior basins of the US, the Amazon and on the Russian platform [6, 7]. Silurian organic-rich shales account for the generation of 9% of the world's petroleum [6, 1].

The Silurian Akkas Formation does not crop out in Iraq and it has been penetrated in several boreholes in the western desert of Iraq (**Figure 1**). The Akkas Formation overlies the Ordovician

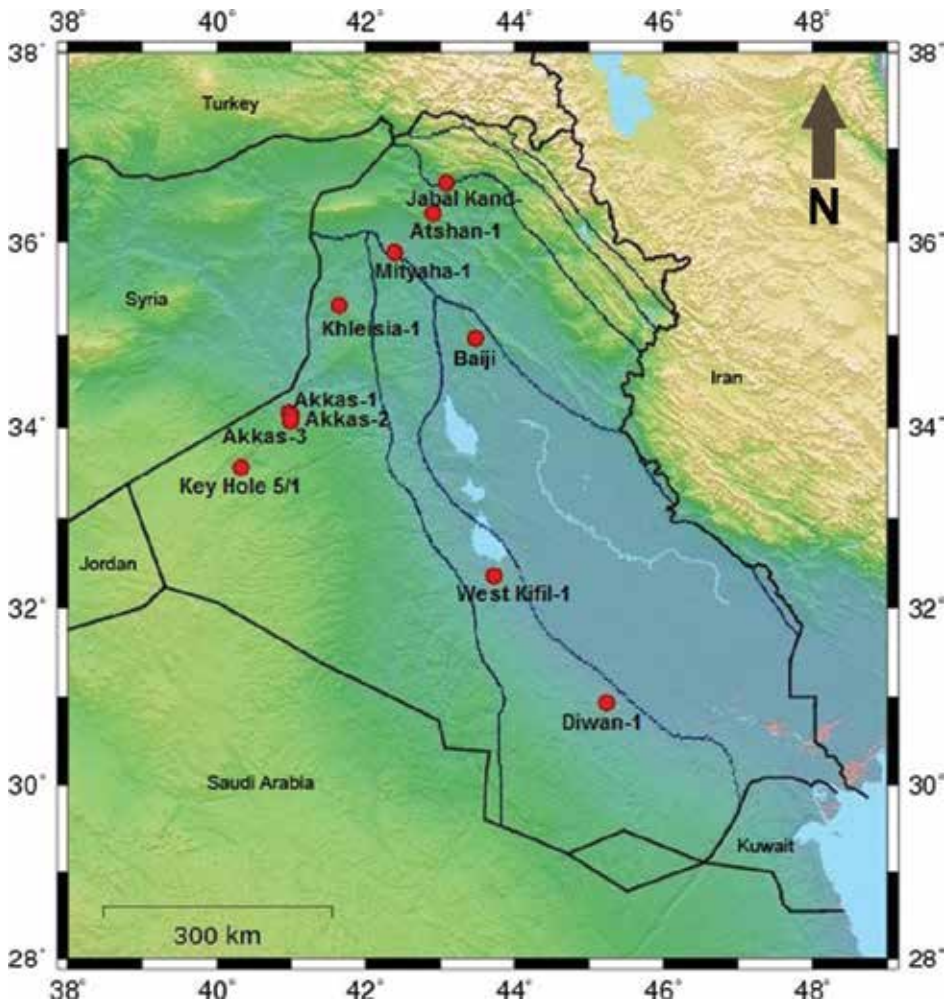

Figure 1. Map of Iraq showing the locations of wells that penetrate the Paleozoic rocks of Iraq including the wells of the current study, Akkas 1-3 (SA 1-3), Khleisia and key hole KH5/1 (source Abd Alwahab 2013, [8]).

http://dx.doi.org/10.5772/intechopen.77246

Khabour Formation and underlies the Devonian Pirispiki Red Beds Formation in surface outcrops in extreme northern Iraq or Kaista Formation in other locations [5]. It consists of black fissile shale with sandstone and siltstone intercalations. It is divided into lower Hoseiba and upper Qaim members. The Hoseiba Member consists of black, gray to dark gray shale, fissile,

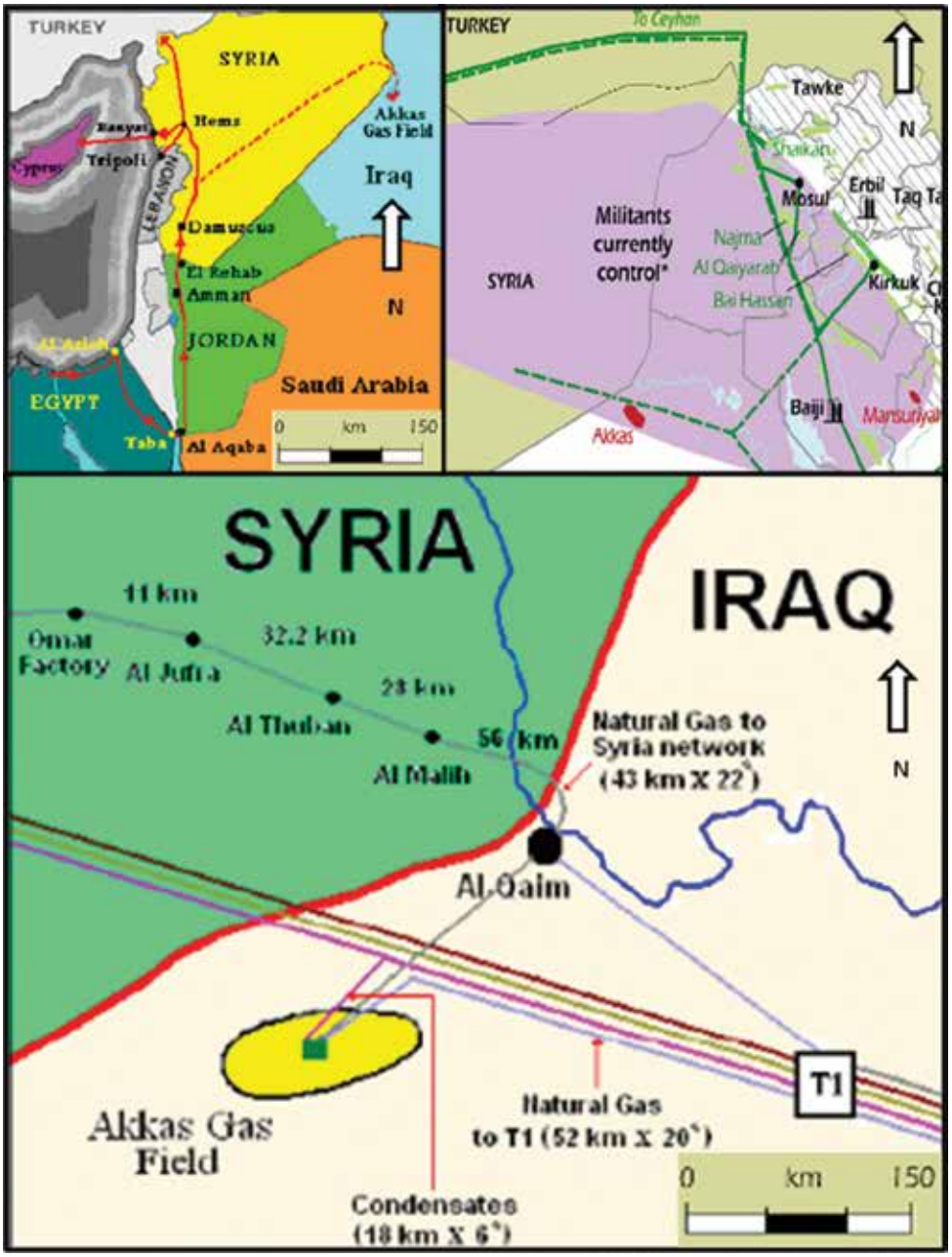

Figure 2. Location of the Akkas field and pipelines connection (source AlShalchi 2008 [9]).

micaceous, non-calcareous, pyritic and silty, with graptolite and brachiopods. It contains two organic-rich black hot shale beds that are fissile with high-gamma uranium radiation. These hot shales also existed in the early Silurian after the melting of the Gondwana polar glaciers.

The study area is located in the Akkas field of western Iraq (**Figure 2**). It is 52 km from the T1 pump station and 285 km from the K3 pump station. The distance between this field and Baji town, where the entire Iraqi gas grid passes, is around 300 km. The nearest industrial complex to the field is the Al-Qaim. Industrial Complex that consists of a fertilizer plant and cement plant is less than 40 km away. The first exploration well in Akkas region took place in August 1992. The drilling program target was to reach a depth of 5000 m, but this did not succeed due to technical difficulties. The drilling reached a depth of 4238 m, and the well test confirmed the presence of natural gas with a flow rate of 6–8 MMscfd.

Akkas is one of the largest gas fields in Iraq. It contains 5.68 tscf of initial gas in place, of which 4.55 tscf is estimated to be recoverable. There is also the potential of condensate and other prospects in deeper formations. In 2001, the development of Akkas-Saladin gas field was referred to the Syrian Petroleum Co. The commitment was to drill five horizontal wells and redrill the Akkas-1 (SA-1) discovery well horizontally. An average well test for another five wells demonstrates more than 9 MMscfd on the largest choke.

The present chapter aims to illustrate the importance of the gas-rich shale from Akkas field of western Iraq in terms of geological and hydrocarbon potential clues and with the available limited information to calculate the probable reserves and design the plan of development for the field.

2. Geological setting

The Akkas Field is a part of the Widyan basin and Interior Platform Province of western Iraq and northern Saudi Arabia [10]. The gas fields of the Widyan basin-interior platform in western Iraq are mainly Lower Paleozoic petroleum systems such as gas in the Ordovician Khabour and lower Silurian Akkas formations. Their main source could be the Khabour Formation and the oil shale of the Akkas Formation. Structural framework of folding and faulting as well as stratigraphic facies changes could form the main traps in these regions. The lower Paleozoic Qusaiba/Akkas petroleum system of Saudi Arabia and western Iraq which consists of one assessment unit "the horst/graben-related oil and gas assessment unit" is characterized by high-gravity, low-sulfur crude oil, as well as natural gas, occurs in horst/graben-related traps that formed prior to, during, and after Hercynian (Carboniferous) deformation [10].

Silurian rocks are not exposed in Iraq. They are absent from outcrops in northern Iraq due to erosion at the late Devonian unconformity (Van Bellen et al. [11]). However, they have been penetrated in several boreholes in the Western Desert of Iraq. The Silurian (Llandovery and Wenlock) succession consists of shales with a basal hot shale unit encountered in the wells Akkas-1 and Khleisia-1 (**Figure 1**). The thickness of the basal hot shale is 19 m and occurs about 60 m above the top of the basal Silurian hot shale unit. The basal Silurian hot shale is believed to be the main Paleozoic source rock in the western and southwestern deserts of Iraq and to be

http://dx.doi.org/10.5772/intechopen.77246

the source rock of the light oil and sweet gas discovered in the Akkas field. In Akkas-1, the total organic carbon (TOC) ranges between 0.96% and 16.62%, and in Khlesia-1 it ranges from 1.0% and 9.94%, with a hydrocarbon potential of about 49 kg HC/tonne [12].

The maturation distribution is complicated by an intense Hercynian-age horst-graben relief; therefore, Silurian hot shales could be over-mature in deeper areas of the region while they are immature in shallower areas [12].

The Paleozoic hydrocarbons of the Western Desert of Iraq are almost free of H_2S and composed of up to 85% methane and ethane. Silurian shale was deposited under dysoxic to anoxic conditions in an intra-shelf basin located north of the Central Arabian Arch.

3. Methodology

Graptolite chitinozoan identification is conducted on a dark gray, indurated graptolitic shale from Silurian shale from a depth between 2213 m and 2221 m, from the Akkas-1 well, drilled in 1993 by the Iraqi Oil Exploration Company in the western desert of Iraq (**Figures 3**, **4A**). The graptolites were measured with an eyepiece graticule. For chitinozoan extraction, the standard HCl-HF-HCl processing method was employed, which was done at School of Earth and Environmental Sciences, University of Portsmouth, UK.

Samples were prepared and analyzed for the type organic matters at laboratories of Wollongong University, Australia, according to the procedures of Falcon and Snyman [13]. Five black shale samples are chosen for this part of study. Selected types of organic matters are illustrated in (**Figure 4B**, **C**).

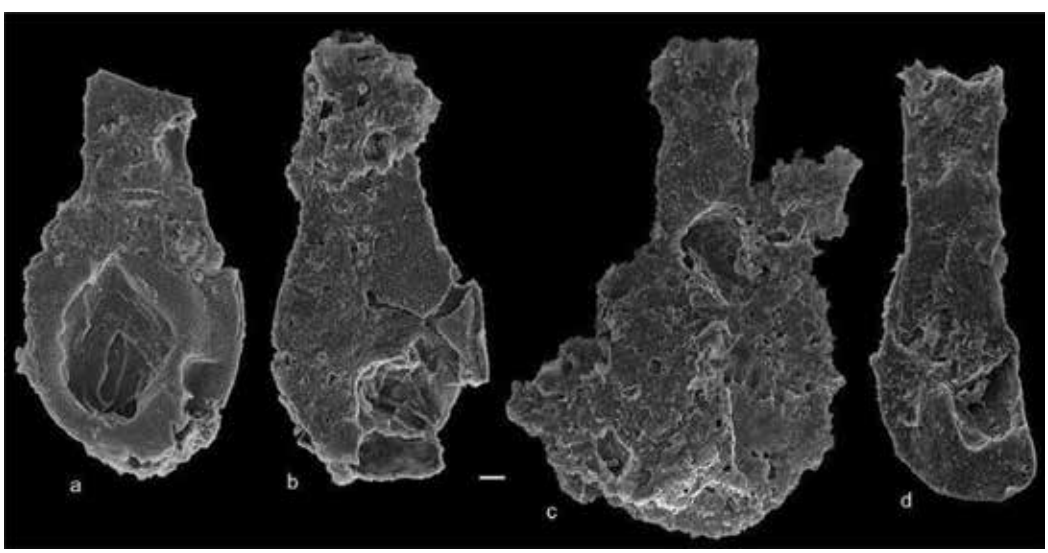

Figure 3. Chitinozoans from Silurian shale in Akkas-1 well, western Iraq; a–c: *Sphaerochitina sphaerocephala* (Eisenack [16]), d: Angochitina sp., scale bar (10 μm), after Loydell et al. [3].

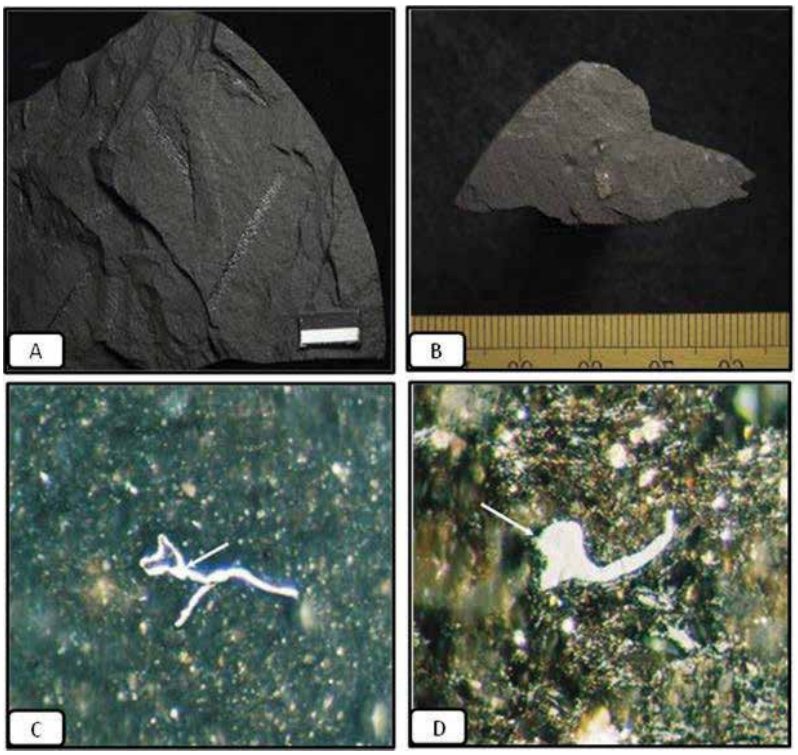

Figure 4. A: Graptolites in hand specimen of black fissile hot shale. B: Pyrite crystal in the hot shale. Both samples are from the Silurian Akkas formation, C: Tasmanite in Silurian hot shale, X50, D: Vitrinite (arrow) common with a lot of organic matter in Silurian shale, x50, Akkas formation, Akkas-1 well western Iraq.

A representative portion of each sample was manually ground to a fine powder using a ceramic mortar and pestle. The powder was packed into a recessed plastic holder and preferred orientation was minimized. The samples were analyzed using a Philips X-ray diffractometer (PW3710) scanning from 4 to 60° 2θ. Ten samples from both hot and cold shales are selected and representative diffractograms are shown in (**Figure 5**). The generator was controlled using Philips PC-APD software. Peak identification was enabled using PDF/ICCD database and quantification using Rietveld analysis using commercial program Siroquant (Sietronics, Australia). Analysis was done at laboratories of the department of Earth Sciences, Royal Holloway University of London.

A scanning electron microscope (SEM) helps identification and description of the mineral phases. The SEM also reveals their morphology, textural relationship and growth habits. SEM analyses were carried out with magnifications between 100X and 12,000X with gold-coated samples. The coater is a EDWARDS RV3, using a quartz crystal thickness monitor. Analysis was carried out at the scanning microscope unit of MTA Ankara, Turkey, using FEI QUANTA 400 scanning electron microscope from JKMRC Technical Company. Several clay and non-clay minerals were recognized in the studied Silurian shales from the same above-mentioned ten samples analyzed for XRD analysis (see **Figure 6**). TOC (total organic carbon) values (wt%) were obtained using a Leco instrument by combustion in oxygen. Samples were analyzed by Geomark Research Ltd. (Houston, Texas, USA).

http://dx.doi.org/10.5772/intechopen.77246

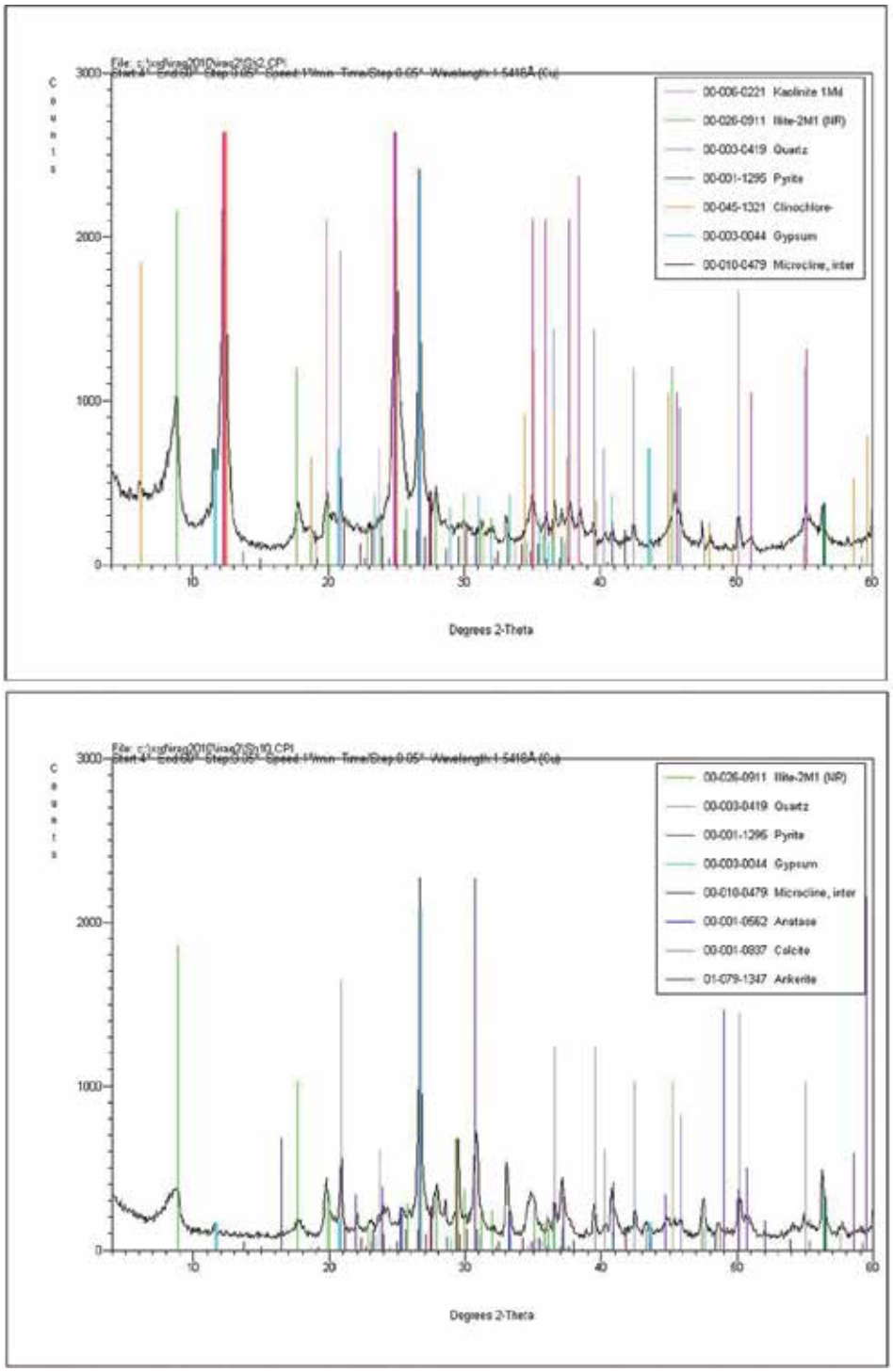

Figure 5. X-ray diffractograms for bulk hot shale sample in the well Akkas-1 (SA-1), illustrating the main clay and non-clay components. Samples represent the cold shale (upper) and hot shale (lower).

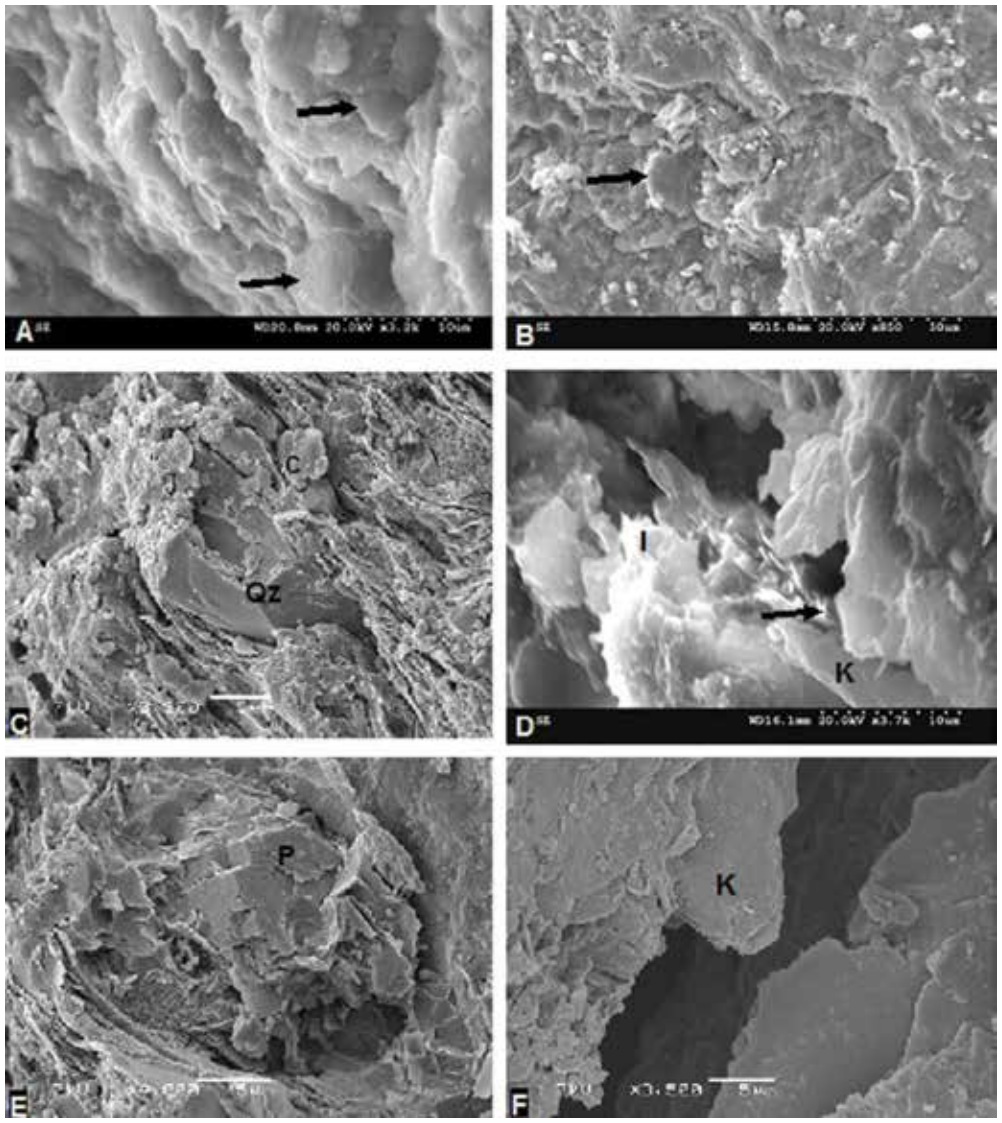

Figure 6. Scanning Electron Microscopic Images (SEM) from the hot shale, A- kaolinite hexagonal plates some are degraded (black arrows), B- illitization of kaolinite, C- Authigenic quartz (Qz) and carbonates (C), D- fine illite fibers (I and arrow) and kaolinite booklets (K). E- Cubes of pyrite (P), F- common kaolinite booklets mostly are degraded (K).

4. Significance of Silurian shale in Iraq

4.1. Stratigraphic importance

Graptolites are important index fossils for dating Paleozoic (Silurian) rocks and are used to delineate the time transgressive depositional advance of marine clastics across the Arabian Peninsula

after the melting of Ordovician glaciers. After the peak of the late Ordovician glaciations during the Hirnantian [14], ice melting led to a rapid eustatic sea-level rise and a far-reaching southward transgression which commenced during the latest Ordovician persculptus graptolite Zone. This must have been a very rapid transgression (or sediment-starved) because shallow-marine sand waves, strandlines and rippled sandstones, resulting from littoral reworking, were preserved during the transgression and were subsequently buried beneath graptolitic shales [15].

Graptolites from 'hot' shale from western Iraq demonstrate that it is of early Wenlock Monograptus riccartonensis Zone age, somewhat younger than the Llandovery age previously ascribed to it [2]. A post-Llandovery age also is indicated from chitinozoan study from western Iraq [3], (**Figure 3**).

During these short periods, a favorable combination of factors in parts of North Gondwana led to the deposition of exceptionally organic-rich shales. The Silurian post-Rhuddanian shales are, in general, organically lean and do not make a significant contribution to petroleum generation.

The restriction of the hot shales to the Rhuddanian Stage implies that palaeohighs, which during the latest Ordovician-early Silurian transgression were flooded only during post-Rhuddanian times, are likely to be devoid of the Silurian hot shales. The palaeorelief, therefore, controlled not only the timing of the onset of shale deposition but also the presence or absence and probably the thickness of the hot shales.

The environment of deposition was anoxic before, during and after deposition of the 'hot' shale, except for some very brief incursions of more oxygenated water that enabled the development of a very limited burrowing benthos and graptolite preservation as three-dimensional pyrite internal molds [3].

4.2. Petrology and mineralogy

The Silurian shale of the Akkas Formation contains common graptolites Monograptus convolutes (**Figure 4A**). A lot of organic matter is also present in addition to abundant vitrinite and pyrite (**Figure 4B**). Large fragments of vitrinite and some grainy organic matter of marine algae (Tasmanites) are also observed (**Figure 4C–D**).

The mineralogical composition of the studied shale units in western desert of Iraq is studied using X-ray diffraction (XRD) and scanning electron microscopy (SEM) techniques. The main clay minerals observed are illite and kaolinite, while the non-clay minerals include quartz, feldspars (microcline), pyrite, apatite, anatase, carbonates (calcite and rare dolomite) and ankerite (**Figure 5**).

SEM analysis shows that kaolinite is commonly present as hexagonal plates mostly are degraded (**Figure 6A**, **D**, **F**). Illite grew from precursor kaolinite (illitization of kaolinite, see **Figure 6B**), this characteristically occurs during burial diagenesis. Illite also is commonly present as fibers and fine white flakes (**Figure 6D**). Quartz is the next most common non-clay mineral observed in the studied shales. Detrital quartz grains and few diagenetic quartz overgrowths were observed using the SEM (**Figure 6C**). SEM analysis shows that the carbonates

Sample number	L. Depth (m)	Leco TOC (WT%)	S1 mg/g	S2 mg/g	S3	HI	OI	S1/S1 + S2	TMAX C	% Carbonate
Sh1	1750	0.58	0.22	0.21	0.25	36	43	0.51	385	3.7
Sh3	1895	0.33	0.15	0.51	0.24	155	73	0.23	431	6.2
Sh5	2030	0.63	0.23	0.31	0..28	49	44	0.43	401	7.2
Sh8	**2222**	**9.59**	**6.27**	**24.91**	**0.48**	**260**	**5**	**0.20**	**438**	**16.7**

Table 1. Organic geochemical results for the analyzed shale samples.

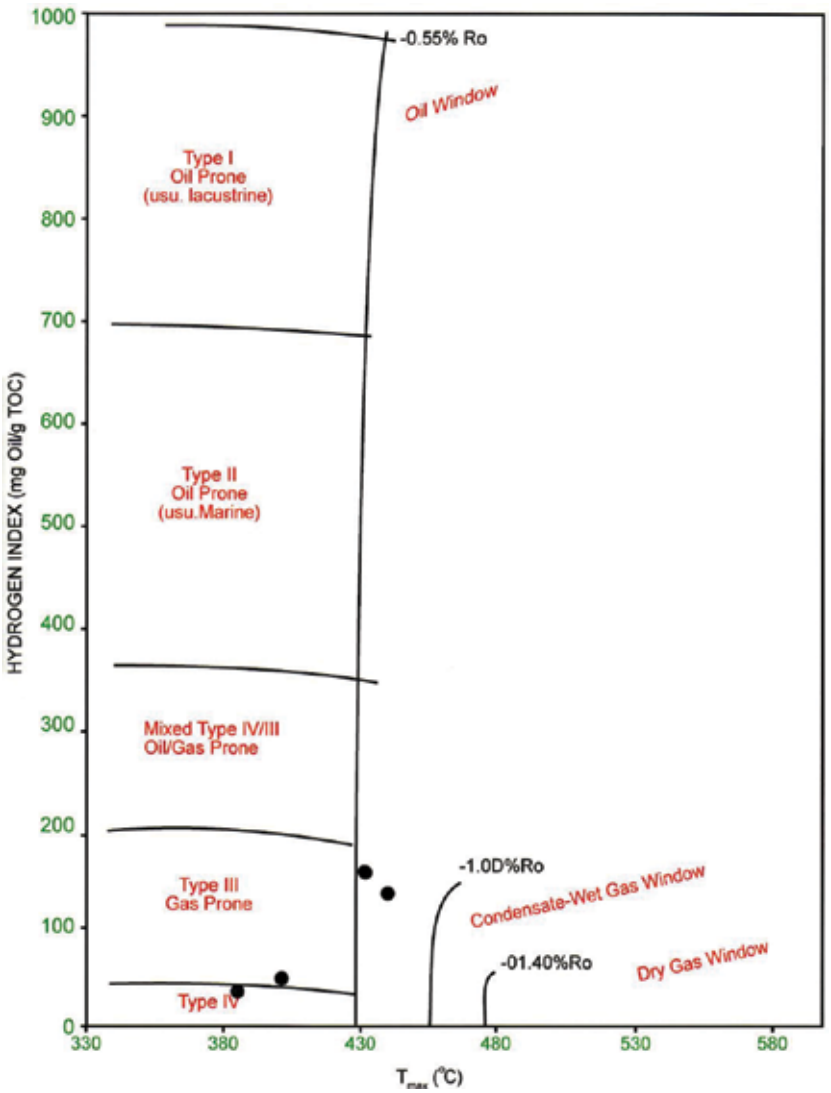

Figure 7. Plot of rock-Eval Tmax versus HI (hydrogen index) for Silurian hot shales (the right two samples) from western Iraq [17].

are either filling fractures or randomly distributed in the sample (**Figure 6C**). Pyrite cubes are also common in the Silurian hot shales (**Figure 6E**).

4.3. Hydrocarbon source rock

Paleozoic shale is organic rich and the most likely source rock of the low-sulfur, high-gravity oil, condensate, and gas in the Paleozoic rocks of western Iraq. Lithologically, similar Silurian sequences were deposited over most of the broad stable shelf of Gondwana from the Middle East to the African Sahara.

In the basal Silurian hot shale in Akkas-1, western Iraq, the TOC ranges between 0.96% and 16.62% compared to that in Khlesia-1 which ranges from 1.0% and 9.94%, with a hydrocarbon potential of about 49 kg HC/tonne [12]. The organic geochemical analysis of the hot shale is summarized in **Table 1**. In some deeper areas of the Southwestern Desert the Silurian hot shales could be over-mature, whereas in other shallower western areas, they might be immature [12]. The maturation distribution is complicated by an intense Hercynian-age horst-graben relief. The Paleozoic hydrocarbons of the Western Desert of Iraq are almost free of H_2S and composed of up to 85% methane and ethane [1].

In the present chapter, TOC value over 9% and a hydrogen index of 260 and Tmax of 438°C for the upper hot shale sample reveal that this sample could be within the oil window. Results are presented on diagrams of hydrogen index versus Tmax (**Figure 7**). These plots indicated the presence of kerogen Types II and III which is at oil-gas window maturities.

5. Hydrocarbon potential and reservoir development estimation

5.1. Hydrocarbon potential

The formations with hydrocarbon potential in Akkas field are as follows:

The Ora, Kaista and Harur formations at 1365–1424 m is a sequence of sandstone, a compact shale layer of low and medium porosity, followed by dolomite and limestone.

- The Akkas Formation at 1993–2002 m is sandstone with compact shale layers of low porosity.
- The Khabour Formation, at 2332–2360 m in Akkas-1, 2365–2375.5 m in Akkas-2, and 2341–2355 m in.

Akkas-3 (SA-3), is sandstone and compact shale layers of low porosity. The specific gravity of the tested gas was 0.726–0.6953 and of the condensate was 0.7792.

In Akkas-1 (SA-1), there are indications of light oil (density 0.8326 gm/cu cm). An Akkas-4 (SA-4) test showed gas, and the author believes condensate may also be present in this well.

Samples of cores and cuttings were collected from the Khabour, Akkas and Upper Devonian Kaista formations in wells Akkas 1–6 (SA 1–6), Khleisia-1, KH 5-6, and KH 5-1. Their diagnostic

organic matters are abundant and a few spores and chitinozoa as well as scolecodonts, graptolite siculae, cuticles and amorphous organic matter are present (see **Figures 3** and **4**) [19].

Hydrocarbon generation potential is assessed by plotting organic matter up to 16% TOC, especially the hot shale of the Akkas formation, which is very low asphaltene and sulfur. The saturated and aromatic hydrocarbons of more than 96% and high peaks of C2-C20 gas chromatography could indicate predominant gas generation with some light oils.

The associated gases are mainly methane and ethane of CH4, C4H6 and C3H8. Accordingly, source potential for wet gas and condensate could be assessed at a depth of 2750–3000 m and dry gas at a depth of 3570–3650 m in Akkas-1 only from the Khabour Formation. Little oil might be generated from the Akkas Formation in Akkas-1 (SA-1) well (**Figure 8**) [8, 19].

These potential source rocks are extended toward neighbor countries. Accumulation sites of these generated gases and a little oil could be within the sandstone porosities of 10–17% and permeability of 500 md sealed by the non-permeable shale along closures of the structured anticline fold and fault of this field as well as along the unconformity of the boundary of the Akkas Formation with the Kaista Formation.

Accordingly, Lower Paleozoic Total Petroleum System of generation, migration and accumulation that could be assessed for a basin includes West Iraq and extensions in the neighboring regions.

5.2. Formation evaluation

In Akkas-1 (SA-1), the borehole generated condensates and wet and dry gas of mainly 85% methane and ethane. Little oil could have been generated from the upper part of the Lower Silurian rocks.

Increasing thermal alteration (>170° C., TAI = 3.8) applied to rocks containing more than 0.5% TOC would be a reason for generating gas from Ordovician rocks. Trapped gas and oil could be accumulated along anticline and fault structural traps within Ordovician and Silurian sandstone's interlayers in western Iraq. **Table 2** shows summarized characteristics of the Akkas gas obtained from the tests made in the Akkas-1 well [19]:

5.2.1. Wet gas and condensate generation

The Akkas-1 borehole has total organic carbon of 0.71–1.42 wt% at 2750–3000 m.

The biodegradation and thermal alteration of the organic matter resulted in abundant amorphous organic matter (70–75%).

The Khabour B rock unit started the generation of wet gas and condensates hydrocarbons during the Mississippian time and continued until now with the expulsion quantity of 65% of its proven reserve [19].

5.2.2. Dry gas generation

The Akkas-1 borehole has TOC of 0.5–1.0% at 3570–3650 m.

http://dx.doi.org/10.5772/intechopen.77246

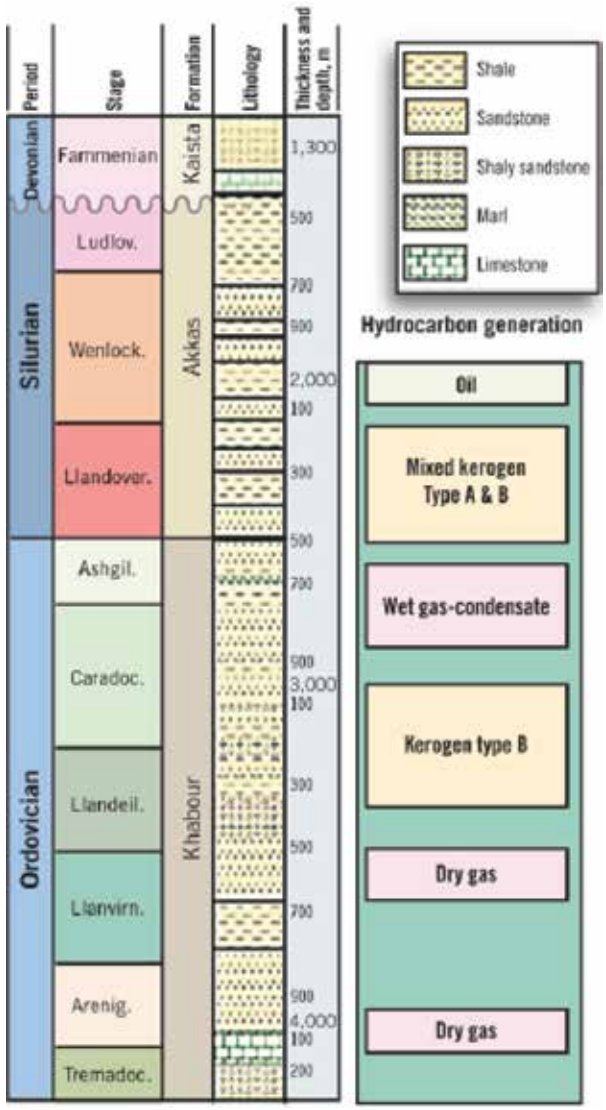

Figure 8. The hydrocarbon generation and the stratigraphy column of Akkas-1 (SA-1) well (Bujak et al. [18]).

The biodegradation and thermal alteration of the organic matter led to abundant amorphous organic matter. The analysis for this shale unit (Khabour D) gives results of starting dry gas generation during Silurian time and ended generation during late Triassic.

5.2.3. Oil generation

Potential source rocks for oil have been encountered from the Akkas Formation depths of 2280–2330 m in Akkas-1. The analyses for this lithostratigraphic unit of Akkas hot shale have resulted in no hydrocarbon generation although it has very high organic content [8, 9, 19].

5.3. Subsurface condition

Low sulfur content of the generated hydrocarbons in Akkas field could be explained by the presence of iron in these clastic marine rocks that combines with sulfur and precipitates as iron pyrites (which is found in abundance with the organic kerogen). The free sulfur content is reduced in the organic matter and in the released hydrocarbons. In addition, an increase in the geothermal gradient due to the presence of radioactive shales has caused the breakdown of long chain hydrocarbon compounds into simpler compounds forming very light oil, condensate and gas with low sulfur contents [1, 3, 19].

This was proven by the test results from Akkas-1, which has 42° gravity light oil in sandstone units at the base of Silurian and free sweet gas in the upper part of the Khabour Formation. The results of bitumen analysis from the shale source rock unit, at the base of Silurian, indicated that saturated hydrocarbons and aromatics make up 96 wt% and asphalt compounds 3.89 wt% of the extract. The saturated compounds are of low molecular weight (C2-C20) by gas chromatography and hence could indicate predominant gas generation with some light oils.

5.4. Reservoir and seal

This principal reservoir (Khabour Formation) is the oldest known sedimentary rock unit in Iraq. It consists entirely of siliciclastic sequences, comprising thin-bedded, fine-grained sandstone, quartzite graywackes and silty micaceous shale with some intercalation of dolomite and limestone.

The base of the formation, which may be more than 1000 m thick, has not been reached in wells. It was deposited in shallow marine inner to outer neritic environments that prevailed over the entire eastern part of the Arabian Plate. In Akkas field, the Khabour Formation is found at depths below 2310 m and exhibits good reservoir properties. It comprises sandstone with silty shales and has a gross thickness of approximately 38 m and an average thickness of 25 m.

Core analysis of the reservoir intervals generally indicated an average porosity of 10% and permeability of 500 md. Its depth in Akkas-1 is at 2040 m below sea level. Formation temperature is 146°C at 3300 m. The high temperature is caused by the Silurian shales' radioactivity and decreases downward in the Khabour Formation to normal gradients. The gross hydrocarbon reservoir column is about 80 m.

A secondary reservoir is provided by the Akkas Formation found above the Khabour Formation at a drilled depth of 1465–2326 m. It is comprised of a sandstone unit interbedded within the basal hot shale unit, with a gross thickness of 10 m and net thickness of 1.5 m. Core analysis of the reservoir intervals indicated porosity of 17% and a permeability of 500 md. The Akkas Formation was found to contain 42° gravity light oil only from the

GIIP	5.680 Tcf	N2	0	Wellhead Pressure	2015 lb/in2
Condesate Gas Ratio	Condesate Gas Ratio	Water Salinity	120000	Pressure at Sep.	1190 lb/in2
Cond. Gas Spec.Garv.	0.779	Gas Density at 1 at	0.89	Chock Temp.	135 F
Conden. Gas Gravity	50 API	Reservoir Temperature	210 F	Pipe temp.	130 F
Conden. Water Gas Ratio	0.20%	Reservoir Piessure	3720 lb/in2	Survey Depth	2100/3000/1000 m
Condens. H2S	0.05	Flow rate	17.3 MMscfd	Pipe lenghts to Sep.	1000 m
Gas Spec. Garvity	0.726	Flow Pressure	3045 lb/in2	Tubing Depth	2150 is 3.5 inch
CO2	0.04	Chock Size	0.5 inch		

Table 2. Published data of Akkas gas field from the Akkas-1 (SA-1) well.

thin sandstone horizon sandwiched between the hot shales at the base; it is therefore considered a minor reservoir. The overlying Silurian shale of the Akkas Formation is an effective local regional seal.

5.5. Reservoir engineering

The author's MBAL material balance model indicates that cumulative recoverable gas at Akkas would be 3.553 tscf.

A possible production profile plateau is 500 MMscfd from 50 wells and for contract; the reason can be 55 wells. Published data show many uncertainties in the reservoir like bottomhole pressure, wellhead pressure, density and downhole equipment. From published information, it is impossible to calculate the vertical lift performance (VLP) and the inflow performance relationship (IPR). The author estimated the wellhead pressure according to the given reservoir pressure of 3720 psi.

In order to design and allow for the building of reliable and consistent well models with the ability to address each aspect of wellbore modeling, PVT (fluid characterization), vertical lift performance (VLP) correlations (for calculation of flow line and tubing pressure loss) and IPR (reservoir inflow), the author used Prosper. According to the available data from Akkas-1, the Prosper model shows the absolute open flow of 214 MMscfd (**Figure 9**). It shows VLP and inflow performance relationship (IPR) with production rates of 17.4 MMscfd (**Figure 10**).

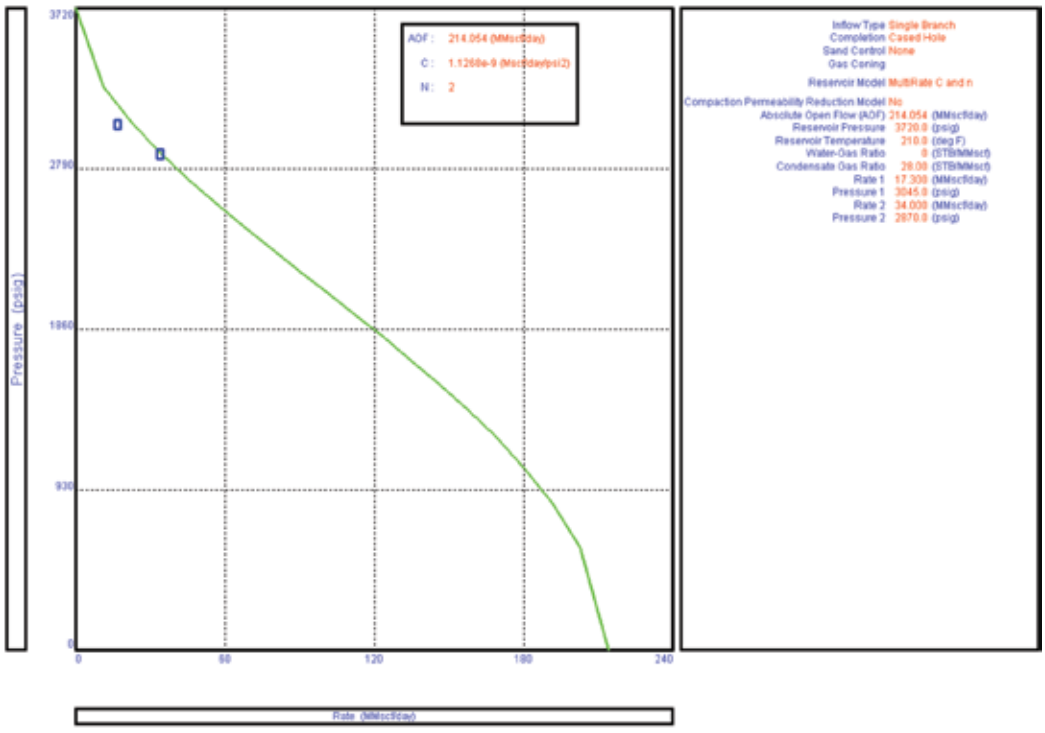

Figure 9. Absolute open flow (AOF), IPR plot multi rate C and n.

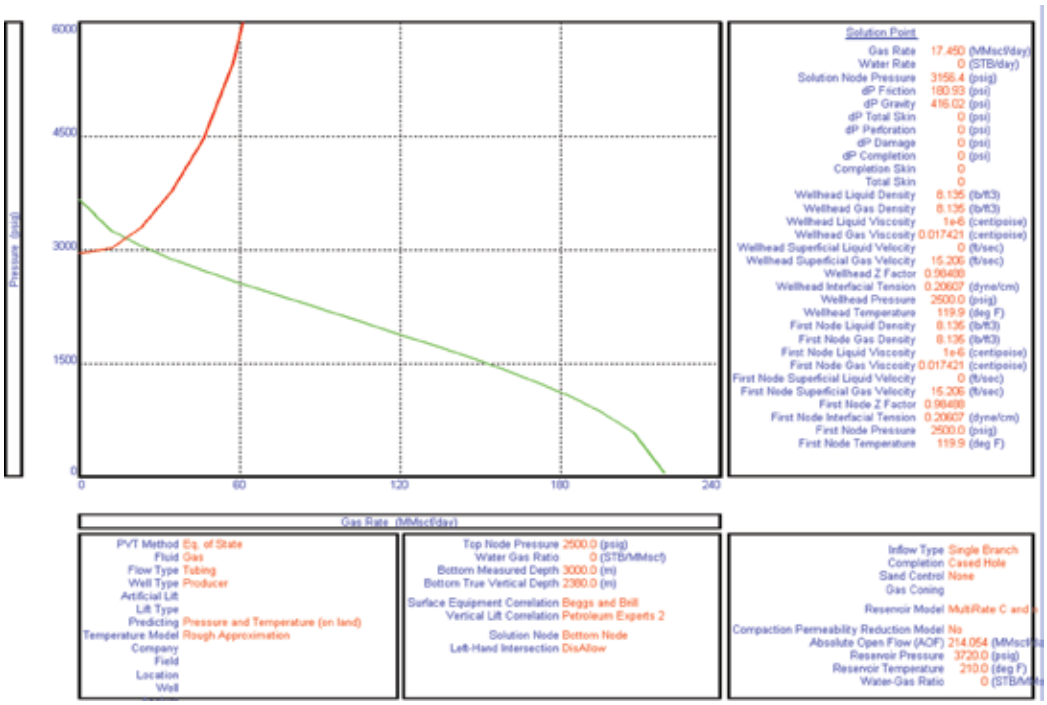

Figure 10. Inflow (IPR) versus outflow (VLP).

Efficient reservoir development requires a good understanding of reservoir and production systems.

Figure 11 shows the rough MBAL model for the tank Akkas-1 (SA-1) and extrapolated rates of the 50 wells including the five existing wells. According to the well test rates from the exploration wells, conservative average production of 10 MMscfd/well was taken.

5.6. Condensate production profile

From the extent geological knowledge of the area, the author estimated one of the deeper layers to contain recoverable condensate of 14 billion barrel (**Figure 12**).

5.7. Field development plan

Iraq proposed a strategy plan and wished to use methane to satisfy domestic power/water demand, C1-, C2-, C3-based petrochemicals for export. Ethane and propane are used for olefins production. Butane and condensates are for domestic use, export and petrochemical production.

The proposed development plan can be divided in two phases: The first phase is 250 MMscfd gas rate. Power generation and methanol use natural gas. Propane, butane and condensate are for export. The second phase is an additional 250 MMscfd gas processed including ethane recovery for olefin production.

http://dx.doi.org/10.5772/intechopen.77246

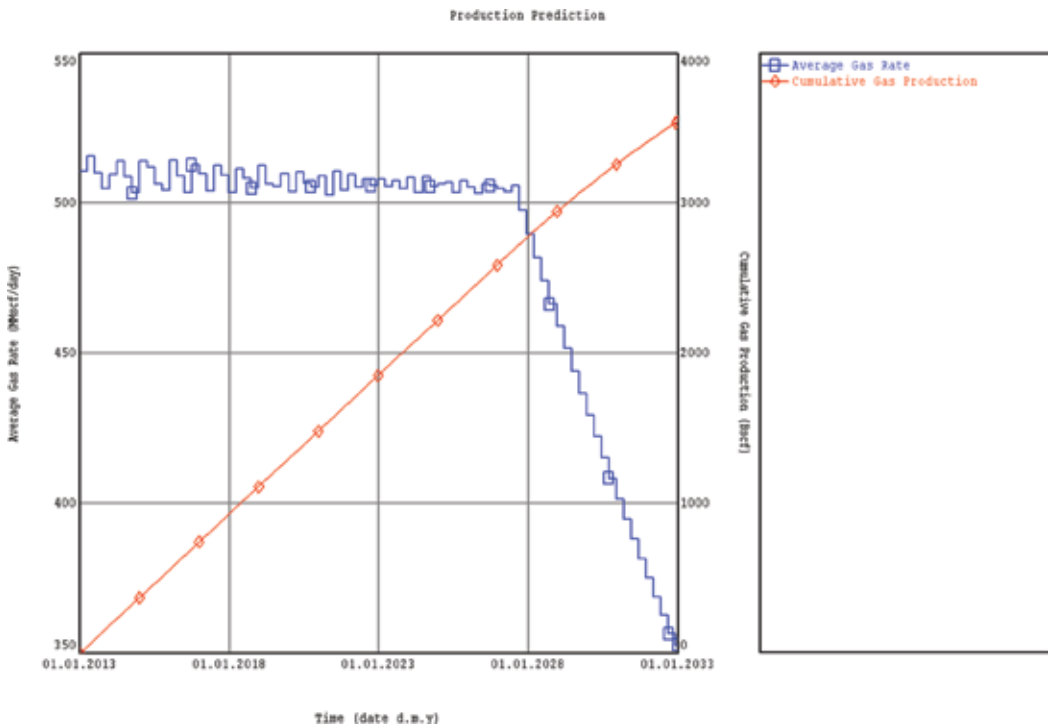

Figure 11. Production profile of the 50 production wells.

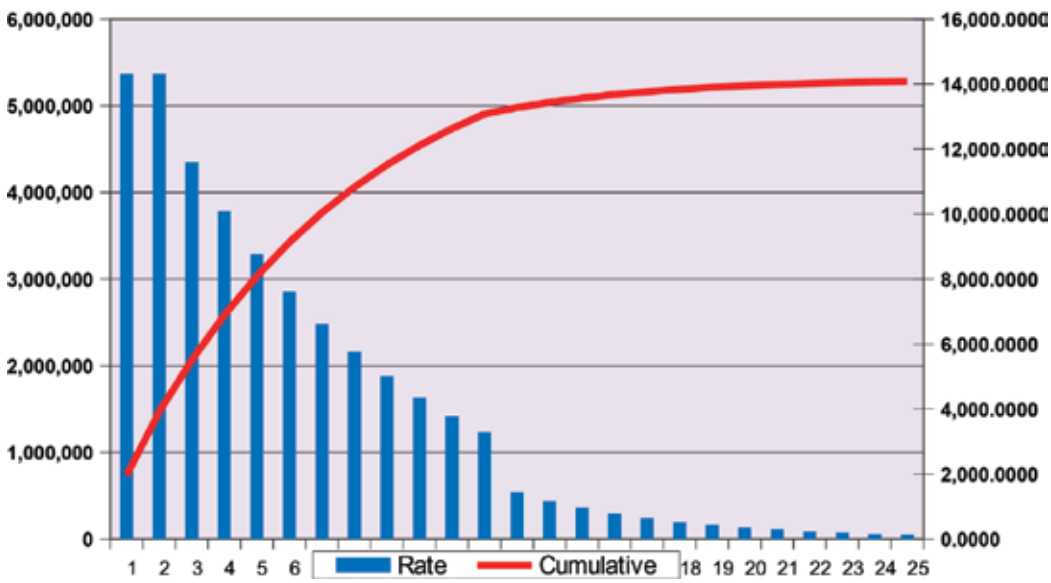

Figure 12. Estimates of condensate production profile.

Furthermore, power generation and ammonia use the incremented gas. Ethane is to be used for ethylene production, with the option to use some propane and butane. Polyethylene production is the main ethylene derivative.

5.8. Gas and condensate specifications

The samples are taken from the separator (**Tables 3** and **4**).

Reference: oil ministry Iraq, report 2004.

5.9. Central plant facility

The proposed central plant facility is according to the possible development scenarios of the field and the use of the hydrocarbon and their derivatives (**Figure 13**).

5.10. Pipelines and route connection

There are many possibilities to transport the gas and their products. The optimized way is to use the route of T1 to the Baniyas port in Syria (**Figure 2**).

5.11. Possible contract conditions

Currently the main Iraq has only the service contracts, which still do not have the approval of political actors and public organs. The term service contracts encompass those various contracts in which the host government has a contract with a service company or an international oil company for the performance of services related to the exploitation of petroleum resources.

Component	SA-1 (2332-2360m)	SA-2
N_2	1.54	0
C_1	80.49	80.5299
C_2	8.92	8.9407
CO_2	2.2	2.0683
H_2S	-	-
C_3	3.54	3.3636
I-C_4	0.4	0.3788
n-C_4	1.0	0.9898
i-C_5	0.35	0.2924
n-C_5	0.41	0.3768
C_6	0.54	0.6784
C_7	0.39	0.7881
C_8	0.22	1.593
Specific Gravity	0.726	0.787
Density 15.5, 1AT-G/L	0.89	-
Molecular Weight	21.02	22.811
Heating Value Kcal/m^3 - Gross: Net:	10702 9700	-

Table 3. Specifications of the free gas from the wells Akkas-1 (SA-1) and Akkas-2 (SA-2).

http://dx.doi.org/10.5772/intechopen.77246

Specifications	SA-1	SA-2	SA-3
Specific Gravity	0.779	0.7538	0.7448
Water Content (% by volume)	0.2	Nil	Nil
Sulphur Content (% by weight)	0.06	0.0163	0.0131
Asphalt Content	Nil	Trace	Nil
Pour Point (°F)	- 30	- 45	- 45
Kinematics Viscosity (Cst) at:			
80 °F	1.52	0.98	1.016
100 °F	1.27	0.82	0.941
120 °F	1.08	0.75	0.876

Table 4. Specification of the condensates.

The risk service contract appears similar to the production-sharing contract but differs in certain important matters. Its basic distinctive feature is that it reimburses the contractor in cash, not in crude oil or gas, although it may have provisions permitting the contractor to buy back an amount of crude oil at an international selling price equivalent to the amount to be paid to the contractor.

A pure service contract is an agreement between a contractor and a host country that typically covers a defined technical service to be provided or completed during a specific period. The service company investment is typically limited to the value of equipment, tools and personnel used to perform the service.

In most cases, the service contractor's reimbursement is fixed by the terms of the contract with little exposure to either project performance or market factors. Payment for services is normally

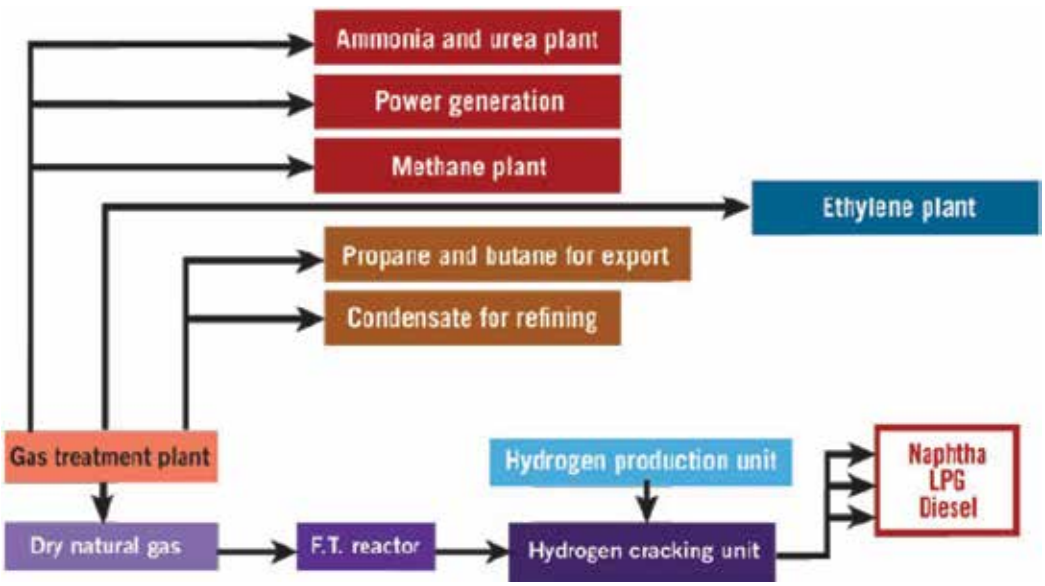

Figure 13. Possible design of the CPF, use of the hydrocarbons and their products, reference: Oil ministry Iraq, report 2004.

Year	Seismic	G&G	G&A	Drilling	Facilities Mn USD	Pipelines Mn USD
	Mn USD	Mn USD	Mn USD			
1	14	5	10	40	70	18
2	14	5	10	80	80	
3				120	60	
4				120		
5						
6						
7						
8				40		
Workover rig rates will be around $20,000/day.						

Table 5. Cost estimations of the proposed development.

based on daily or hourly rates, a fixed rate or some other specified amount. Payments may be made at specified intervals or at the completion of the service. Payments, in some cases, may be tied to the field performance, operating cost reductions or other important metrics.

These agreements are similar to the production-sharing agreements with the exception of the contractor payment. With a risk service contract, the contractor usually receives a defined share of production (in kind). As in the production-sharing contract, the contractor provides the capital and technical expertise required for exploration and development. If exploration efforts are successful, the contractor can recover those costs from the sale revenues and receive a share of profits through a contract-defined mechanism.

5.12. Cost estimation

The approximate cost estimation for Akkas development phases are illustrated in **Table 5**. The calculations have been made for operating costs, based on the gas price for October 2010.

The annual fixed operating costs for the central processing facility will be in the range of $30–40 million/year. In addition, the fixed operating costs for the existing Iraqi pipelines will be $2 million/year. The variable operating costs are 20–30¢/bbl of oil or condensate and 4.5–7.5¢/Mcf.

6. Discussion and conclusion

The Silurian hot shales are believed to be the main Paleozoic source rocks in the western and southwestern deserts of Iraq [1].

Hot shales of the Akkas Formation in the Akkas-1 well of western Iraq were deposited in anoxic-dysoxic marine shelf environment that extended across the northern margin of the Gondwana Continent characterized by provincial achritarchs, [19]. These deposits were extending from outer to inner neritic with effects of local upwelling currents. The presence

of marine algae such as Tasmanites (**Figure 4C**) and prasinophyte achritarchs [19], in the ecosystem of the lower Silurian Akkas Formation sediments could delineate highly oil-prone materials following Tyson's [20] simple classification of sedimentary organic matter types for rapid assessment of hydrocarbon potential.

According to the organic geochemical, the studied Silurian shales especially those of the hot shales could be considered as source rocks for oil in the western Iraq. TOC of 9.6 wt%, HI 260 and Tmax 438°C, and with TAI 2–3, VRo up to 1 and brown acritarch colors of (Al-Ameri, [19]).

Higher compositional organic matter contents for the marine algae Tasmanites and prasinophyte algae may hold their ability to generate light oil. In the present study, the organic matter types of algal-type Tasmanites and traces of vitrinite are common in hot shale samples from the Akkas-1 (SA-1) well (**Figure 4C** and **D**). This marine algal phytoplankton Tasmanites sp. is an important type of organic matter in the Paleozoic (Ordovician to Devonian black shales of the Appalachian basin.

They correspond to types I and II kerogen that appear to be derived from extensive bacterial reworking of lipid-rich algal debris [21]. Silurian hot shales form the main source rock in the Paleozoic sequence of western Iraq and it has regional extent in Jordan [22] Syria, Libya and Saudi Arabia [23]. Modeling of the Silurian hot shales in well Akkas-1 [12] indicates that the unit has remained in the oil generation window since Late Paleozoic times. Variation in maturation between the lower hot shales and the overlying shale horizons may relates also to the effect of the intense Hercynian-age extensional tectonics in the area under study.

Various clay and non-clay mineral constituents are observed in the Silurian shale from western Iraq (**Figure 5**). Illite and kaolinite are the main clay minerals observed, while quartz, carbonates (calcite dolomite and/or siderite, feldspars (microcline)), pyrite, rare apatite, anatase and occasional gypsum are the main non-clay minerals. Clay minerals illite, kaolinite, show an overall increase with depth especially in the lower and upper hot shale samples.

Increase in illite accompanied with organic matter increase in deeply buried shale. Transformation of smectite (suggested to be a source for the present illite since the Silurian shale is of marine origin) to I-S and finally to illite may be coeval with generation of oil in sedimentary basins. The top of most oil-bearing horizons in the US Gulf Coast Tertiary horizons occur at depth intervals where reactions, transformation and illite formation are manifested [24].

Scanning electron microscopy gives clues for better identification of the authigenic and detrital components of the studied shale (**Figure 6**). Quartz authigenic syntaxial overgrowth (**Figure 6C**) also is recorded in the studied shale. Compaction on the shale beds enhanced the transformation of smectite to illite, and thus represents a possible source for the silica for quartz overgrowth formation. Additionally, burial depth conditions may led to feldspar dissolution as well as partial and/or complete replacement of detrital silicates (quartz and feldspar) by calcite and is an alternative source for silica [25].

Pyrite is present as clusters of crystals in cubic forms or as discrete euhedral crystals (**Figure 6E**). The stagnant reducing conditions during deposition of organic matter were favorable for sulfate-reducing bacteria to reduce the sulfate ions of seawater to sulfide ions which then reacted with any available iron to form pyrite (FeS2). These conditions prevailed during deposition of the Silurian shales.

Calcite and ferroan dolomite (ankerite) also are recorded in the XRD analysis (see **Figure 5**) and some scattered carbonates (calcite) are also revealed by SEM investigation (see **Figure 9C**). Conversion of smectite to illite during burial is a common diagenetic process which is capable for releasing large amounts of Fe, Mg, Ca, Na and Si. Some of these elements may enhance late-stage dolomitization process [26].

Organic matter type of the Silurian hot shale of Saudi Arabia consists of amorphous matter, marine algae (phytoplankton), intertinite, and occasional chitinozoans and graptolites. Generally, they are dark gray to black, organic-rich, oil-prone, marine shales [27].

7. Recommendation concerning development of Akkas field

Concerning the development of the Akkas field, the inconsistency between the downhole pressure, reservoir pressure and the wellhead pressure published numbers is solved by estimation. The possible production rate and plateau is based on a conservative production development scenario. Akkas field shows very high gas rate potential. The following steps should further be taken:

- Analyze samples from Akkas wells to evaluate their biomarkers and thereby confirm the oil and gas sources in order to find other oil and gas pays in Akkas and oil and gas fields in the west of Iraq.
- Analysis of local oil seeps has been conducted to find their affinity and the structural relation to Akkas oil and gas fields. It is also possible that they lead to other oil fields that have been charged by oil migration from Mesopotamian basin to structural closures in western Iraq.
- It is important to drill deeper at least in the exploration/appraisal phases to find possible gas accumulations.

It is well known that the Iraq government would like to develop Akkas and is looking for new discoveries in the Western Desert of Iraq. This region has not yet been explored and may hold potential.

The development plan for the use of Akkas gas is more likely to serve the national grid of electricity, future and existing petrochemicals and other industrial plants. Part of the derivatives will be exported. Most likely Iraq will follow the Saudi Aramco plan that uses the gas for development of national industry and demand. Those can multiply the profits from the petrochemicals and other industries of the petroleum resources.

The Iraq government chooses the service contracts for different political and regulatory reasons (like delays or unapproved petroleum law). The long-term service contracts in Iraq are similar to PSAs, the SC is signed without the agreement of the parliaments; it can lead to escalation between IOCs and future governments in Iraq.

In order to have clean and transparent business for all participants, the IOCs should press to have the right regulation and a law to cover legal activities (investment), tax and environmental issues related to the oil industry in Iraq.

The political turbulence and mismanagement in the country make the development of the oil and gas industry and the country development questionable. There can be no concrete development of oil and gas fields without the parallel development of the infrastructure of the country; without this, turbulence may arise.

The CAPEX for the exploration and development phases and OPEX are simulated with cost simulation taking into account the security factor. Even with high contingencies, still the 4.5–7.5¢/Mcf is low compared with that of other OPEC countries.

Author details

Ali Ismail Al-Juboury[1]* and Muhammed Abed Mazeel Thani[2]

*Address all correspondence to: alialjubory@yahoo.com

1 Geology Department, Mosul University, Iraq

2 Petroleum Engineering Department, Brunel University, London, UK

References

[1] Lüning S, Craig J, Loydell DK, Štorch P, Fitches B. Lower Silurian hot shales in North Africa and Arabia: Regional distribution and depositional model. Earth Science Review. 2000;**49**:121-200

[2] Loydell DK, Butcher A, Frýda J. The middle Rhuddanian (lower Silurian) 'hot' shale of North Africa and Arabia: An atypical hydrocarbon source rock. Palaeogeography, Palaeoclimatology, Palaeoecology. 2013a;**386**:233-256

[3] Loydell DK, Butcher A, Al-Juboury AI. Biostratigraphy of a Silurian 'hot' shale from western Iraq. Stratigraphy. 2013b;**10**(4):249-255

[4] Al-sharhan AS, Nairn AEM. Sedimentary Basins and Petroleum Geology of the Middle East. Amsterdam: Elsevier; 1997. p. 978

[5] Al-Hadidy AH. Paleozoic stratigraphic lexicon and hydrocarbon habitat of Iraq. GeoArabia. 2007;**12**(1):63-130

[6] Klemme HD, Ulmishek GF. Effective petroleum source rocks of the world: Stratigraphic distribution and controlling depositional factors. American Association of Petroleum Geologists Bulletin. 1991;**75**:1809-1851

[7] MacGregor DS. The hydrocarbon systems of North Africa. Marine and Petroleum Geology. 1996;**13**:329-340

[8] Abd Alwahab NS. Basin analysis of Paleozoic succession, Iraq. Unpublished PhD thesis. Iraq: Mosul University; 2013. p. 234

[9] AlShalchi W. Development of Akkas Gas Field in Iraq. Jordan: Amman; 2008. p. 33

[10] James EF, Ahlbrandt TS. Petroleum geology and total petroleum systems of the Widyan Basin and interior platform of Saudi Arabia and Iraq. United State Geological Survey Bulletin, 2202-E; 2002, 26p

[11] Van Bellen RC, Dunnington H, Wetzel R, Morton, DM. Lexique Stratigraphique International, Paris, Centre National recherché Scientifique Fasc 10a, Iraq; 1959: 333p

[12] Aqrawi AAM. Paleozoic stratigraphy and petroleum systems of the western and south-western deserts of Iraq. GeoArabia. 1998;**3**:229-248

[13] Falcon RMS, Snyman CP. An introduction to coal petrography: Atlas of petrographic constituents in the bituminous coals of southern Africa. The Geological Society of South Africa. 1986. 27p

[14] Brenchley PJ, Marshall JD, Carden GAF, Robertson DBR, Long DGF, Meidla T, Hints L, Anderson TF. Bathymetric and isotopic evidence for a short-lived late Ordovician glaciation in a greenhouse period. Geology. 1994;**22**:295-298

[15] Beuf S, Biju-Duval B, De Charpal O, Rognon D, Gariel O, Bennacef A. Les gres du Paleozoique inferieur du Sahara: Sedimentations et discontinuities, evolution structural d un craton. Paris: Editions Technip; 1971

[16] Eisenack A. Neue Mikrofossilien des baltischen Silurs. II. (Foraminiferan, Hydrozoen, Chitinozoen u.A.). Palaeontologische Zeitschrift. 1932;**14**:257-277

[17] Thompson CL, Dembiki HJ. Optical characteristic of amorphous kerogen and the hydrocarbon generation potential of source rocks. International Journal of Coal Geology 198;**6**: 229-249

[18] Bujak JP, Barss MS, Williams GL. Offshore East Canada's organic type, color, and hydrocarbon potential. Oil Gas Journal. 1977;**75**:198-201

[19] Al-Ameri TK. Palynostratigraphy and the assessment f gas and oil generation and accumulations in the lower Paleozoic, western Iraq. Arabian Journal of Geosciences, Springer. 2010;**3**(2):155-179

[20] Tyson R. Palynofacies analysis. In: Jenkins DJ, editor. Applied Micrpaleontology. Dordrecht: Kluwer; 1993. pp. 153-193

[21] Peters KE, Moldowan JM. The Biomaker Guide. Englewood Cliffs, New Jersey: Prentice Hall; 1993. p. 363

[22] Lüning S, Shahin Y, Loydell J, and et al. Anatomy of world-class source rocks: Silurian organic rich shales in Jordan. Proceeding of the 8th Int. Conf. of Jordanian Geol. Assoc, abstract; 2004: 71p

[23] Al-Ameri ThK. Palynology, biostratigraphy and palaeoecology of subsurface mid. Paleozoic strata from the Ghames Basin, Libya, PhD thesis. Kings College London; 1980

[24] Eberl DD. Clay mineral formation and transformation in rocks and soil. Philosophical Transactions. Royal Society of London. 1984;**A31**:241-257

[25] McBride EF. Quartz cement in sandstones: A review. Earth Science Reviews. 1989;**26**: 69-112

[26] McHargue TR, Price RC. Dolomite from clay in argillaceous or shale associated marine carbonates. Journal of Sedimentary Research. 1982;**52**(3):873-886

[27] Cole GA, Halpern HI, Aoudeh SM. The relationships between iron–sulfur–carbon and gamma-ray response, Silurian basal Qusaiba shale, northern Saudi Arabia. Saudi Aramco Journal of Technology, Fall-Winter. 1994/95:9-19

Chapter 4

Current Technologies and Prospects of Shale Gas Development in China

Yunsheng Wei, Ailin Jia, Junlei Wang,
Yadong Qi and Chengye Jia

Additional information is available at the end of the chapter

http://dx.doi.org/10.5772/intechopen.76054

Abstract

Shale gas in China has realized the great-leap-forward development because of the significant strides of development technique for marine shale resource, becoming the second largest shale gas producer only to the USA. Benefits from the progress of technique advance, a complete technique series for the development of shale resource buried less than 3500 m has been established by operating technique research and field trail, including five main key techniques of geological evaluation, optimum and fast drilling, multistage hydraulic fracturing, productivity evaluation, and development parameters optimization. At present, shale resource in China has not been fully exploited besides the marine shale resource (<3500 m). It would be the future development trend to enhance ultimate recovery of shale gas (<3500 m). Moreover, two-thirds of recoverable resource are stored in the formation (>3500 m). With the further process of development technique for marine shale, shale gas is expected to the single type of gas reservoir contributing to the highest annual production rate in the near future. Therefore, based on the success in shale industry, this work is organized by reviewing the advances and challenges of current evaluation techniques, and then discussing the possible development trend of shale gas performance evaluation in the future.

Keywords: shale gas, reservoir characteristics, productivity evaluation, horizontal section length, fracture parameter, development well spacing, production system

1. Introduction

China has abundant organic-rich shale resource, and there is 31.6×10^{12} m^3 technically recoverable reserves (predicted by EIA [1]), ranking the second only to the USA. China has

already become one of few countries besides North America making breakthrough in the aspect of shale gas development. Especially for the last 2 years, China has greatly promoted the shale gas development, annual production rapidly increasing from 2×10^8 m^3 in 2013 to 45×10^8 m^3 in 2015, and become the second largest shale gas producer only to the USA [2, 3]. In the structure of total natural gas output in China, shale gas has surpassed the coalbed methane (CBM) and becomes the second largest gas reservoir type only to tight gas.

Shale gas industry in China has realized the great-leap-forward development because of the significant strides of development technique for marine shale resource. Encouraged by government investment and subsidy policy during the 12th five-year plan, a complete technique series for the development of shale resource buried less than 3500 m has been established by operating technique study and field trail, including five main key techniques of geological evaluation, optimum and fast drilling, hydraulic fracturing, productivity evaluation, and development parameters optimization (**Figure 1**). These technique trials and applications result in enhancing production rate of gas well and reducing investment costs on single well, which has laid the technical foundation of large-scale development of shale resource.

Although shale gas enjoys vast development prospects in China, shale resource in China has not been fully exploited besides the marine shale resource buried less than 3500 m, a very low development degree. Considering the supply–demand relation in the natural gas market in China, it would be the future development trend to enhanced ultimate recovery of shale gas. Moreover, two-thirds of recoverable resource are stored in the formation buried more than 3500 m [4, 5]. With the process of development technique for marine shale and the breakthrough of development technique for land and transitional shale with large areas in the northern China, shale gas is expected to the single type of gas reservoir contributing to the highest annual production rate in the near future.

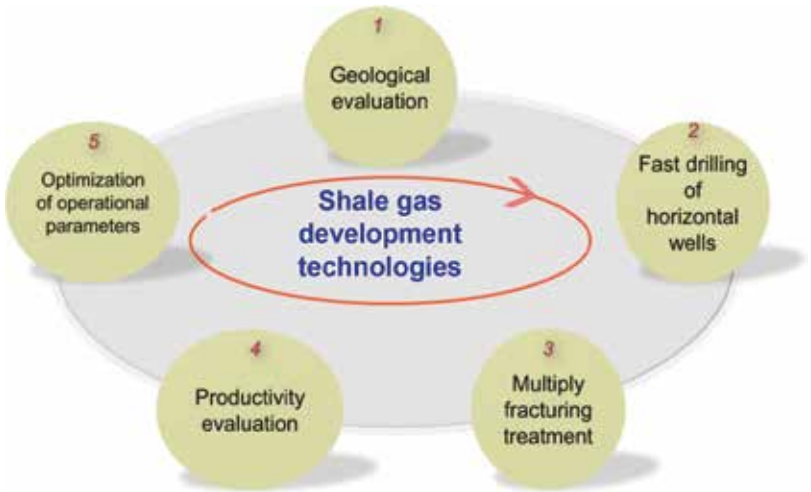

Figure 1. Schematic diagram of shale gas development technologies.

This chapter compares the shale gas developing conditions between China and the United States, reviews the developing practice and technological innovations and gives a summary of progress in key technologies of evaluating shale gas development in the past few years, in the hope of providing instructive references for the development of China's shale gas industry.

2. Development status of China's marine shale gas

Shale gas exploration and development in China have made a great breakthrough during the 12th five-year plan period. A series of major theories, systematic innovations and technology progresses fueled commercial development of China's shale gas from 2014 to 2015. By the end of 2015, 198 evaluation wells, 393 horizontal wells of marine shale gas had been finished, 267 wells had been fractured and put into production, with the productivity of 77×10^8 m^3, and three marine shale gas demonstration areas, Fuling, Changning-Weiyuan and Zhaotong had been built [2, 6].

The selection of "sweet spot," optimized and accelerated drilling and volume artificial fracturing technologies have made major progress through research and test during the 12th five-year plan, which has supported the transition of invalid resource to effective production, lowered the total investment of single well from 100 million Yuan in the early days to 7 0 million Yuan now, and brought about the rapid increase of shale gas production from 12.8×10^8 m^3 in 2014 to 44.6×10^8 m^3 in 2015. How to translate effectively production into scale production is the most important research direction in the 13th five-year plan period.

According to the characteristics of marine shale gas in southern China, CNPC and SINOPEC have come up with the four modes of efficient exploration and development, "well deployment on wellpad, factory drilling and fracturing, skid-mounting of production and storage equipment, and integrated organization and management." They have also worked out "cooperative evaluation, development test stage, and scale development stage" three kinds of scale development regimes for shale gas, which have promoted the technical progress, lowered cost and increased efficiency.

- In the stage of cooperative evaluation stage (2007–2011), the main work was focus on explorating technologies for shale gas development, and building out shale gas development strategies.
- In the stage of development test stage (2012–2015), the main technologies for shale gas development were developed, tested and determined rapidly, and single well production and EUR were increased rapidly.
- In the stage of scale development stage (2016-), single well production and EUR kept increasing steadily, and development technologies were optimized continuously. As a result, annual production is increased rapidly.

In summary, the shale gas production has increased rapidly in China since 2013, similar to the historic period of tight gas from 2005 to 2008 [7], as shown in **Figure 2**. As a consequence,

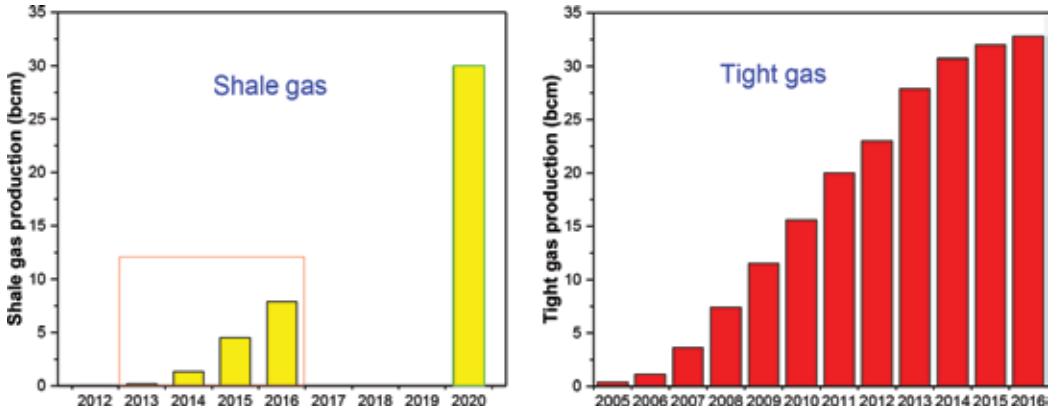

Figure 2. Comparison of annual production and forecast of shale gas and tight gas in China.

recoverable resources have been proved, daily production of single well almost doubled, and the development costs declined.

3. Current status of applied techniques in shale gas development

3.1. Geologic evaluation of marine shale gas in China

Shale reservoir description is characterized by acquiring, processing and interpreting 3D seismic and logging data from shale in mountainous area. As a result, high-quality shale interval in vertical distribution and sweet spot in lateral distribution are recognized by integrating comprehensive geological evaluation technology with outcrop, core, geochemical data and sedimentary setting model. These techniques provide guidance for the target optimization of drilling horizontal well and the mass arrangement of multiwell pad.

Seismic survey. An integrated technique has been established to conduct 3D seismic acquisition, process and interpretation as shown in **Figure 3**. Here, 2D seismic technique is used to perform structure evaluation and predict reservoir-characterized parameters [8]. After using this integrated technique, the consistency of parameters prediction with actual parameters is up to 80% in 3D seismic acquisition areas.

Well logging. China has conducted independent development of LWF (Logging While Fishing) technologies, as shown in **Figure 4**. As a result, the interpretation of parameters such as TOC, porosity and gas content has the consistency of up to 90%.

Reservoir evaluation. Geological evaluation is performed on the basis of flow unit appraisal (**Figure 5**). The gas bearing layer is the lower part of the Longmaxi Formation with thickness of 30 m. The drilling target has been optimization to the lower zone with thickness of 15 m. Reserve abundance is reevaluated: the development zone has average abundance of 0.45 bcm/km^2, the lower unit is 1.2 bcm/km^2.

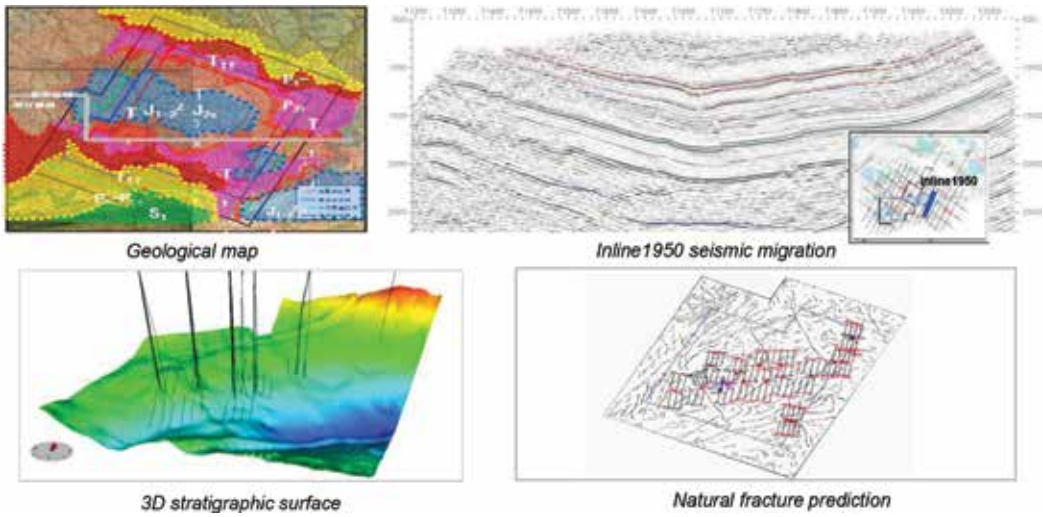

Figure 3. Technical frame of integrated 3D seismic interpretation.

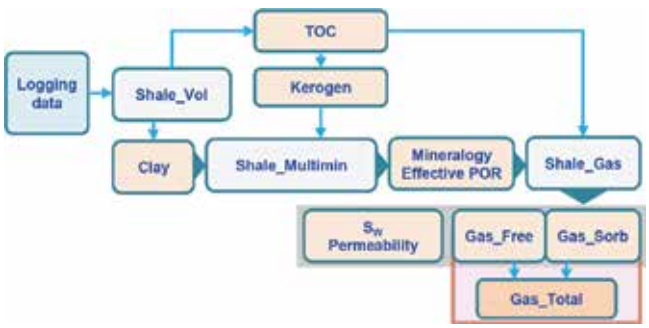

Figure 4. Shale gas well logging interpretation flow chart.

As a result, stratigraphy was correlated by using logging and core data, and Longmaxi Formation is divided into three members according to the characteristics of lithology, fossils and logging curves [9, 10]. We find that Longmaxi Formation and its favorable reservoirs are stable in thickness, which make good targets for horizontal wells; the good seal condition leads to an abnormal high pressure, which is the key to high production; The carbonaceous or siliceous shale with abundant organic matters, which deposited in restricted or semi-restricted sea basin, is ideal as favorable reservoirs (sweet spots). In addition, geological factors such as TOC, gas content, porosity and pressure coefficient control the quantity of resources (geological sweet spots), and engineering factors such as brittleness, Young modulus and Poisson ratio control the fracturing efficiency (engineering sweet spots), seen in **Figure 6**.

3.2. Fast drilling of horizontal well

It was not until 2013 that there was a total shit to horizontal wells for developing shale in the Changning-Weiyuan shale as well as other China shale basins that followed. Now that the

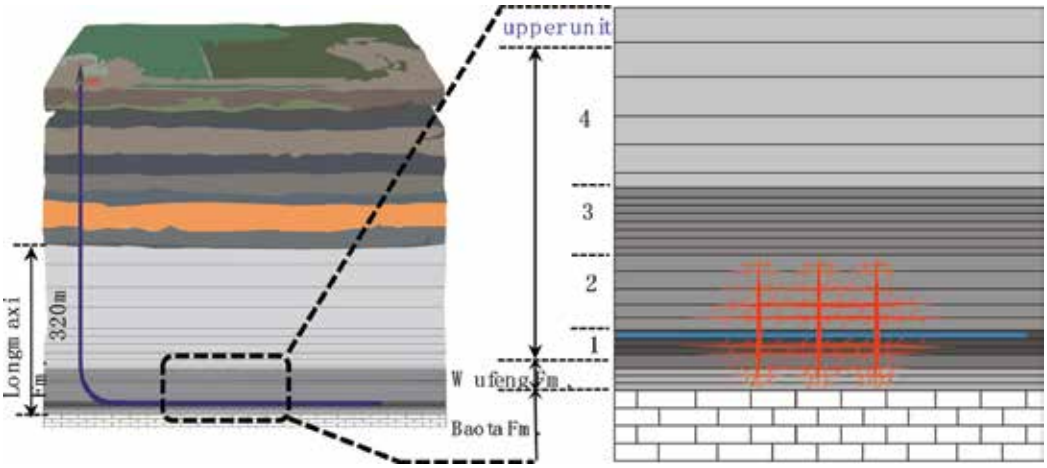

Figure 5. Stratigraphy structure and OGIP evaluation for producing layers in Changning area.

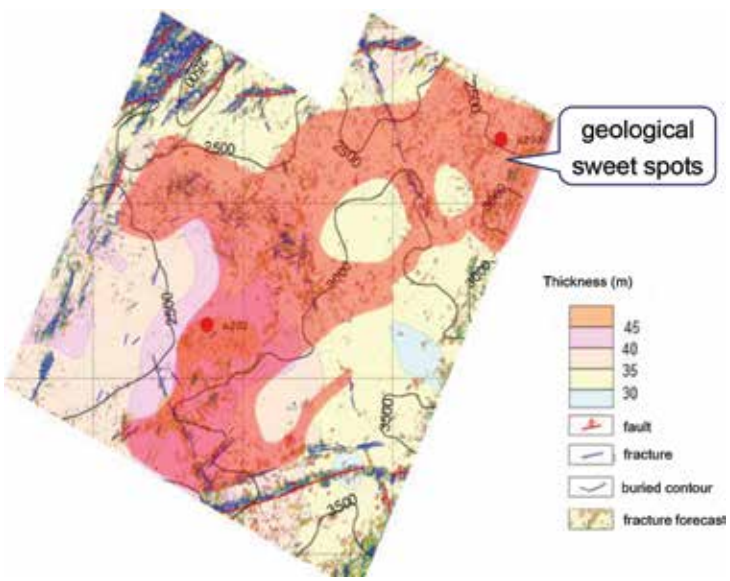

Figure 6. Sweet spots prediction based on 3D seismic interpretation.

template has been set for shale gas drilling in China, service companies have been successfully reducing drilling costs through optimized drilling and new technology [11]. The advance of drilling technique makes the drilling cycle reduce from 139 to 69 days with the help of hole structure optimization, straight hole high-efficiency motor, individualized PDC bits, rotary steerable drilling system, gas factory drilling progress management (**Figure 7**).

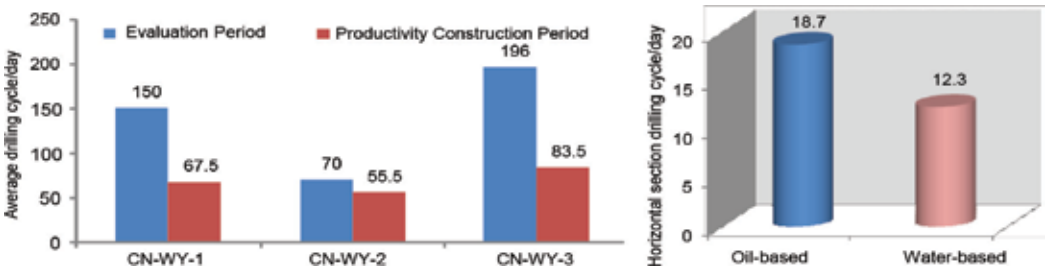

Figure 7. Drilling cycle of different period.

Listed in the following are some of the current typical practices used for drilling horizontal wells:

- Optimum lateral lengths are now preferred over "longer lateral lengths. "Length of horizontal sections varies from play to play, and ranges from 1500 to 2000 m for main shale play.
- High-efficiency water-based drilling fluid was also chosen prior to drilling the curve and lateral to reduce the environmental risks. It is understood that most international horizontal wells will be probably be drilled with water-based drilling fluid.
- Mud weights depend on formation, which range from normal to overpressured.
- Poly-diamond crystalline (PDC) bits were used by oil companies in China.
- Wells are drilled in the direction of minimum horizontal stress.
- The practice of pad drilling (6–8 wells per pad) was quickly adopted by China operators, and currently over 90% shale wells are being drilled from pads.
- The "drilling cost "constitutes 40–50% of the total well cost.

3.3. Multiple fracturing treatments

Fracturing the rock and propping open the induced fractures creates high permeability pathways, which allows the reservoir formation to produce at much higher flow rates than it could naturally [12]. As shown in **Figure 8**, China has built a framework of volume fracturing by integrating zipper-style volume fracturing using high-displacement low-viscosity slick water, low-density moderate-intensity proppant and soluble bridge plug. As a result, the testing production is increasing from 105,000 to 163,000 m^3/d through, and Gas factory reduces the drilling cycle by 30%, and increases the fracturing efficiency by 50%, which reduces the fracturing cycle of half-platform to 30d.

Listed in the following are some of the current typical practices used for hydraulic fracturing:

- high-displacement low-viscosity slick water has the ability of providing sufficient propped flow capacity to develop a gas productivity shale, and overcoming the tendency of the proppants to settle.

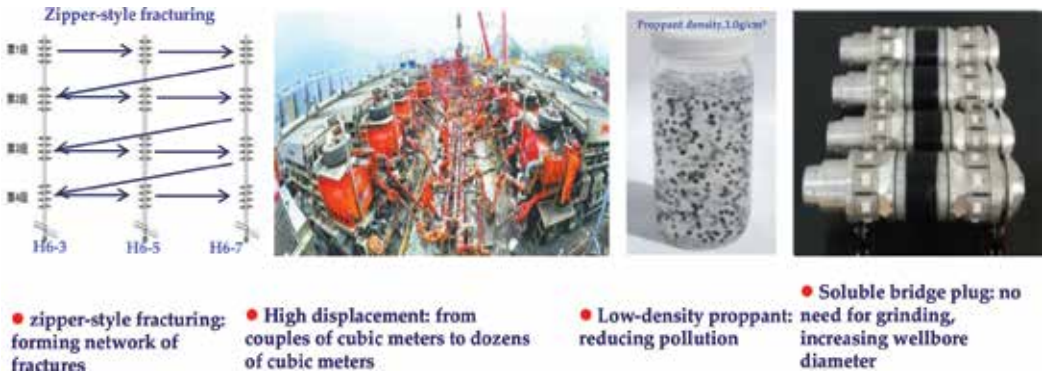

Figure 8. Framework of integrated fracturing techniques.

- Up to three wells could be zipper fractured, although no documentation could be found on more than two zipper fractures at a time. Brittleness of the shale likely has some control on the success of zipper fracturing.

3.4. Productivity evaluation technologies of shale gas

It is critical for investors to investigate the potential benefits and prospective risk in order to determine whether the given shale source should be invested. Performance evaluation is an integrated technique of well testing, production data analysis for quantitatively extracting reservoir (i.e., gas-in-place and reservoirs permeability) and stimulation information (i.e., fracture properties), based on incorporating the statistic data from geoscience research, production log, lab measurement, micro-seismic, well completions and stimulation, and the dynamic data from historical pressure/rate surveillance [13, 14]. This aims at calculating reserves and estimated ultimate recovery (EUR), forecasting future production for prospect analysis, and optimizing the development of shale gas field, and highlighting effectiveness, economy and convenience.

China has present a probabilistic methodology (**Figure 9**), which incorporates the risk and uncertainty with the complexity of flow mechanisms and fracture networks when evaluating shale gas performance.

The method is described for integrated use of newly developed empirical model and modified analytical model incorporating pseudo-variables accounting for changes in fluid properties and reservoirs properties and in operational conditions (variable flow rate and flowing pressure), which is threefold. (1) Establish reliable equations of parameter combinations by dynamic data analysis and linear regression method ($x_fK^{0.5}$ is a constant). (2) Determine the probability distribution model of fundamental parameters such as formation thickness and permeability, etc., by statistical analysis (**Figure 9a**), it is worth noting that the lower limit of permeability is from core testing and the upper limit is determined by the formula of radius probing [12]. (3) Sample randomly from the permeability values based on stochastic simulation to calculate the unknown parameters combined with constraint equations. (4) Rearrange the results from

http://dx.doi.org/10.5772/intechopen.76054

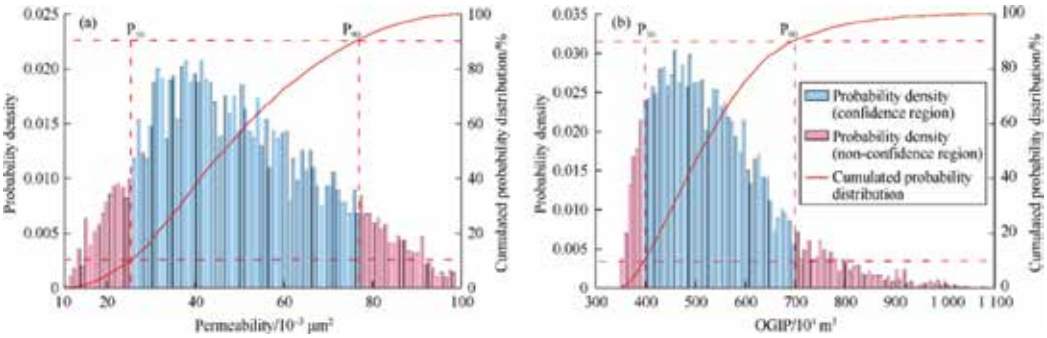

Figure 9. Permeability and OGIP versus confidence region.

small to large, to get the probability distribution and corresponding confidence range of unknown parameters (**Figure 9b**).

The production performance of shale gas wells was predicted with the linear flow model, based on the permeability and controlled reserves of single well at the probability of P10, P50 and P90, furthermore, quantitative risk assessment of production dynamic and cumulative production were performed (**Figure 10**). Average cumulative production of single wells at P50 is $(0.6–1.0)\times10^8$ m^3 according to the production data of 270 stimulated horizontal wells in China (**Figure 11**).

3.5. Parameter optimization technologies for shale gas development

Technology demands of shale gas well development can be basically satisfied by combining geological evaluation, drilling, fracturing and productivity evaluation technologies, but to realize reasonable development of shale gas, the length of horizontal section, fracture placement, production systems and well spacing need to be optimized.

Optimization of horizontal section length and fracture parameters. Optimizing the fracture parameters of horizontal wells requires an integrated optimization of several parameters simultaneously. Gas well productivity is strongly influenced by the horizontal section length

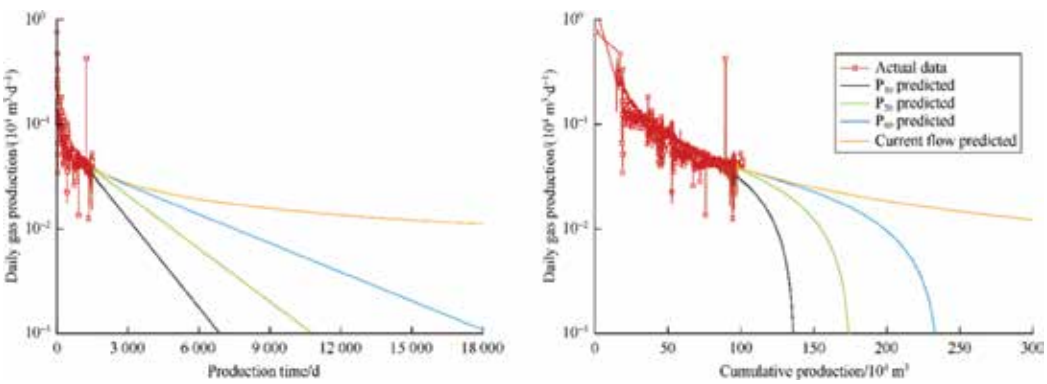

Figure 10. Prediction of production performance at different confidence levels.

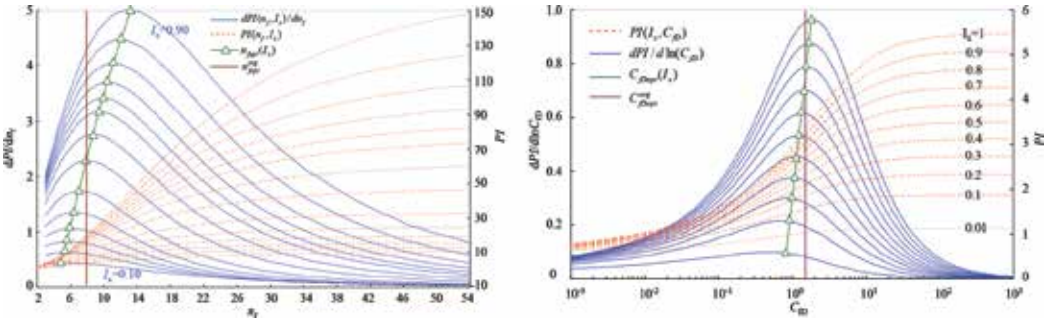

Figure 11. Prediction of productivity performance at different proppant number.

of the fractured well, number of fractures, flow conductivity and fracture length [15]. The optimization idea is: (1) enlarging the contact area between the fracture network system and formation by increasing the fracture number and length; (2) balancing the relationship between inflows and outflows of fracture network through adjusting the limited fracture conductivity; (3) reducing the interference between fractures by regulating the fracture spacing and relative location with the closed boundary. The relationship of multiple fracture parameters is shown in **Figure 12**.

In addition, shale gas development is marginal in benefit now, so the costs of various engineering links are stringent, and parameters of horizontal well and fracturing should be comprehensively demonstrated by combining the theoretical research and actual operation conditions.

Optimization of well spacing. At present, horizontal well deployment from wellpad, factory-like drilling and fracturing, and large-scale continuous operation are widely adopted in drilling shale gas horizontal wells. If the well spacing is too large, some remaining gas reserve will be left behind forever; on the contrary, if the spacing is too small, the cumulative production of single well will decrease, which will lower the development economic benefit. The production

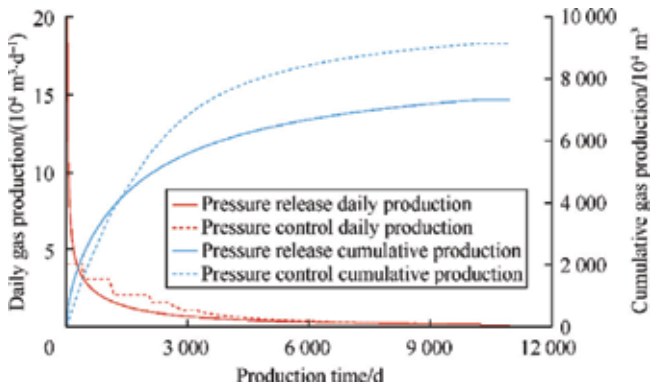

Figure 12. Comparison of predicted production between pressure release and pressure control production system considering stress-sensitivity.

Area	Horizontal section length (m)	Well controlled area (km^2)	Average well controlled area (km^2)	Average well spacing (m)	Proppant dosage of single stage (t)
Barnett	1219	0.24–0.65	0.45	280	129.7
Haynesville	1402	0.16–2.27	0.50	260	162.3
Marcellus	1128	0.16–0.65	0.42	260	181.2
Eagle Ford	1494	0.32–2.59	0.60	300	112.6
Southern Sichuan Basin	1448	0.36–1.10	0.65	400–500	97.5

Table 1. Comparison of well spacing between typical areas in Southern Sichuan and the United States.

history of China's shale gas is short, and the well spacing is determined mainly based on micro-seismic monitoring results in the early stage of development. But the monitoring of test production performance to date shows that the well spacing determined from micro-seismic monitoring is too large [16]. It can be seen from **Table 1**, compared with the four major shale gas fields in the United States, the average proppant dosage of single stage in shale gas developing areas of south Sichuan Basin is much lower. Besides that, the length of fracture is shorter due to the bedding restriction. Therefore, reasonable well spacing should be smaller [17, 18]. Development well spacing should be optimized through theoretical study, interference well-testing and dynamic data analysis, in combination with field test.

Optimization of production system. Barnett and Marcellus shale gas fields are produced in free pressure release and large pressure difference mode. In contrast, in Haynesville shale field, because of high formation pressure and pressure-sensitivity of the shale formation, the wells are produced at controlled pressure and production [19, 20]. Shale gas plays of CNPC have high pressure in general, so wells in Changning and Weiyuan are producing at big pressure difference, while wells in Zhaotong area are producing at controlled pressure and production. Since the two demonstration areas take different fracturing technologies, they cannot be compared quantitatively. Theoretically, pressure release production will lead fast pressure drop in major fractures, consequently, pressure sensitive effect will cause rapid permeability decline in areas around the major fractures, thus the fast formation of reservoir damage area, which would forbid peripheral gas getting into the major fractures and cause production decrease of well (**Figure 12**). Numerical simulation based on the data of production wells shows that different production systems differ widely in cumulative production (**Figure 7**); and pressure controlling production gets 28% higher cumulative production than pressure release production. Therefore, comparison test between nearby wellpads or wells in the same wellpad could be conducted to select the better production system.

4. Development prospects and technical direction of shale gas

As a new source of energy, shale gas has huge exploration and development potential. According to the latest evaluation of CNPC shale gas project team of nation project on oil & gas, recoverable

resources of marine shale gas in southern China are $8.82\times10^{12}m^3$, in which 2.10×10^{12} m^3 are in Fuling, eastern Sichuan Basin, and 4.37×10^{12} m^3 in Changning, Weiyuan, Fushun-Yongchuan, Zhaotong, in southern Sichuan Basin. With the promotion of geologic theories and progress of technologies in China, the marine shale gas production is expected to reach 300×10^{12} m^3 by 2020; the shale gas is likely to become the most productive type of natural gas by 2030. But due to the complex geological conditions in China and the current low prices of oil and gas in the world, large-scale efficient development of China's shale gas is facing lots of problems.

Theories of China's shale gas are still not complete, and comparative studies between sub-layers and regions need to be deepened further. Although existent studies have revealed the basic laws and features of shale gas accumulation, in such studies, shale formations are often taken as homogenous reservoirs, differences between different layers and areas have not been examined carefully; therefore, calculation of reserves and selection of production relay block lack effective guidance.

Percolation mechanism and shale gas productivity evaluation methods based on the artificial fracture network and nanometer pores should be further improved. Pores in shale are mostly nanoscale, which lead to gas flow state different from conventional reservoirs, especially in complex fracture network system created by volume fracturing, the combined effect of multiscale flow space and nanoeffect makes the flow space description and seepage pattern characterization very complex, and brings about huge challenge to productivity evaluation.

The key technologies of shale gas development have not finalized. Development policies are essential issues for scientific and efficient development of oil or gas fields. For example, well spacing influences the ultimate recovery of gas reservoir, production system affects the cumulative production of single wells. The determination of these key technology policies only depend on theoretical analysis and simulation so far, because of the deficiency of practical data or big error caused by improper test methods. Therefore, it is of great significance to demonstrate key technologies of shale gas development comprehensively by combining theories with and field data.

From the viewpoint of economic benefits, even if the costs of shale gas drilling and fracturing in China have reduced considerably in recent years, they are still too high. The comprehensive cost of signal well should be less than 50 million to achieve an internal rate of return of 12%, at the current gas price. To transfer resource into production as soon as possible, further improvement and innovation should be encouraged in both technology and management.

5. Summary

By now, China companies have proposed a customized method of developing shale gas resource for our own geologic feature and current level of engineering technology. In summary, the method consists of four aspects, which are summarized as follows:

1. Shale reservoir description is characterized by acquiring, processing and interpreting 3D seismic and logging data from shale in mountainous area; high-quality shale interval in

vertical distribution and sweet spot in lateral distribution are recognized by integrating comprehensive geological evaluation technology with outcrop, core, geochemical data and sedimentary setting model. These techniques provide a guidance for the target optimization of drilling horizontal well and the mass arrangement of multiwell pad.

2. The geology-engineering workflow is integrated to realize optimum and fast drilling technique by incorporating hole structure optimization, individualized PDC bits, rotary steerable drilling system and implementing the factory drilling model of "double-drilling rigs pattern, mass batched drilling, standardized operation." As a result, single-well drilling cycle is shortened by more than 50%.

3. On the basis of importing, absorbing and innovating foreign technology, China has formed a mature technical system of volume fracturing including high-displacement slick water, low-density proppant, soluble bridge plug, zipper-style fracturing and factory drilling pattern. As a consequence, fracturing efficiency is enhanced by 50%, and associated testing production rate is improved to $20 \times 104\ m^3/d$.

4. A production performance model is built by incorporating multiscale fracture network and multimechanism flow model to perform production performance analysis of shale gas well. Based on the model, an uncertainty productivity method is proposed to quantify probabilistic production forecasts and the probable range of estimated-parameter outcomes. A systematic optimization of fracturing parameters and well spacing is established by type curve matching, production performance modeling, and analogy with exploited shale field in North America.

In spite of great strides in the development of shale gas in China, there still exists much room for improvement. Based on periodic development regulation of other unconventional resources (such as tight gas), more advanced development techniques are required to be improved with the help of

1. strengthening geological research and technical development for the purpose of realizing cost-effective producing at low gas price;

2. reducing investment costs on single well and increase economic benefits. Draw lessons from tight gas development in China and explore low-cost development for shale gas;

3. reducing investment costs on single well and increase economic benefits;

4. performing sustainable improvements on drilling and completion to reduce low production wells.

6. Conclusion

Compared with the United States, shale gas in China has deeper buried depth, more complicate structures and surface conditions, which add difficulties to the shale gas development. At present, shale gas reservoirs less than 3500 m deep have been put into preliminary scale

development. Shale gas exploration is heading toward deeper formations, and shale gas development has wider prospects.

An evaluation criterion of shale gas well classification considering dynamic and static parameters and economic indicators has been basically established, but needs further improvement. Unstable mathematic seepage flow model of horizontal wells and probabilistic evaluation method of productivity based on multiscale space and various flow states are nearly perfect.

Optimization of horizontal section length, fracture placement, production system and well spacing are the keys to ensure the overall proper development of shale gas reservoirs. The theoretical research is basically mature, and field testing is urgently needed.

Establishment of shale gas development theory, optimization of evaluation methods and control of development cost are the core tasks in large-scale shale gas development.

Acknowledgements

The authors are indebted to PetroChina Southwest Oil&Gasfield Company and PetroChina Zhejiang Oilfield Company for their great support. This article was supported by the National Major Research Program for Science and Technology in China (No. 2017ZX05037, No. 2017ZX05063).

Conflict of interest

No conflict of interest exists in the submission of this manuscript, and manuscript is approved by all authors for publication.

Author details

Yunsheng Wei*, Ailin Jia, Junlei Wang, Yadong Qi and Chengye Jia

*Address all correspondence to: weiys@petrochina.com.cn

PetroChina, Research Institute of Petroleum Exploration and Development, Beijing, China

References

[1] Energy Information Administration. Shale in the United States [2016-07-26]. https://www.eia.gov/energy_in_brief/article/shale_in_the_united_states.cfm

[2] China Geological Survey. China Shale Gas Resources Survey Report. Beijing: China Geological Survey; 2014

[3] Ailin J, Yunsheng W, Yiqiu J. Progress in key technologies for evaluating marine shale gas development in China. Petroleum Exploration & Development. 2016;**43**(6):1035-1042

[4] Caineng Z, Dazhong D, Yuman W, et al. Shale gas in China: Characteristics, challenges and prospects. Petroleum Exploration & Development. 2016;**43**(2):166-178

[5] Wenrui H, Jingwei B. To explore the way of Chinese-style shale gas development. Natural Gas Industry. 2013;**33**(1):1-7

[6] Dazhong D, Yuman W, Xinjing L, et al. Breakthrough and prospect of shale gas exploration and development in China. Natural Gas Industry. 2016;**36**(1):19-32

[7] Ailin J, Jianlin G, Dongbo H. Perspective of development in detailed reservoir description. Petroleum Exploration and Development. 2007;**34**(6):691-695

[8] Xing L, Tingshan Z, Yang Y, et al. Microscopic pore structure and its controlling factors of overmature shale in the lower Cambrian Qiongzhusi Fm, northern Yunnan and Guizhou provinces of China. Natural Gas Industry. 2014;**34**(2):18-26

[9] Min G, Xuefu X, Yungui D, et al. The inorganic composition, structure and adsorption properties of the shale cores from the Weiyuan gas reservoirs, Sichuan Basin. Natural Gas Industry. 2012;**32**(6):99-103

[10] Ruyue W, Wenlong D, Dajian G, et al. Logging evaluation method and its application for total organic carbon content in shale: A case study on the lower Cambrian Niutitang formation in Cegong block, Guizhou province. Journal of China Coal Society. 2015; **12**(40):2874-2883

[11] Jun Y, Hai S, Zhaoqin H, et al. Key mechanical problems in the development of shale gas reservoirs. Scientia Sinica Physica, Mechanica & Astronomica. 2013;**43**(12):1527-1547

[12] Anderson M, Nobakht M, Moghadman S, et al. Analysis of production data from fractured shale gas wells. In: Proceedings of the SPE Unconventional Gas Conference (SPE 131787); 23-25 Feburary 2010; Pennsylvania. USA: SPE; 2010. pp. 1-15

[13] Yusheng W, Sepehrnoori K. Optimization of multiple hydraulic fractured horizontal wells in unconventional gas reservoirs. In: Proceedings of the SPE Unconventional Gas Conference (SPE 164509); 23-26 March 2013; Oklahoma. USA: SPE; 2013. pp. 1-15

[14] Junlei W, Ailin J, Bo N, et al. Analysis of the un-steady production data of a gas well based on pseudo-time function. Natural Gas Industry. 2014;**34**(10):1-7

[15] Valko PP, Economides MJ. Heavy crude production from shallow formations: Long horizontal wells versus horizontal fractures. In: Proceedings of the SPE International Conference on Horizontal well Technology (SPE 50421); 1–4 November 1998; Alberta. USA: SPE; 1998. pp. 1-11

[16] Junlei W, Ailin J, Yunsheng W, et al. Pseudo steady productivity evaluation and optimization for horizontal well with multiple finite conductivity fractures in gas reservoirs. Journal of China University of Petroleum (Edition of Natural Science). 2016;**40**(1):100-107

[17] Dongxiao Z, Tingyun Y. Environmental impacts of hydraulic fracturing in shale gas development in the United States. Petroleum Exploration and Development. 2015;**42**(6): 801-807

[18] Weiyao Z, Qian Q, Qian M, et al. Unstable seepage modeling and pressure propagation of shale gas reservoirs. Petroleum Exploration and Development. 2016;**43**(2):261-267

[19] Mirani A, Marongiu-Porcu M, Wang HY, et al. Production pressure drawdown management for fractured horizontal wells in shale gas formations. In: Proceedings of the SPE Annual Technical Conference and Exhibition, Dubai, UAE, 26-28 September, 2016

[20] Okouma V, Guillot F, Sarfare M, et al. Estimated ultimate recovery (EUR) as a function of production practices in the Haynesville shale. In: Proceedings of the SPE Annual Technical Conference and Exhibition; 30 October-2 November; Denver, Colorado, USA. 2011

Chapter 5

Capture of CO_2 from Natural Gas Using Ionic Liquids

Raghda Ahmed El-Nagar, Alaa Ali Ghanem and
Maher Ibrahim Nessim

Additional information is available at the end of the chapter

http://dx.doi.org/10.5772/intechopen.75577

Abstract

This chapter will be divided into three parts; introduction, experimental and result and discussion.

Introduction: This includes introduction about ionic liquids, their history and types which were used in different applications such as removal of carbon dioxide from natural gas.

Experimental: This deals with chemicals, solvents, and scheme of synthesis of different types of ionic liquids and their characterizations using different traditional techniques. The synthesized ionic liquids were used to capture carbon dioxide from natural gas using bubbling technique and gas chromatography as indicator.

Result and discussion: The results which obtained from synthesis and the applications briefed in this section and the quality of removal will be determined.

Keywords: ionic liquids, bubbling technique, natural gas, carbon dioxide

1. Introduction

Natural gas is the cleanest consuming non-renewable energy source, essentially because of its ignition creates low levels of carbon dioxide (CO_2) emissions; it is half the amount compared to coal and 30% compared to petroleum. Also it is widely available and easy to transport [1, 2].

For these reasons, there is a global trend for natural gas to be the main non-renewable energy source. According to the EIA (The Energy Information Administration), in 2011, the United States of America uses natural gas to produce 21% of its electricity and covering the equivalent of 24% of the energy demand. Global demand of natural gas, like the United States, is expected to increase or at least remains constant [3].

Natural gas is divided into two types according to its source of extraction; the first type is conventional gas (relatively easy to recover) comes from relatively high permeable reservoirs such as siltstone, sandstone and carbonate reservoirs in which the rock pores act like a trap for the gas particles with permeability of more than 1000 microdarcy. On the other hand unconventional natural gas is found in low permeable reservoirs such as; coal bed, tight sand formations with permeability of 1–100 microdarcy and shale with permeability of 1 microdarcy or less, where the accumulation of gas have a tendency to diffuse and spread over extensive geological ranges making it more hard to extract [4].

2. General overview of shale gas

Shale gas is known as one of the unconventional natural gas; extracted from shale rocks and has risen as a standout among the most encouraging vitality sources in the last few decades. Shale revolution started in the United States of America, with the discovery of huge reserves of recoverable shale gas, and kept spreading out in other countries all over the world. [5, 6].

EIA [3] reported that; the shale gas production in the United States in 2005 was only about 2% from the produced natural gas. Nowadays, the U.S. has become the largest gas producer in the world, as shale gas represents about 34% of the total U.S. produced natural gas and it aims to be above 50% by the year 2040. It was reported that U.S. natural gas production will increase from 23 trillion cubic feet in 2011 to 33.1 trillion cubic feet in 2040, with an increase of 44%. Almost all of this increase in natural gas production is due to projected growth in the shale gas [3, 7]. There are many countries who once thought they were had no or limited amounts of conventional hydrocarbon reservoirs are finding and exploring shales for gas and oil. As shown in **Figure 1** beside USA, a lot of countries like Britain, Ukraine, south Africa, Canada, Brazil, Argentina, Mexico, Poland, Australia, china and several north African countries are interested in exploiting and development of shale gas industry [8].

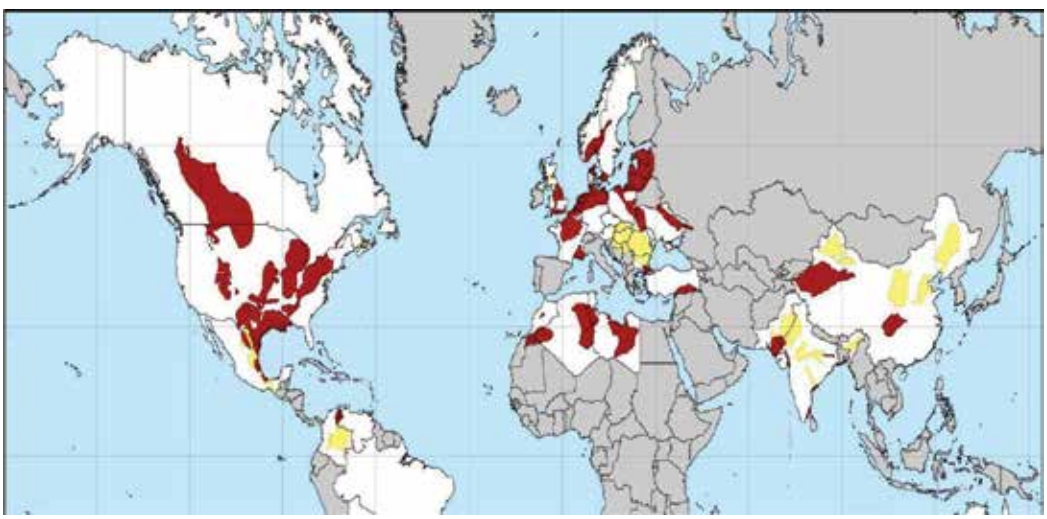

Figure 1. Sedimentary basin worldwide containing significant shale gas resources. Source: U.S. Energy Information Administration [8].

3. Shale gas composition

Shale gas is a natural gas, mainly methane, was trapped within the shale rocks during the Devonian epoch. Shale rock like sandstone and limestone is a fine-grained sedimentary rock which formed by the accumulation of deposits at the surface of the earth or at the bottom of relatively closed bodies of water. Gases from conventional and unconventional reservoirs have relatively the same composition. Both contain various amounts of acid gases (H_2S and CO_2). Also the amount of produced water varies among formations. Shale gas is quite dry; on the contrary of coal bed methane production is accompanied with a lot of water [9].

4. Shale gas production

Although the sources of shale gas and its extraction techniques are known a long time ago, its extraction from very little resources has been considered economically only in the last few years. This is thanks to George Mitchell's ideas on hydraulic fracturing, horizontal drilling and well stimulation techniques [7].

5. Hydraulic fracturing

Hydraulic fracturing method is a well stimulating technique used to fracture the rocks of the reservoir. It consists of two main stages: the first one is injecting fracking fluid which is a high pressure fluid (fracking fluid consists mainly from water and suspended proppants such as sand or aluminum oxide with the aid of a thickening agent) into the reservoir to increase the downhole pressure and create cracks in the formation rocks. These cracks enable the trapped gases to flow. The second stage is known as flow-back in which some of the injected water is released and comes out to the surface with the produced gas. Flow-back fluids can be treated and reused in another hydraulic fracture job which can decrease the volume of the generated wastewater. After the fracking pressure effect is over, the sand grains or aluminum oxide holds the fractures open [8].

Recent advances in horizontal drilling and hydraulic fracturing techniques have allowed access to the production of large quantities of shale gas that were previously uneconomical to produce [4].

6. CO_2 removal

Removal of carbon dioxide increases the calorific value and transportability of the natural gas. Carbon dioxide content in the natural gas obtained from gas or oil well can vary from 4 to 50%. On the other hand, purged gas from a gas re-injected EOR (enhanced oil recovery) well can contain as much as 90% carbon dioxide. Before a natural gas rich in carbon dioxide can be transported, it must be pre-processed so as to meet the typical specification of 2–5%

carbon dioxide. To meet such a specification, the natural gas is most commonly treated with an aqueous alkanolamine solution in absorption columns. The major advantages of the amine treatment are that it is a widely commercialized technology in which the hydrocarbon loss is almost negligible. However, the capital and operating cost shoots up very rapidly as the concentration of carbon dioxide in feed gas increases [10].

Carbon dioxide, which falls into the category of acid gases (as does hydrogen sulfide, for example) is commonly found in natural gas streams at levels as high as 80%. In combination with water, it is highly corrosive and rapidly destroys pipelines and equipment unless it is partially removed or exotic and expensive construction materials are used. Carbon dioxide also reduces the heating value of a natural gas stream and wastes pipeline capacity. In LNG plants, CO_2 must be removed to prevent freezing in the low-temperature chillers.

7. Experimental

7.1. Materials

Lactic acid (99%), ethanol amine (99%), diethanolamine (99%) and N,N-dimethylethanolamine (99%) were purchased from Fluka. 1-Methyl imidazole (99%), 1,2 dimethylimidazole (98%), 2-bromoethylaminehydrobromide (98%), 3-bromopropylamine hydrobromide (99%), sodium tetrafluoroborate (99%) and lithium bis(trifluoromethylsulfonyl)imide (99%) were purchased from Sigma-Aldrich. Sodium methoxide (99%), ethanol (absolute), dry methanol (98%), acetone (99%), acetonitrile (99%) and methylene chloride (99%) were purchased from Merck Chemicals Company. PVDF membrane was obtained from Whatman incorporation.

7.1.1. Synthesis of ionic liquids (ILs)

7.1.1.1. Synthesis of ethanolamine lactates

Ethanolammonium ionic liquids were synthesized by direct neutralization of different ethanolamines with lactic acid [11].

Ethanolamines were loaded into 100 ml flask in water bath; the system was equipped with liquid filler, a reflux condenser and N_2 under vigorous stirring at constant rate. Lactic acid (0.05 mol) was then added drop wise into the stirring reaction mixture for about 15 min and the reaction was allowed to proceed for 30 min. The solution was treated with acetone, removed by evaporation under vacuum and then dried for 48 h at 50°C. The synthesized reaction for the ethanol ammonium ILs is expressed in **Scheme 1**:

Scheme 1. Synthesis of hydroxyl amine lactate. I: (R = CH_3, R_1 = H, R_2 = H, R_3 = HO─CH_2─CH_2─); II, (R = CH_3, R_1 = H, R_2 = HO─CH_2─CH_2─, R_3 = HO─CH_2─CH_2─); and III, (R = CH_3, R_1 = CH_3, R_2 = CH_3, R_3 = HO─CH_2─CH_2─).

7.1.1.2. Synthesis of imidazolium bis(triflouromethylsulfonyl)imides

Solution containing one equivalent of 1-methyl imidazole (0.25 M) in acetonitrile was added to stirring solution of one equivalent n-bromoalkyl amine hydrobromide (ethyl and propyl, respectively), dissolved in a minimal amount of ethanol, it was stirred at room temperature. Solvent was removed under vacuum yielding dark solid color. Methylene chloride and ethanol (50:50)% were added to yield white precipitate and solvent was removed by evaporation. The amine moiety was deprotonated with 1.2 equivalence of sodium methoxide in dry methanol. Solvent was evaporated and methylene chloride was added to precipitate out the sodium bromide as by-product which was filtered off. Methylene chloride solution was added to 1.1 equivalence of lithium bis(tri fluoromethylsulfonyl)imide overnight and the organic layer was repeatedly washed with water to remove bromide. Methylene chloride and water were removed under vacuum. The synthesized product was expressed in **Scheme 2**.

7.1.1.3. Synthesis of imidazolium tetraflouroborates

Solution containing one equivalent of 1-methyl imidazole (0.25 M) in acetonitrile was added to a stirring solution of one equivalent of n-bromoalkyl amine hydrobromide (ethyl and propyl, respectively) dissolved in a minimal amount of ethanol, it was stirred at room temperature [12]. Solvent was removed under vacuum yields dark color. Methylene chloride was added to ethanol (50:50)% to yield white precipitate, and solvent was removed by evaporation. The amine moiety was deprotonated with 1.2 equivalence of sodium methoxide in dry methanol. Solvent was evaporated and methylene chloride was added to precipitate the sodium bromide as by-product which was filtered off. Methylene chloride solution was reacted with 1.1 equivalence of sodium tetraflouroborate, dissolved in water overnight and the organic layer was repeatedly washed with water. Methylene chloride and water were removed under vacuum. The synthesized reaction was expressed in **Scheme 3**.

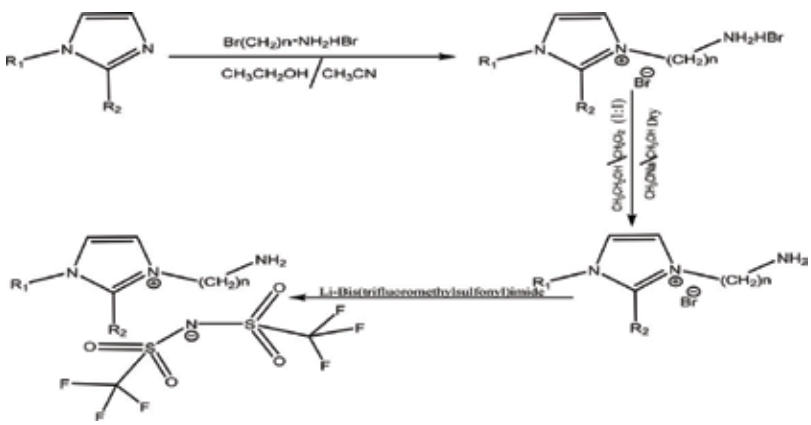

Scheme 2. Synthesis of imidazolium bis(triflouromethylsulfonyl)imides. IV = (n = 2, $R_1 = CH_3$, $R_2 = H$); V = (n = 3, $R_1 = CH_3$, $R_2 = H$); VIII = (n = 2, $R_1 = CH_3$, $R_2 = CH_3$); and IX = (n = 3, $R_1 = CH_3$, $R_2 = CH_3$).

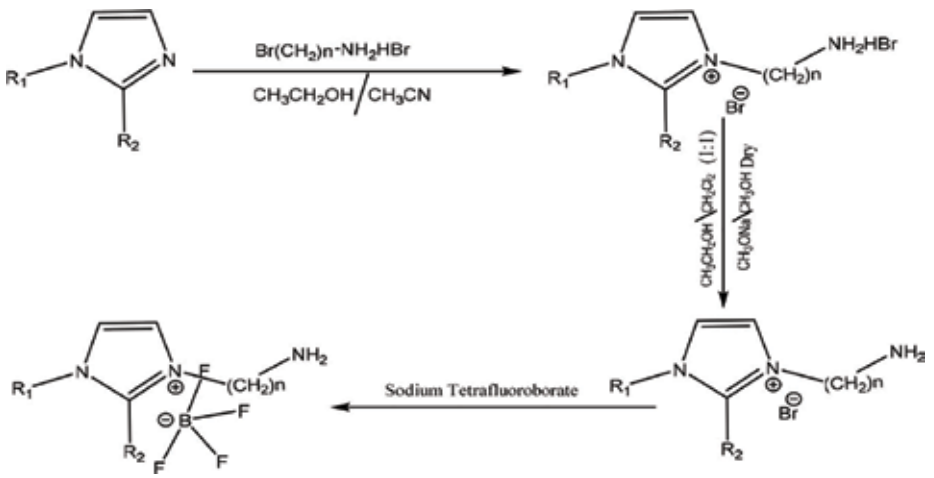

Scheme 3. Synthesis of imidazolium tetraflouroborates. VI = (n = 2, R_1 = CH_3, R_2 = H); VII = (n = 3, R_1 = CH_3, R_2 = H); X = (n = 2, R_1 = CH_3, R_2 = CH_3); and XI = 3 (n = 3, R_1 = CH_3, R_1 = CH_3).

7.1.2. Capture of carbon dioxide (CO_2)

7.1.2.1. Bubbling technique

Using methanol as a blank solution, 0.1 mol solution of ionic liquid prepared, was put in the bubbling cell and the system run as follows [13, 14]:

- The system was adjusted as in **Figure 2** where: (a) cylinder of He, (b) cylinder of CO_2/CH_4, (c) valve, (d) water bath at 25°C, (e) bubbling cell, (f) needle, (g) mass flow meter, (h) sampling valve, and (i) gas chromatography.
- The system was evacuated using He gas first.
- CH_4/CO_2 gas were flowed to the system and passed to the solution through thin needle.
- Outlet gas was characterized by gas chromatography.

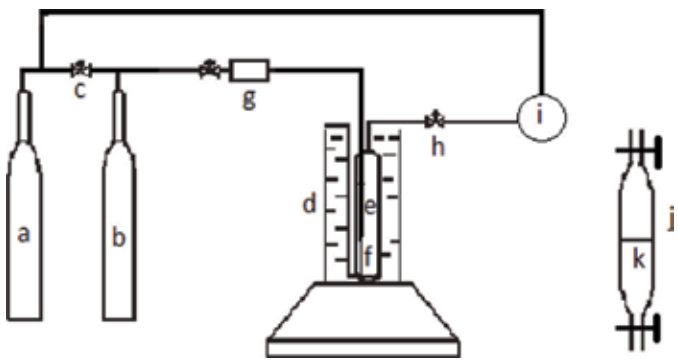

Figure 2. Flow sheet of CO_2 captures experimental apparatus.

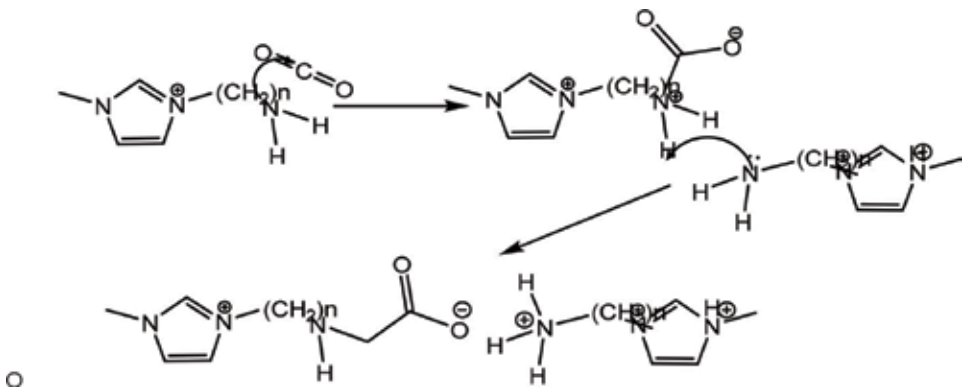

Scheme 4. Mechanism for bubbling technique A (amine interaction).

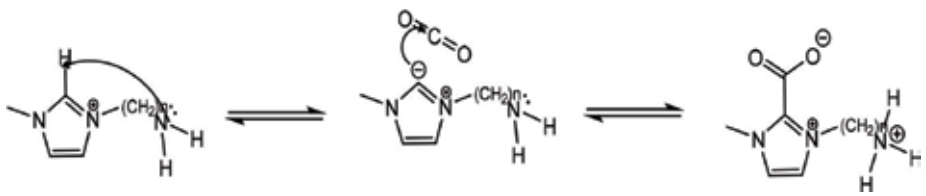

Scheme 5. Mechanism for bubbling technique B, carbene interaction.

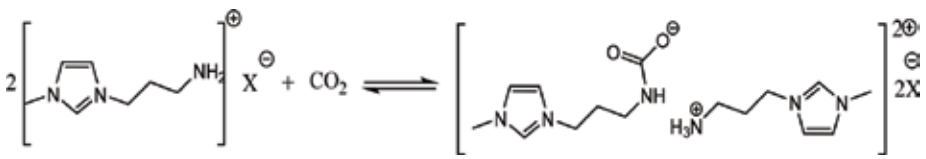

Scheme 6. Proposed amine interaction.

In amine interaction carbon dioxide is attacked by the amino group through it is lone pair of electrons, consequently the amino group of another molecule of ionic liquid capture a proton from the first one to form a bimolecular compound. In carbine reaction, the active proton of the imidazolium nucleus migrates to the amino group of the chain part to form the carbenium ion; this anion formed can attack the carbon dioxide molecule to get the Zwitterion (**Schemes 4** and **5**).

In this work the proposed mechanism is amine inter action and can be illustrated in **Scheme 6** [15].

7.1.2.2. Membrane technique (adsorption)

The system was adjusted as above (**Figure 2**), where bubbling cell was replaced by the membrane cell [(j)—membrane cell, (k)—supported ionic liquid membrane] (SILM) were prepared by immersing PVDF membrane in ionic liquid till saturation, put the SILM in membrane cell, pass CO_2/CH_4 through the cell, and the outlet gases passed to gas chromatography to be characterized.

7.1.3. Regeneration of ionic liquids

The used ionic liquids could be recycled by two ways. When we use heating, we can ride of captured CO_2. Also by washing with distilled water and then evaporating it.

8. Results and discussions

8.1. Technique of CO_2 removal

Methanol was used as solvent for the prepared ionic liquid solutions as it has no effect on absorption of CO_2 (CO_2 = 21.430).

To reach the optimum conditions, the gas rate was changed and the percent of CO_2 captured was determined in presence of the prepared ionic liquid solutions. By using a rate of 0.7 sccm, the amount of ionic liquids took more time to be saturated with carbon dioxide, whereas by using a rate of 2 sccm we did not reach to a complete chemical reaction between the ionic liquids under investigation and the total amount of carbon dioxide flowed (**Figures 3** and **4**). While at 1 sccm rate, a complete reaction between the ionic liquid solutions and the flowed CO_2 took place with suitable time, i.e. the optimum rate was 1 sccm.

Figures 1–17 show that:

- The traditional ionic liquids (I–III) are of good efficiency in carbon dioxide removal from the natural gas and the order of increasing efficiency was II < III < I.
- The time of saturation of ionic liquids (I–III) by carbon dioxide followed the order of II < I < III.
- By using 1-methyl imidazole ionic liquids (IV–VII) in carbon dioxide capture, the results showed that the efficiency will be as follows: VII < VI < V < IV, this means that, the efficiency increased by:
  - **a.** Increasing the chain length of the aliphatic amine part.
  - **b.** Changing the anion part from bis(trifloromethylsulonyl)imide to tetraflouroborate so the second is better.
- This observation was also obtained by (VII–XI) ionic liquids.
- The derived imidazolium cations (1,2 dimethyl imidazole) affect the efficiency of synthesized ionic liquids as shown in the following order: XI < X < IX < VIII.

8.2. Regeneration of ionic liquids

Ionic liquids (I–XI) can be recycled. In chemical reaction the reacted species in the loaded solvent are decomposed by heating to liberate carbon dioxide and regenerate the ionic liquids that reacted with carbon dioxide. In another way, ionic liquids are recycled by washing them

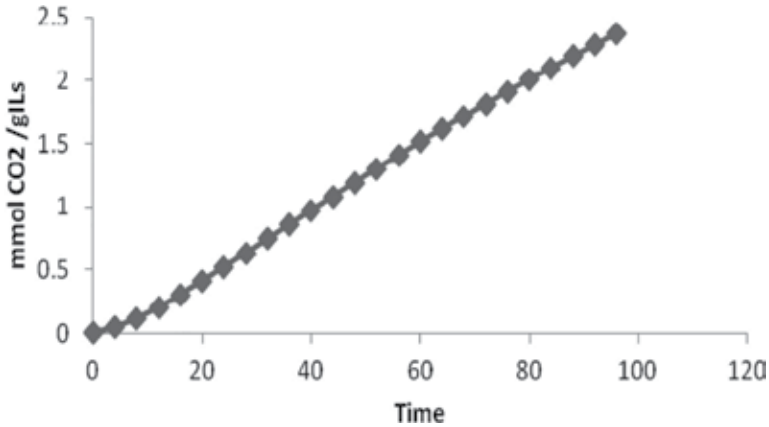

Figure 3. Capture of CO_2 using ionic liquid vat rate 0.7 sccm.

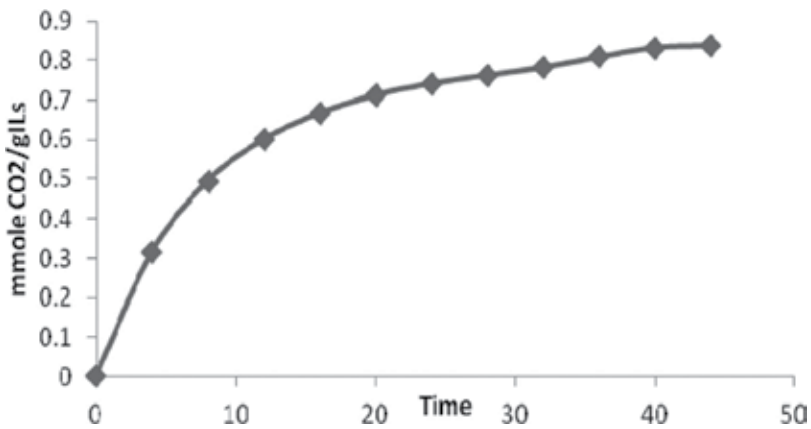

Figure 4. Capture of CO_2 using ionic liquid VII at rate 2 sccm.

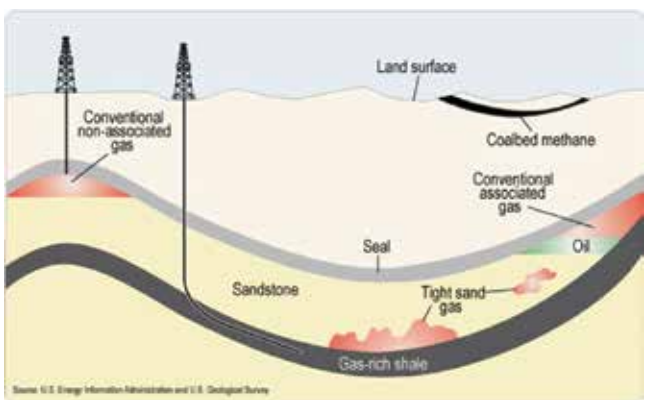

Figure 5. Conventional and non-conventional gas reservoirs [4].

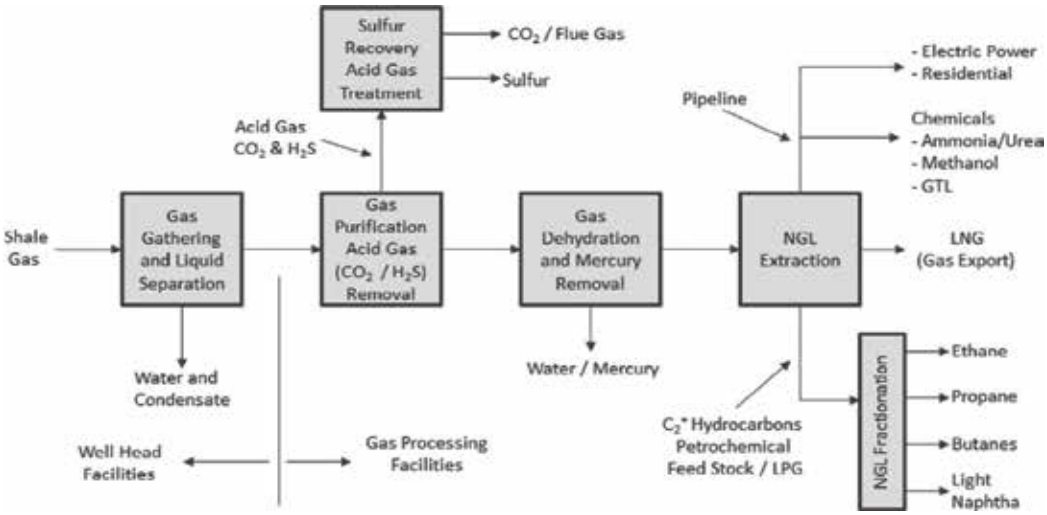

Figure 6. Shale gas overall infrastructure block diagram [4].

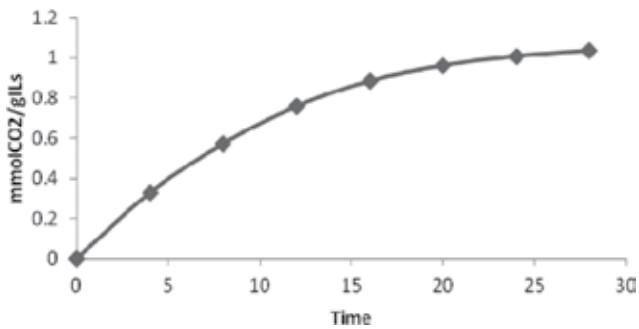

Figure 7. Absorption of CO_2 using synthesized ionic liquid I.

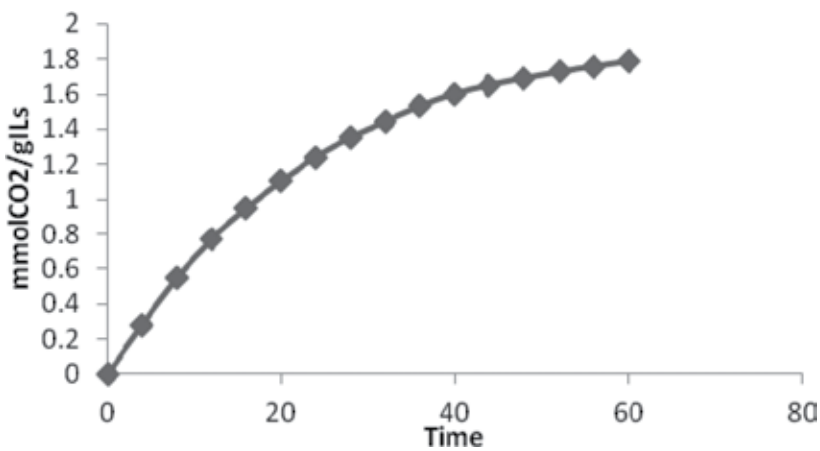

Figure 8. Absorption of CO_2 using synthesized ionic liquid II.

http://dx.doi.org/10.5772/intechopen.75577

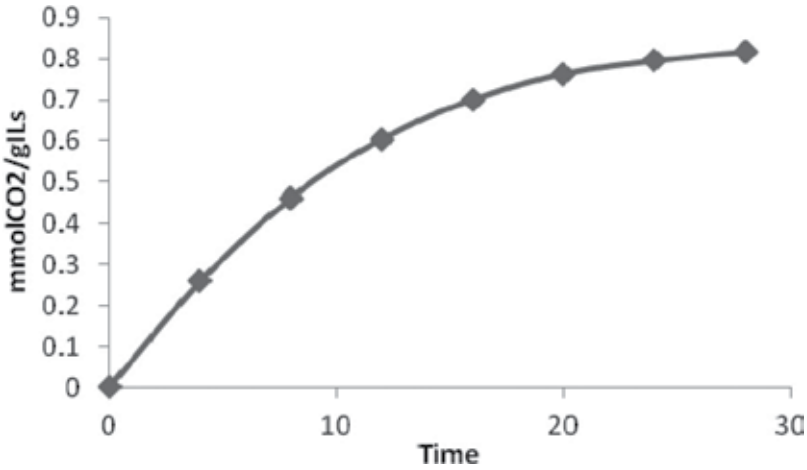

Figure 9. Absorption of CO_2 using synthesized ionic liquid III.

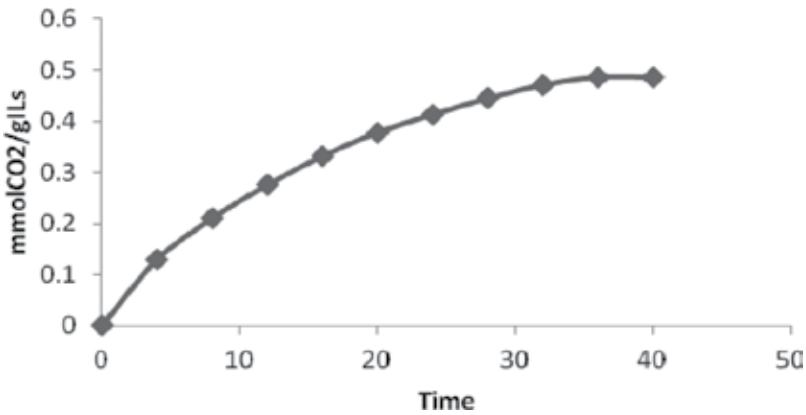

Figure 10. Absorption of CO_2 using synthesized ionic liquid IV.

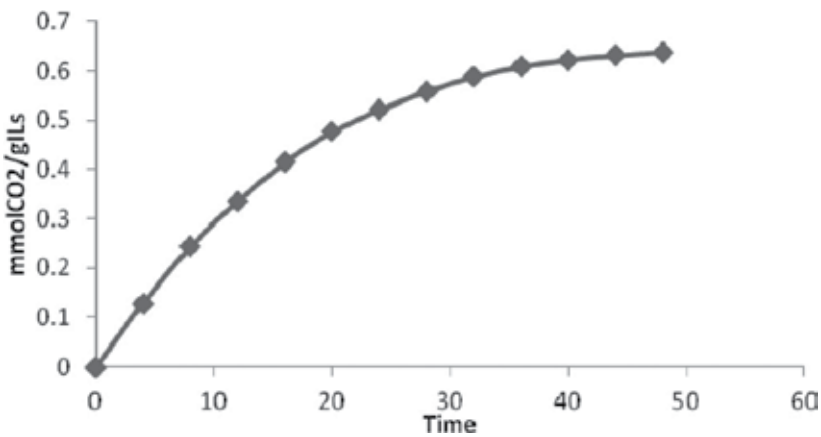

Figure 11. Absorption of CO_2 using synthesized ionic liquid V.

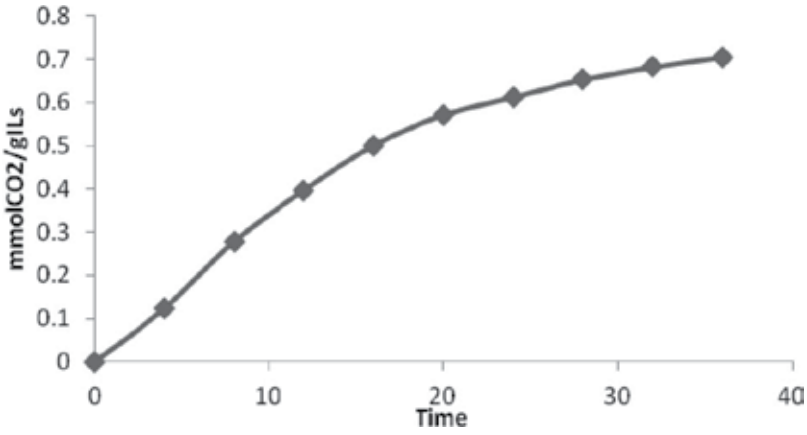

Figure 12. Absorption of CO_2 using synthesized ionic liquid VI.

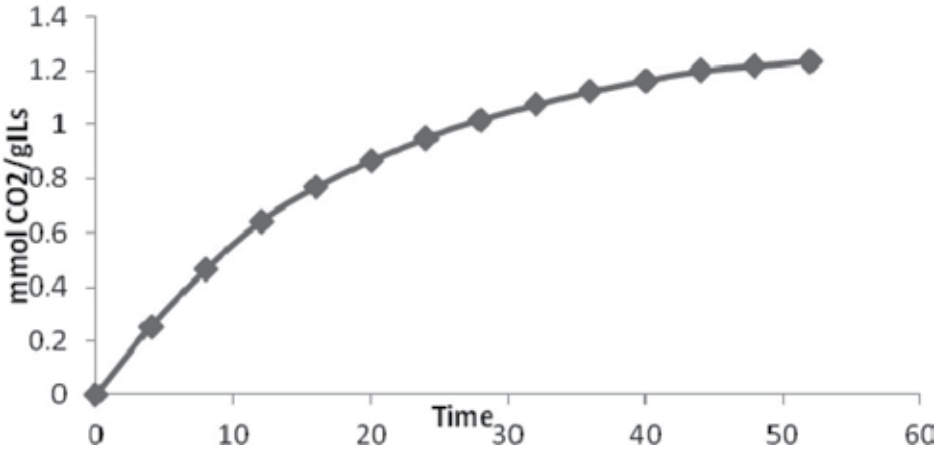

Figure 13. Absorption of CO_2 using synthesized ionic liquid VII.

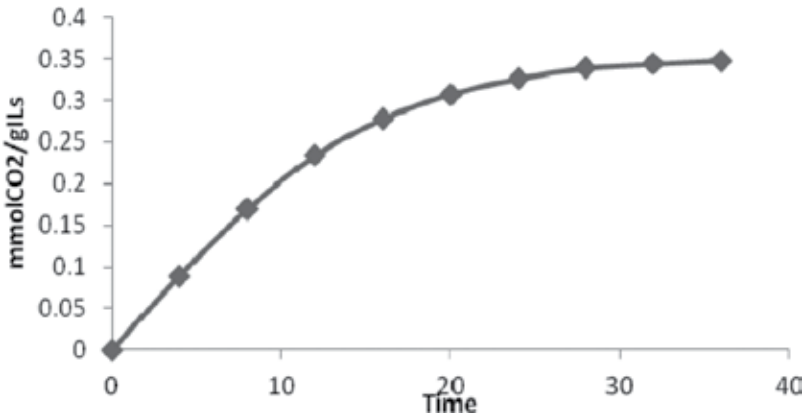

Figure 14. Absorption of CO_2 using synthesized ionic liquid VIII.

http://dx.doi.org/10.5772/intechopen.75577

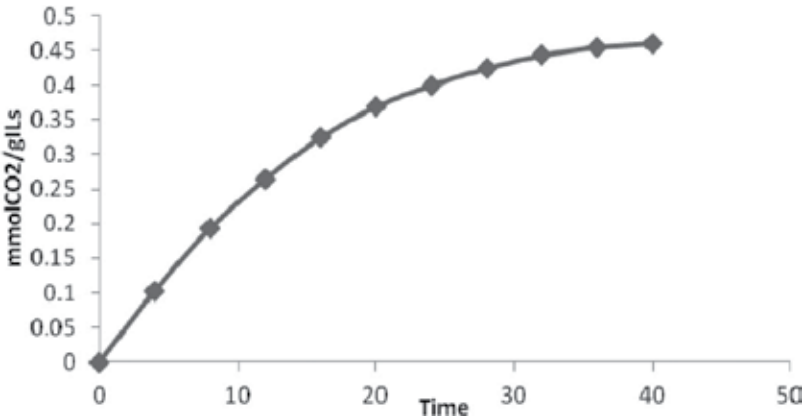

Figure 15. Absorption of CO_2 using synthesized ionic liquid IX.

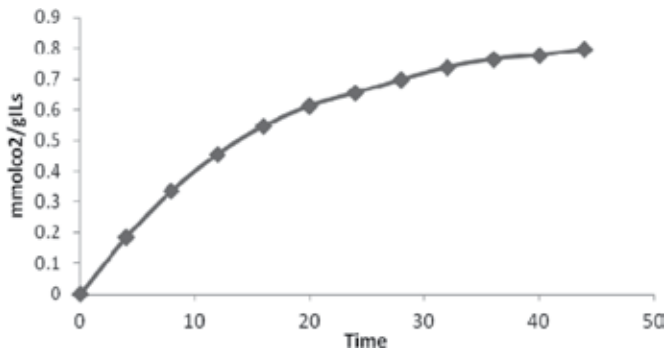

Figure 16. Absorption of CO_2 using synthesized ionic liquid X.

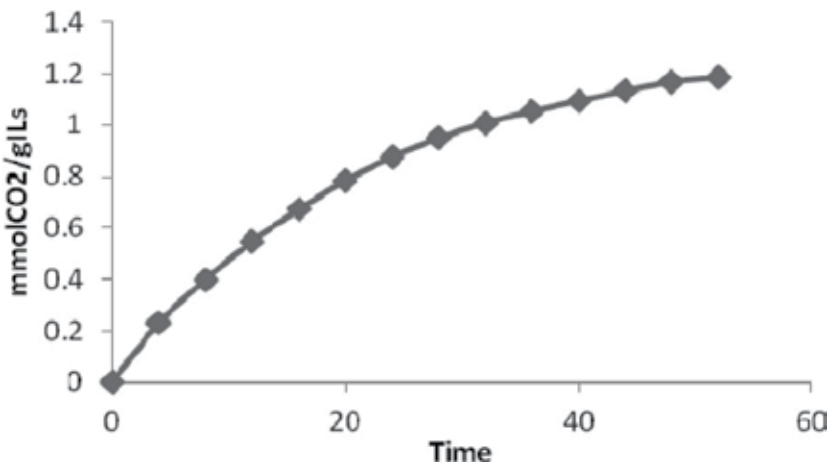

Figure 17. Absorption of CO_2 using synthesized ionic liquid XI.

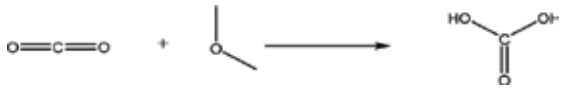

Scheme 7. Regenerated mechanism.

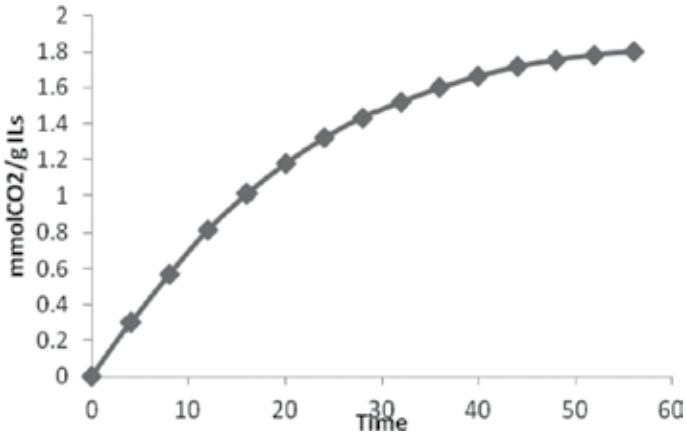

Figure 18. Absorption of CO_2 using regenerated ionic liquid I.

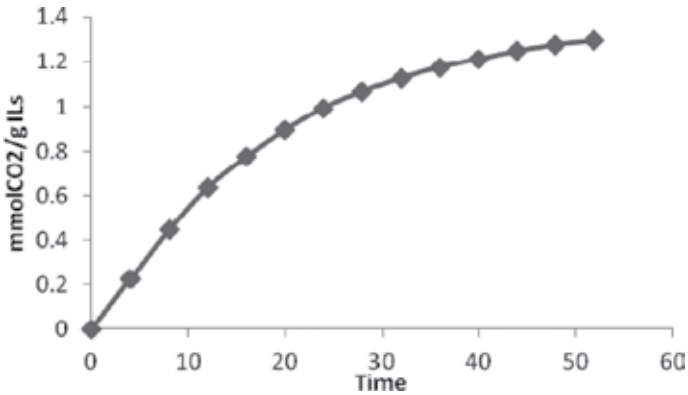

Figure 19. Absorption of CO_2 using regenerated ionic liquid II.

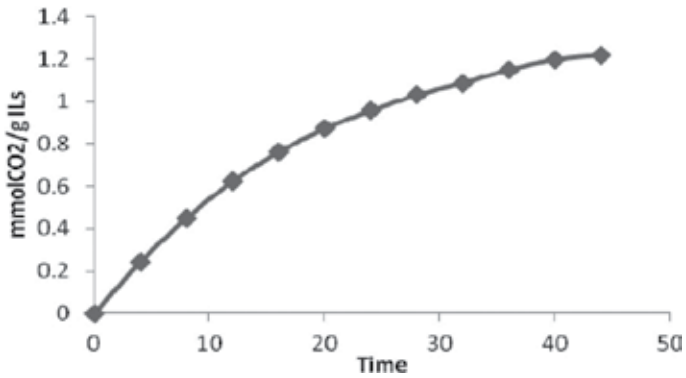

Figure 20. Absorption of CO_2 using regenerated ionic liquid III.

http://dx.doi.org/10.5772/intechopen.75577

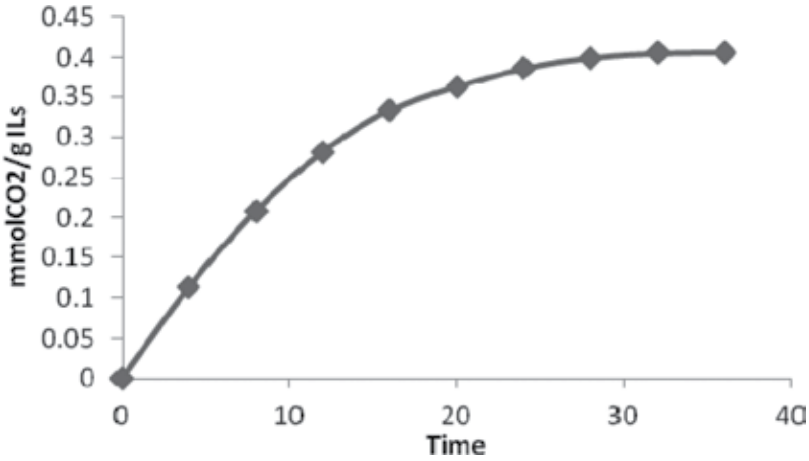

Figure 21. Absorption of CO_2 using regenerated ionic liquid IV.

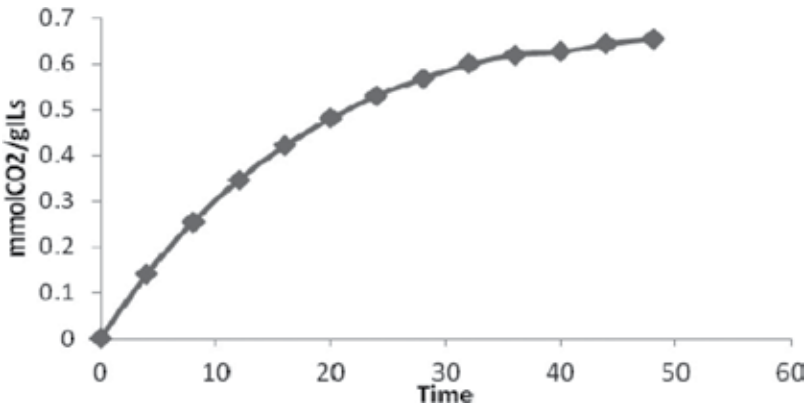

Figure 22. Absorption of CO_2 using regenerated ionic liquid V.

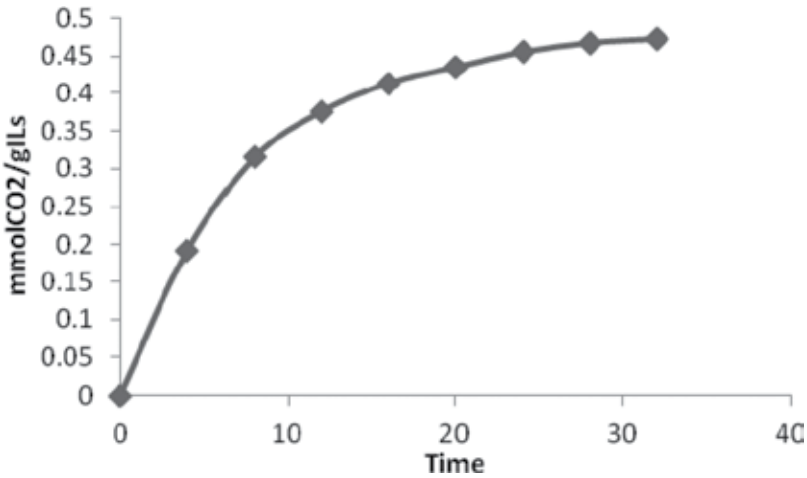

Figure 23. Absorption of CO_2 using regenerated ionic liquid VII.

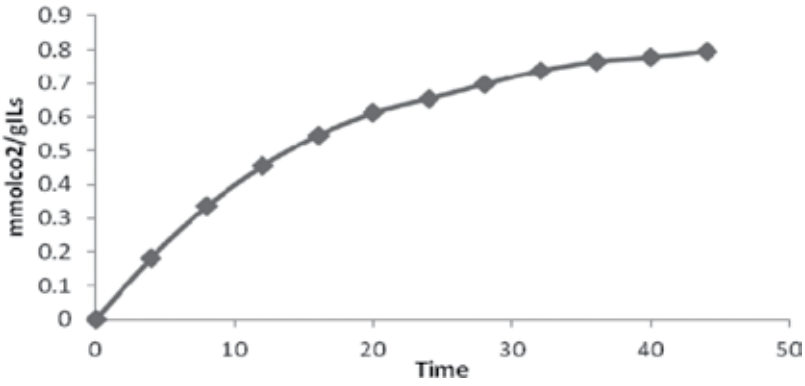

Figure 24. Absorption of CO_2 using regenerated ionic liquid X.

with distilled water, and consequently the captured carbon dioxide reacted with water to yield carbonate [16] (**Scheme 7**). Then, the ionic liquids were obtained by decantation and evaporation to get rid of any water. In this work, ionic liquids (VI, VIII, IX and XI) are soluble in water so, it cannot be regenerated through the second way. The regenerated ionic liquids are used to capture carbon dioxide from natural gas with high efficiency as shown in **Figures 18–24**.

Abbreviations

EIA	the Energy Information Administration
EOR	enhanced oil recovery
SILM	the supported ionic liquid membranes
sccm	standard cubic centimeters per minute

Author details

Raghda Ahmed El-Nagar*, Alaa Ali Ghanem and Maher Ibrahim Nessim

*Address all correspondence to: raghda_elnagar@yahoo.com

Egyptian Petroleum Research Institute (EPRI), Egypt

References

[1] Jaramillo P, Griffi WM, Matthews HS. Environmental Science and Technology. 2007;**41**:6290-6296

[2] Gregory KB, Vidic RD, Dzombak DA. Elements. 2011;**3**:181-186

[3] EIA—Annual Energy Outlook 2011. United States Department of Energy, Energy Information Administration DOE/EIA-0383. 2011. Available from: www.eia.doe.gov/forecasts/aeo/

[4] Kamal SH. Journal of the Combustion Society of Japan. 2013;**55**:13-20

[5] Deutch J. Foreign Affairs. 2011;**90**:82-93

[6] Jacoby H, O'Sullivan F, Paltsev S. The influence of shale gas on US energy and environmental policy. Economics of Energy & Environmental Policy. 2012;**1**:37-51

[7] O'Sullivan F, Paltsev S. Shale gas production: Potential versus actual greenhouse gas emissions. Environmental Research Letters. 2012;**7**:044030. 6p

[8] Soeder DJ. Shale gas development in the United States. In: Al-Megren H, editor. Advances in Natural Gas Technology. InTech. ISBN: 978-953-51-0507-7. Available from: http://www.intechopen.com/books/advances-in-natural-gas-technology/shalegas-development-in-the-united states

[9] Stephenson T, Valle JE, Riera-Palou X, American Chemical Society. Environmental Science & Technology. 2011;**45**:10757-10764

[10] Datta AK, Sen PK. Journal of Membrane Science. 2006;**283**:291-300

[11] Zhai L, Zhong Q, He C, Wang J. Journal of Hazardous Materials. 2010;**177**:807-813

[12] Myers C, Pennline H, Luebke D, Ilconich J, Dixon JK, Maginn EJ, Brennecke JF. Journal of Membrane Science. 2008;**322**:28-31

[13] El-Nagar RA, Nessim M, Abd El-Wahab A, Ibrahim R, Faramawy S. Journal of Molecular Liquids. 2017;**237**:484-489

[14] Nessim MI, Abdallah RI, Elsayed GE, El-Nagar RA. Life Science Journal. 2013;**10**:1716-1723

[15] Zhijun Z, Haifeng D, Xiangping Z. Chinese Journal of Chemical Engineering. 2012;**20**:120-129

[16] Figueroa JD, Fout T, Plasynski S, McIlvried H, Srivastava RD. International Journal of Greenhouse Gas Control. 2008;**2**:9-20

Edited by Ali Al-Juboury

Natural gas, particularly shale gas, is one of the main sustainable energy sources in the current century. It is an abundant energy resource, playing an active role in future energy demand and enabling nations to transition to higher support on renewable energy sources. The book aims to add some contributions and new advances in technologies and prospects on shale gas reserves in selected regions of the world, in terms of new technologies of extraction, new discoveries of promising reserves, synthesis and applications to get high quality of this cleanest consuming non-renewable energy source.

Published in London, UK

IntechOpen

ISBN 978-1-83881-479-3